

Synthesis and Studies Directed Toward Multidrug Resistance-Modulating Natural Products

by

Christopher Allen Lee

BS, Saint Michael's College, 1998

MS, University of Pittsburgh, 2002

Submitted to the Graduate Faculty of
Arts and Sciences in partial fulfillment
of the requirements for the degree of
Doctor of Philosophy

University of Pittsburgh

2004

UNIVERSITY OF PITTSBURGH
FACULTY OF ARTS AND SCIENCES

This dissertation was presented

by

Christopher Allen Lee

It was defended on

October 25, 2004

and approved by

Scott G. Nelson
Professor of Chemistry

Christian E. Schafmeister
Professor of Chemistry

Jack C. Yalowich
Professor of Pharmacology

Dr. Paul E. Floreancig
Professor of Chemistry
Dissertation Director

Synthesis and Studies Toward Multidrug Resistance-Modulating Natural Products

Christopher Allen Lee, PhD

University of Pittsburgh, 2004

Studies directed toward the enantioselective preparation of dihydroagarofuran natural products are presented. The purpose of this project is to synthesize dihydroagarofuran natural products in order to study what structural features are required for inhibition of Phosphoglycoprotein (P-gp) induced multidrug resistance in this family of molecules. Once an optimal synthetic route is established, analogs can be synthesized to probe P-gp function at the molecular level. Three synthetic routes to the dihydroagarofuran family of natural products were investigated. Each synthesis utilized (*R*)-(-)-carvone, an inexpensive terpene available in high enantiomeric purity, as the sole source of chirality. Our studies have shown that the dihydroagarofuran tricyclic skeleton can be prepared in as few as eight steps from (*R*)-(-)-carvone. Each synthesis is substantially shorter than previously published routes to similar ring systems.

In conjunction with our studies toward interesting multidrug resistance modulating natural products, a short and enantioselective route to the tetrahydropyran (THP) bryostatin B ring was developed. This new method utilizes a cyclic acetal to generate a reactive oxocarbenium ion, which was subsequently trapped with a tethered silyl enol ether. The resulting diastereoselective reaction gives exclusively 2,6-*cis*-tetrahydropyranone rings in excellent yield. Unlike previous routes to create oxocarbenium ions from acetals, our approach uses Ce(NO₃)₃ an exceptionally mild Lewis acid. Ce(NO₃)₃ is inexpensive, non-toxic, and easy to separate from reaction mixtures. The use of acetals as oxocarbenium ion precursors is an attractive method for complex molecule synthesis, since acetals can be constructed under extremely mild conditions. This new method can be easily extended to the enantioselective preparation of other complex THP ring containing macrolide natural products, such as (+) Phorboxazole A or (+) Leucascandrolide A.

TABLE OF CONTENTS

PREFACE.....	xi
1. Multidrug Resistance	1
1.1. Introduction to Multidrug Resistance	1
1.2. The Role of Phospho-glycoprotein in MDR.....	2
1.3. Disease Associated with P-gp.....	3
1.4. Function of P-gp	4
1.5. Recognition of Substrates by P-gp.....	5
1.6. Structure of P-gp.....	7
1.7. Inhibition of P-gp.....	9
1.8. Cytochrome P450 and P-gp	12
2. Dihydroagarofuran Natural Products.....	15
2.1. A Model for the Structural Basis of MDR Modulation	17
2.2. Advantages of Using Dihydroagarofurans.....	18
2.3. Previous Dihydroagarofuran Syntheses.....	20
3. Work Towards the Construction of the Dihydroagarofuran Ring System	26
3.1. Orbiculin A as an Initial Target	26
3.2. A Ring Closing Metathesis Route to Celafolin A-1	46
3.3. A Revised Route to Celafolin A-1	59
3.4. Summary	74
4. Studies Directed Toward Bryostatin 1: A MDR Modulating Natural Product.....	76
4.1. A Mild Method for Constructing 2,6- <i>cis</i> -THP Rings	79
4.2. The Bryostatins: Isolation and Biological Activity	82
4.3. Previous Bryostatin Syntheses.....	84
4.4. A Model System for the Bryostatin B Ring.....	85
4.5. Enantioselective Preparation of the B Ring of Bryostatin 1	93
4.6. Summary	100
Experimental Procedures	103
BIBLIOGRAPHY.....	144

LIST OF TABLES

Table 1 MDR reversing dihydroagarofurans	16
Table 2 A comparison of the ^1H NMR data from six aldol diastereomers	43

LIST OF FIGURES

Figure 1 Phospho-glycoprotein.....	2
Figure 2 Alternating catalytic site model.....	5
Figure 3 Low-resolution image of P-gp.....	7
Figure 4 Topology of P-gp.....	8
Figure 5 Representative MDR reversing compounds.....	9
Figure 6 Dihydroagarofuran MDR reversing agents.....	10
Figure 7 The FRET technique.....	12
Figure 8 Feed-forward / feed-back mechanism for SXR.....	13
Figure 9 Dihydroagarofuran numbering.....	15
Figure 10 Representative dihydroagarofuran natural products.....	17
Figure 11 Comparison of carvone and the dihydroagarofuran skeleton.....	18
Figure 12 Structurally diverse MDR reversing agents.....	19
Figure 13 White and coworkers (\pm)-euonyminol synthesis.....	21
Figure 14 Completion of (\pm)-euonyminol.....	22
Figure 15 Li and coworkers (-)-isocelorbicol synthesis.....	23
Figure 16 Completion of (-)-isocelorbicol.....	24
Figure 17 Retrosynthesis for orbiculin A.....	27
Figure 18 Oxidation of (<i>R</i>)-(-)-carvone using Davis' oxaziridine (28).....	28
Figure 19 Rubottom oxidation of (<i>R</i>)-(-)-carvone.....	29
Figure 20 Epimerization at C-6.....	30
Figure 21 A tandem conjugate addition-aldol reaction.....	32
Figure 22 Closed and open transition state models.....	33
Figure 23 Cyclic carbonate NOE analogs.....	34
Figure 24 1D NOE results for carbonate (38) of the aldol reaction major product.....	35
Figure 25 1D NOE results for carbonate (40) of the aldol reaction minor product.....	36
Figure 26 Zimmermann-Traxler model.....	37
Figure 27 Half-chair conformations for enone (32a).....	37
Figure 28 Aluminum chelate and open transition state models.....	38
Figure 29 Attempted (<i>Z</i>)-vinyl iodide synthesis.....	39
Figure 30 A comparison of the original route (top) and the new route (bottom).....	40
Figure 31 An improved preparation of 4-iodopent-4-enal.....	41
Figure 32 A selective tandem conjugate addition-aldol reaction.....	42
Figure 33 A successful <i>cis</i> -decalin synthesis.....	44
Figure 34 The KAPA mediated olefin isomerization.....	45
Figure 35 Retrosynthesis of celafolin A-1.....	46
Figure 36 Grignard addition into a neopentyl ketone.....	47
Figure 37 Construction of the A and B ring of celafolin A-1.....	49
Figure 38 Substrate controlled addition into the C-5 ketone (63).....	50
Figure 39 Deuterium labeling experiment.....	52
Figure 40 ¹ H NMR coupling constant analysis for the RCM product (65).....	53

Figure 41 C-10 NOE enhancements	54
Figure 42 Attempted Pummerer rearrangement	55
Figure 43 The Pummerer rearrangement and a competing elimination process	55
Figure 44 Completion of the celafolin A-1 ring system	56
Figure 45 NOE results for diol (68).....	57
Figure 46 Acetate (70) NOE experiment.....	58
Figure 47 Revised retrosynthesis of celafolin A-1	60
Figure 48 Construction of the tetrahydrofuran C ring	61
Figure 49 A successful epoxide-opening route.....	63
Figure 50 Titanocene chloride reductive epoxide opening.....	64
Figure 51 Formation of the tetrahydrofuran C ring	65
Figure 52 Mechanism for C-9 epimerization.....	66
Figure 53 Macromodel Monte Carlo calculations	67
Figure 54 Hydrogen bonding interactions in the <i>trans</i> -decalin ring system.....	68
Figure 55 DBU intramolecular aldol additions.....	69
Figure 56 NOESY for <i>cis</i> -decalin (81).....	70
Figure 57 NOESY for <i>cis</i> -decalin (82).....	71
Figure 58 Transition states for <i>cis</i> - and <i>trans</i> -decalin ring forming aldol reactions.....	72
Figure 59 RCM route to celafolin A-1.....	74
Figure 60 The intramolecular aldol addition route	75
Figure 61 Bioactive THP ring containing natural products	76
Figure 62 Five routes to non-racemic 2,6- <i>cis</i> -THP rings	78
Figure 63 Aqueous Prins and Mukaiyama aldol conditions	80
Figure 64 Chair transition state model.....	81
Figure 65 The oxonia-Cope rearrangement produces side chain scrambling.....	81
Figure 66 An unfavorable [3,3]-rearrangement.....	82
Figure 67 Bryostatin family members	83
Figure 68 Wender and coworkers bryostatin analogs.....	84
Figure 69 An intramolecular Mukaiyama aldol reaction.....	85
Figure 70 Mukaiyama aldol substrates	86
Figure 71 Mukaiyama aldol optimization.....	88
Figure 72 Optimized Mukaiyama aldol reactions.....	90
Figure 73 NOESY results for (93).....	91
Figure 74 Failed Cyclization Reactions.....	92
Figure 75 Retrosynthesis of the bryostatin 1 B ring	93
Figure 76 Asymmetric allylation	94
Figure 77 Asymmetric allylation transition states	95
Figure 78 Bryostatin 1 B ring synthesis.....	96
Figure 79 Transition state for the Mukaiyama aldol.....	98
Figure 80 NOESY for tetrahydropyranone (105).....	98
Figure 81 Evans' application of Fuji's binol phosphonate reagent.....	99
Figure 82 A convergent preparation of Mukaiyama aldol precursors	100
Figure 83 A brief route to the C-9 to C-19 fragment of bryostatin 1.....	101
Figure 84 C-20 to C-29 fragment of (+) phorboxazole A.....	102

LIST OF ABBREVIATIONS

A ^{1,2} strain	Allylic strain
ABC	ATP binding cassette
Ac ₂ O	Acetic anhydride
ADP	Adenosine 5'-diphosphate
ATP	Adenosine 5'-triphosphate
CI	Chemical ionization
DBU	1,8-Diazabicyclo[5.4.0]undec-7-ene
DHP	2,3-Dihydropyran
Dibal-H	Diisobutylaluminum hydride
DIPEA	Diisopropylethylamine
DMAP	4-Dimethylaminopyridine
DMPI	Dess-Martin Periodinane
EI	Electron impact ionization
FRET	Fluorescence resonance energy transfer
GC	Gas chromatography
H, H COSY	Hydrogen correlation NMR spectroscopy
HIV1	Human immunodeficiency virus 1
HPLC	High pressure liquid chromatography
HRMS	High-resolution mass spectrometry
KAPA	Potassium aminopropylamide
LAH	Lithium aluminum hydride
LDA	lithium diisopropylamide

MAINS	A maleimide fluorescence technique
<i>m</i> -CPBA	<i>meta</i> -Chloroperoxybenzoic acid
MDR	Multidrug resistance
MOM	Methoxymethyl
NaHMDS	Sodium hexamethyldisilylamide
NBD	Nucleotide binding domain
NOE	Nuclear Overhauser Effect
NOESY	A 2D NOE related experiment
P-gp	Phospho-glycoprotein
PKC	Protein kinase C
PPTS	Pyridinium <i>para</i> -toluene sulfonate
RCM	Ring closing metathesis
Red-Al	Sodium <i>bis</i> (2-methoxyethoxy)aluminum hydride
SDS	Sodium dodecylsulfate
SEM	Trimethylsilylethylmethoxy
SXR	Substrate xenobiotic receptor
TBAF	Tetrabutylammonium fluoride hydrate
TBDPS	<i>tert</i> -Butyldiphenylsilyl
TBS	<i>tert</i> -Butyldimethylsilyl
TBSOTf	<i>tert</i> -Butyldimethylsilyl triflate
TES	Triethylsilyl
TFA	Trifluoroacetic acid
TFAA	Trifluoroacetic anhydride

TfOH	Trifluoromethanesulfonic acid
THF	Tetrahydrofuran
THP	Tetrahydropyran
TIPS	Triisopropylsilyl
TLC	Thin layer chromatography
TMD	Transmembrane domain
TMS	Trimethylsilyl
TMSOTf	Trimethylsilyl triflate

PREFACE

I would like to thank my research advisor, Dr. Paul E. Floreancig. He has been an exceptional advisor and a devoted mentor. He has allowed me to develop my own ideas and provided me the freedom to take on new responsibilities. I am grateful for his guidance, patience, and support over the past years. Working with Paul has been a truly rewarding experience. Thus far, the best decision I have made in my career has been my choice of advisor.

I would also like to thank Dr. Scott Nelson for serving as my proposal advisor. Thanks to Dr. Christian Schafmeister for his advice and participation on a number of my committees during the past five years. Also, thank you to Dr. Jack Yalowich for his advice and willingness to serve on this committee.

I would like to further express my gratitude to the past and present Floreancig group members especially, Dr. Satish Kumar, Dr. Danielle Aubele, Jason Rech, John Seiders, and Lijun Wang. They have all provided me an exceptional work environment along with their continued friendship. I would like to thank Dr. Fu-Tyan Lin for his help and advice over the past years.

I would also like to thank my entire family, especially my father, for inspiring me to become a chemist and for teaching me the value of hard work long before graduate school. Without his help, this achievement would have not been possible. I would like to thank all of the other important people in my family: Adele, George Jr., Caroline, Kevin, Allison, and Greg. I would also like to thank my new family, Peggy, Mike, and Eric, for their help and support. My family and friends have each helped to give me the things in life that I value the most, including my education.

Finally, I would most especially like to thank my wife, Keri. The past two years have been the ultimate test of her devotion and support. My wife has been a kind, understanding, and patient friend throughout this difficult experience. I would not be the person I am today without her support, undying patience, and love. I am truly lucky to have her by my side.

1. Multidrug Resistance

1.1. Introduction to Multidrug Resistance

The efficacy of any drug is largely dependant upon the drug's active lifetime in the human body, as well as the ability of the drug to reach its intended target. One of the greatest obstacles in the clinical treatment of cancer is due to the malignant cells' ability to rapidly develop a resistance to a multitude of structurally diverse therapeutic agents.¹ This phenomenon, by which a cell can withstand or resist a typically lethal dose of more than one type of drug, is known as multidrug resistance (MDR).¹⁻⁴

Only a small amount is known about what causes cells to become resistant. Presently, multidrug resistance has been identified in cells ranging from simple bacteria to human cancers and poses a major health concern.^{4,5} Although there is still very little known about the recognition process utilized by multidrug resistant cells, research has identified four principle mechanisms that most commonly give rise to MDR:³

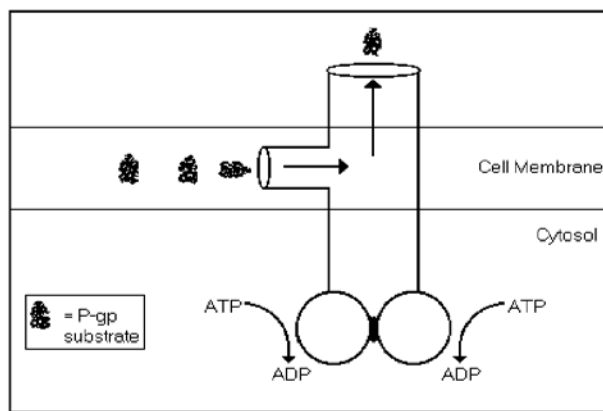
1. Deactivation or modification of drugs by enzymes produced in the target cell.
2. Post-translational modifications and/or mutations that alter the target site.
3. Decreased permeability of the cell wall and outer membrane in bacteria.
4. Active removal by membrane bound multidrug efflux transporters.

Of these four general modes by which cells become resistant, active transport by plasma membrane associated proteins has by far received the most attention.³ Currently, it is believed

that resistance in multiple types of human cancers is largely due to the overexpression of one such transporter known as Phospho-glycoprotein (P-gp).¹⁻²

1.2. The Role of Phospho-glycoprotein in MDR

P-gp is a membrane bound cellular pump which functions to prevent the accumulation of certain hydrophobic molecules within a cell (Figure 1). Normally, P-gp is highly expressed in



Schematic Diagram of P-gp Activity

Figure 1 Phospho-glycoprotein

the cells lining the stomach and the intestines where it functions to inhibit the absorption of drugs and other toxic agents.⁶ It is also found in the endothelial cells of the blood brain barrier, where it plays a key role in preventing certain compounds from being absorbed into the brain through the blood supply.⁷ P-gp, therefore, has an important role in the body's ability to both metabolize and excrete toxic substances.^{8,9}

P-gp becomes problematic when cancer cells overexpress this protein, which then leads to multidrug resistance. Certain types of cancer cells have acquired the ability to use P-gp as a defense mechanism against cytotoxic chemotherapeutic agents.¹⁻² Normally, a non-P-gp expressing cancer cell would die when exposed to a toxic drug. Cells that can overexpress P-gp

prevent the uptake of certain drugs, making the cancer cells immune towards the effects of cytotoxic drugs used in conventional chemotherapy. The overexpression of P-gp by cancer cells is thought to be chiefly due to the exposure of cancerous cells to toxic chemotherapeutic agents. In fact, P-gp induced MDR can be triggered by only a single exposure of the cancer cells to a toxic species.¹⁻² Once a cancer cell has overexpressed P-gp it is not only resistant to the initial toxic species, but can become resistant to a variety of structurally unrelated drugs.² The cancer can then become unresponsive to chemotherapy, leaving few remaining options for treatment.

1.3. Disease Associated with P-gp

P-gp overexpression is the main cause of MDR in human cancer cells.^{1-2,10} To date, it is estimated that over 90% of all research efforts aimed at understanding MDR have focused on the role of active drug efflux pumps like P-gp.¹¹ Research has established that P-gp is encoded for by the *mdr1* gene¹² and drugs are not the only known cause of P-gp overexpression. Many other types of stressors including physical stress, such as X-ray or UV light irradiation, as well as heat shock, can cause the *mdr1* gene to express P-gp.¹³

There is little doubt that P-gp represents a major hurdle for the effectiveness of new chemotherapeutic regimes. It has been estimated, based on examining several hundred different types of human cancers, that nearly 50% will overexpress the *mdr1* gene at some time during drug therapy.¹⁴ Current research has discovered that P-gp is responsible for drug resistance in other diseases, such as parasitic disease¹³ and AIDS.^{13,15} In order to develop effective new drugs to combat disease, we need to improve our understanding of how the defense mechanisms associated with MDR operate. Using this knowledge, we can design drugs that do not induce MDR.

1.4. Function of P-gp

P-gp is a member of the large ATP binding cassette (ABC) superfamily of membrane transporters.^{1-2, 4} The members of the ABC superfamily play a major role in the transport of drugs, natural products, and peptides across the membranes of many different cell types. They differ from other transport proteins in their ability to couple ATP hydrolysis with drug transport. Many transport proteins, even some in the ABC superfamily, are substrate specific. However, P-gp has the ability to recognize and transport a wide variety of substrates.^{1-2, 4}

ATP binding and hydrolysis are essential for the proper functioning of P-gp.^{5, 16-17} In fact, ATP hydrolysis occurs in P-gp even in the absence of a foreign drug or substrate.⁵ One theory is that this basal activity can be attributed to the transport of native lipid molecules.¹⁸ However, ATP hydrolysis is further stimulated by the presence of a P-gp substrate.^{5, 16-17} What is still unclear at the molecular level is how the energy from ATP hydrolysis is coupled with drug transport.

Several models¹⁰ have been proposed to account for the observation that drug binding increases ATP hydrolysis activity. The most commonly accepted theory is known as the alternating catalytic site model (Figure 2).¹⁸ In this model, two drug binding sites act in a cooperative fashion to expel substrates. When a substrate is bound at one site, ATP binding at the other site triggers a conformational change. This leads to hydrolysis of ATP to ADP at the drug bound site. Relaxation of the drug bound site and release of ADP then stimulates dissociation of the drug to the outside of the cell wall. The key aspects of this model, which are supported by

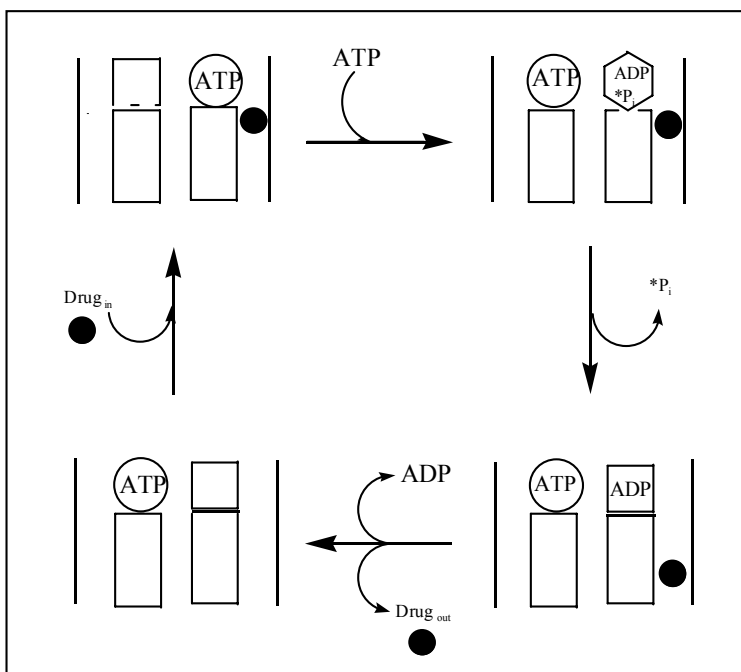


Figure 2 Alternating catalytic site model

experimental results, include: the observation that both nucleotide binding sites are required for active drug transport,¹⁶⁻¹⁷ presentation of the drug seems to occur inside the lipid bilayer,¹⁷ and that drug binding produces a conformational change near the nucleotide binding domain.^{5, 16-18}

1.5. Recognition of Substrates by P-gp

Given that such a large number of P-gp substrates have been reported to date, what remains to be discovered is how so many structurally dissimilar classes of molecules can all interact with a single drug transporter protein. One theory is that there are multiple specific binding sites within the drug binding region, allowing for dissimilar molecule to bind at different locations on the same protein.¹⁷ A second theory speculates the possibility for the existence of a single, conformationally flexible, binding site.^{13, 17, 19} Such a site presumably would have the ability to recognize substrates through less specific interactions. Based upon current evidence,

including X-ray structures of similar proteins, either possibility is valid.²⁰ Ideally, a high-resolution image of P-gp with a bound substrate would be useful in determining how substrates interact with P-gp. Once better techniques to reconstitute and image membrane-associated proteins are found, this type of study might be possible.

Clearly, determining the factors that affect substrate specificity is crucial to rational drug design for inhibiting or modulating P-gp activity. Multiple researchers have attempted to generalize the similarities between various P-gp substrates and inhibitors.^{2, 13, 19-23} One of the first studies suggested that the minimal structural features were a basic nitrogen and two planar aromatic domains.²¹ After examining a broader range of P-gp substrates, it was later realized that molecules lacking a basic nitrogen could also interact with P-gp.²²⁻²³ In fact, one of the only common features observed in these early studies was the relatively hydrophobic nature of P-gp substrates. The Seelig research group has suggested that a key aspect of substrate recognition may be due to the existence of multiple hydrogen bond donating residues, as well as aromatic residues present in the postulated drug interaction sites.^{13,19} Hydrogen bonding and π - π stacking may be very important for drug efflux by P-gp. This would account for the observation that in addition to being hydrophobic, most P-gp substrates contain both aromatic and hydrogen bond accepting groups.

Seelig recently reported that even some hydrophilic substrates could function as weak P-gp substrates.^{13,19} This work suggests that the minimal requirement for substrate recognition is dependant upon having two or three electron donor groups arranged in a specific spatial orientation. Unlike previous reports, Seelig's present work^{13,19} shows that there are predictable trends for substrates that have a higher propensity to trigger P-gp overexpression. Seelig has also examined molecules which are known to reverse or inhibit MDR in certain cancer cells.¹³ The

only drawback to Seelig's approach is that the exact mechanisms for MDR reversal are not known for many of the compounds utilized in her study. Therefore, it cannot be assumed that they all interact at the same binding site or even with P-gp at all.

1.6. Structure of P-gp

P-gp is known to be a 170 kDa membrane bound protein comprised of 1280 amino acid residues.²⁴ Although there is currently no high-resolution structure of P-gp, a low-resolution (2.5 nm) electron microscopy image²⁵ has provided some insight into the three dimensional architecture of P-gp (Figure 3). From this image, it can be estimated that P-gp is approximately 10 nm in diameter and has a large central pore measuring about 5 nm across. Upon examining

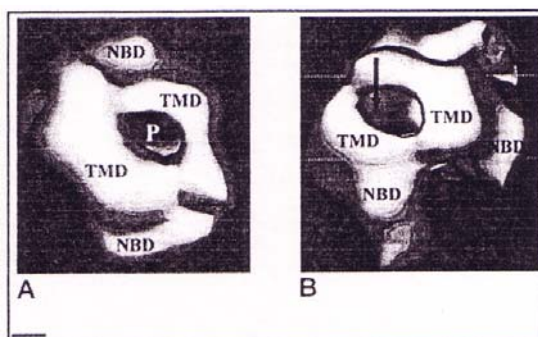


Figure 3 Low-resolution image of P-gp

Reprinted with permission from Rosenberg, M. F. *et. al. J. Biol. Chem.* **1997**, 272, 10685.
Copyright 1997 American Society for Biochemistry and Molecular Biology

both the top (A) and side on (B) view, it can be seen that this pore connects the inner phospholipid bilayer to the outside of the cell wall. Additionally, two 3 nm in diameter lobes can also be seen exposed at the cytoplasmic face of the membrane. These lobes are postulated to be

the nucleotide binding domains (NBD's) of P-gp where nucleotides bind and ATP hydrolysis occurs.²⁵

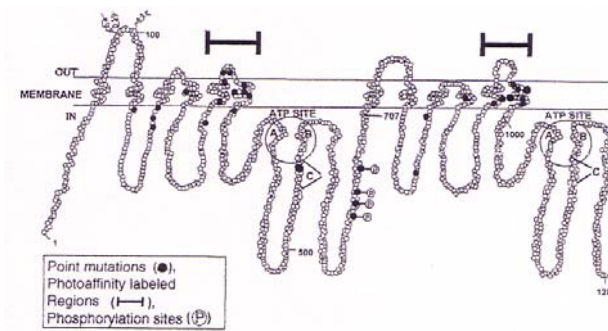


Figure 4 Topology of P-gp

Reprinted with permission from Hrycyna, C.A. *Semin. Cell Dev. Biol.* **2001**, *12*, 247.
Copyright 2001 Elsevier

Most of what is known about P-gp comes from site directed fluorescence^{5, 16-17} and site directed mutagenesis²⁶⁻²⁷ experiments. The most common topological model (Figure 4) depicts P-gp as a dimeric protein consisting of twelve transmembrane domains with two nucleotide binding sites localized in the cytosol.^{1-2, 28} Each half consists of six transmembrane domains connected by a flexible linker region. At least two confirmed drug binding sites have been identified near the transmembrane segments at the phospholipid bilayer.¹⁶⁻¹⁷ Although the number and nature of drug binding sites is poorly defined, site directed mutagenesis and photoaffinity labeling studies have found that the transmembrane domains (TMD's) 5, 6, 11, and 12 make up at least part of the drug binding domains.^{16-17, 26-27}

Biochemical analysis has demonstrated that expression of either half of P-gp alone does not provide a functional multidrug transporting protein.²⁸ An additional experiment verified the protein could not function in the absence of the flexible linker region.³ All of this data seems to

reinforce the idea of a concerted type mechanism for drug transport, rather than each half operating independently.

1.7. Inhibition of P-gp

To date, many small molecule inhibitors of P-gp have been reported (Figure 5).²⁹ However, due to the diversity of these molecules, it has been difficult to determine which structural elements are required for recognition by P-gp or inhibition of P-gp. Very little is known about how P-gp inhibitors function at the molecular level. Like other substrates, inhibitors seem to directly interact with P-gp and compete for binding sites.¹⁷ What distinguishes inhibitors from other substrates is not fully understood. From examining the complex structures

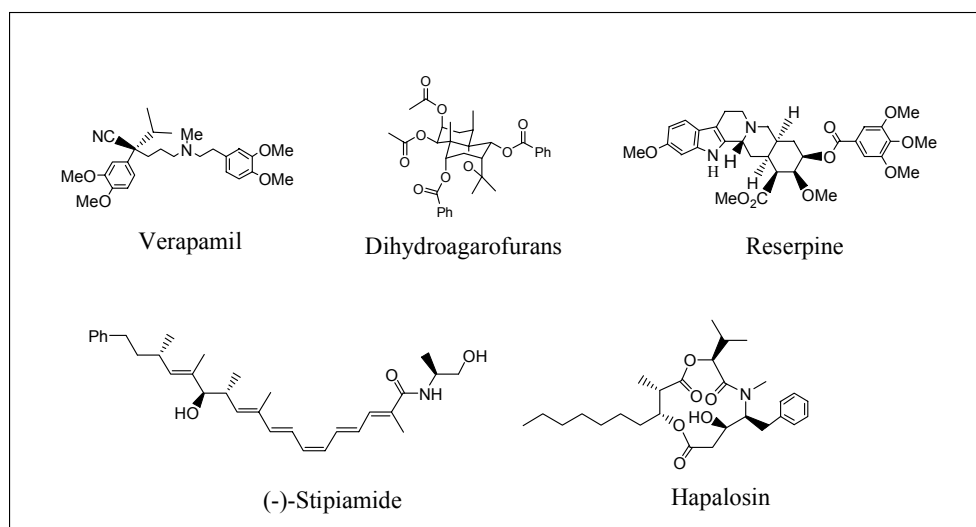


Figure 5 Representative MDR reversing compounds

in Figure 5, it becomes apparent why making any generalizations has proven difficult. We believe that a series of structurally similar analogues would be advantageous. This would enable us to compare and contrast structure versus activity in a meaningful way. One particular family

of molecules, collectively known as dihydroagarofurans, has been recognized to possess multiple features that might facilitate such a study. Recently, it was reported that multiple members of this family (Figure 6), many isolated from the root of *Celastrus orbiculatus*, were more potent than a leading clinical agent in reversing P-gp mediated MDR.³⁰ Lee and coworkers have shown that celafolin A-1 (IC₅₀ 12.4 μM) was more potent than verapamil (IC₅₀ 39.2 μM) for reversing multidrug resistance in the KBV-1 cell line (human nasopharynx carcinoma) to vinblastine. Additionally, celafolin A-1 does not possess any intrinsic cytotoxicity unlike verapamil which is cardiotoxic.³¹ Other members of this family have IC₅₀ values in the 7-70 μM

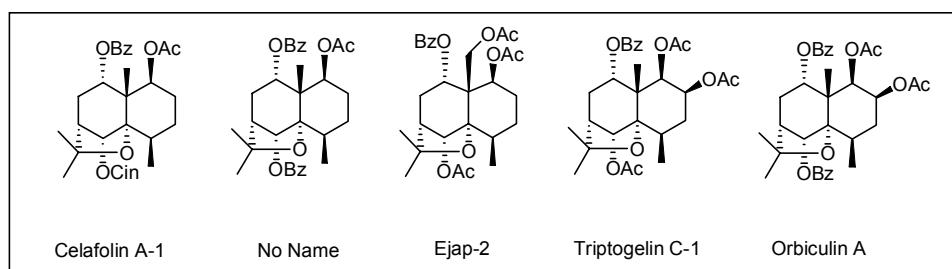


Figure 6 Dihydroagarofuran MDR reversing agents

range and can also reverse resistance to adriamycin and paclitaxel in the KBV-1 cell line and the MCF7/ADR cell line (human breast cancer).³¹

The most attractive aspect of this family of natural products is that they all possess a rigid *trans*-decalin core (Figure 5). This conformational rigidity imparts a well-defined spatial relationship of substituents on the ring system, making these natural products an ideal scaffold for studying the structural aspects of P-gp inhibition. Once a synthetic route for preparing the dihydroagarofuran ring system is developed analogs will be prepared. These analogs will be prepared to test the importance of lipophilicity, hydrogen bond accepting groups, and aromatic

ring stacking interactions. These three elements are reported to be crucial features required for recognition by and binding with P-gp.^{13,19} Carefully designed analogs will be used to study which structural elements and chemical features are required for P-gp inhibition for this family of natural products.

Once these analogs are prepared, their biological activity can be evaluated using a variety of techniques. The MAINS technique, a fluorescence quenching technique developed by Sharom,^{5,16} can be used to determine if these natural products are substrates for Pgp or if they interact at another location. This technique utilizes P-gp tagged with a maleimide fluorophore in the nucleotide binding domain (NBD). When substrates bind for transport a conformational change occurs in the NBD region producing fluorescence quenching. Since this technique is concentration dependent, it can be used to estimate equilibrium constants (K_a) for different substrates.

An alternative to the MAINS labeling approach is available for substrates that fluoresce at the same wavelength as the maleimide fluorophore. This FRET (fluorescence resonance energy transfer) method (Figure 7) utilizes tryptophan residues present in the drug binding regions of P-gp.¹⁷ The principle behind the FRET technique is that if a P-gp substrate can π -stack with a tryptophan residue in the drug binding region, fluorescence quenching will be detectable.

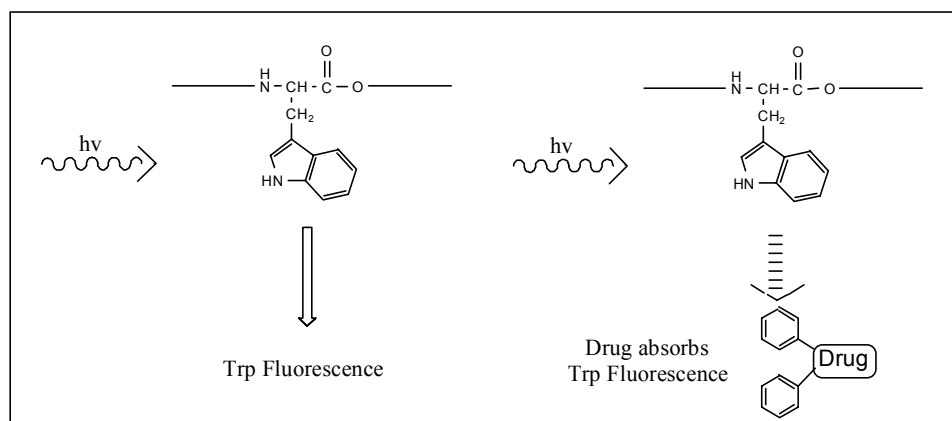


Figure 7 The FRET technique

Dihydroagarofuran natural products should also be investigated to determine if they are true inhibitors of P-gp or just competitive substrates. This can be explored by a simple assay that monitors ATP hydrolysis.³² This assay quantifies ATP hydrolysis by a fluorescence technique that detects the inorganic phosphate byproducts of hydrolysis. Determination of a substrate as an inhibitor or competitive substrate is quite straightforward. Suppression of ATP hydrolysis indicates the substrate is an inhibitor of P-gp while an increase in ATP hydrolysis indicates a competitive substrate. These simple tests can help reveal how dihydroagarofuran natural products are recognized by P-gp. They can also aid in our understanding of how dihydroagarofurans can reverse multidrug resistance.

1.8. Cytochrome P450 and P-gp

In principle, the idea of inhibiting P-gp to enhance the effectiveness of chemotherapeutic agents seems like a straightforward approach. A resistant cancer cell is exposed to a P-gp inhibitor and loses its drug resistance. A cytotoxic agent is then administered and the cancer cell

is killed. This overly simplified model fails to take into account what affect P-gp inhibition could have on other systems inside the body.

Clinically, the benefits of P-gp inhibition have yet to be established and are often complicated due to undesirable side effects produced by P-gp inhibiting agents. One important study demonstrated that some P-gp inhibitors could also inhibit essential drug metabolizing enzymes such as cytochrome P450 3A (CYP3A).³³ Since CYP3A is responsible for the metabolic degradation of more than 50% of all known drugs,⁸⁻⁹ this type of interaction could cause normally safe doses of drugs to become toxic. Fortunately, this study established no strong correlation between good P-gp inhibitors and good CYP3A inhibitors.

To further complicate this situation, research has established that certain P-gp substrates can induce, rather than inhibit, both P-gp and CYP3A expression.⁸ Recently, it was demonstrated that drugs which activate a transcription factor known as the substrate xenobiotic receptor (SXR)

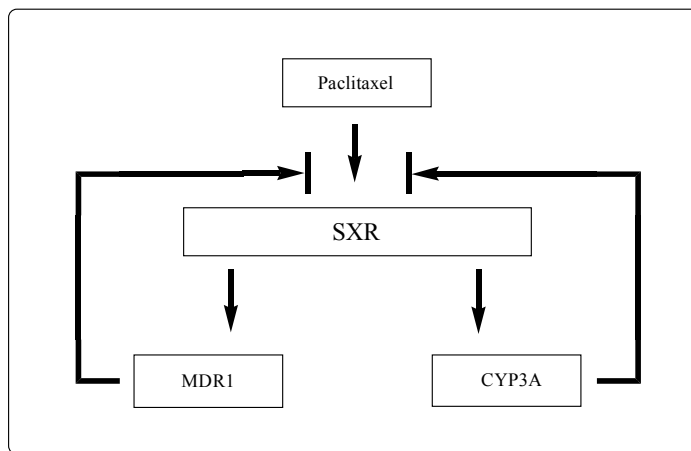


Figure 8 Feed-forward / feed-back mechanism for SXR

can trigger their own metabolism and efflux. For example paclitaxel, a well documented P-gp substrate, induces the expression of P-gp and CYP3A through binding to and activating SXR

(Figure 8).⁹ These clearance pathways lower the concentration of paclitaxel and reduce activation of SXR in a feedback pathway. However, docetaxel, a structural analog of paclitaxel, does not activate SXR and does not induce P-gp or CYP3A expression.⁸⁻⁹ This study suggests that through knowledge of this pathway and manipulation of drug structure it is possible to design drugs invisible to SXR that may then prevent P-gp expression.

One final concern that needs to be addressed is whether P-gp inhibition can be a clinically viable approach to preventing MDR. Since P-gp is also thought to play a crucial role in other parts of the body, inhibition may adversely affect other areas of the body. To test the importance of P-gp in a living system, genetically modified mice, known as knockout mice, were engineered to lack P-gp.³⁴ The results of these knockout mice studies clearly demonstrated that mice were able to survive in the absence of P-gp.

There are certainly many different ways to address the problem of multidrug resistance. Ultimately, the goal of all these approaches is to enable the design of agents to selectively target and inhibit P-gp. Despite advances on many different fronts, it has yet to be determined how P-gp inhibition occurs at the molecular level.

2. Dihydroagarofuran Natural Products

Dihydroagarofurans are terpene-based metabolites of the *celastraceae* family of plants.³⁵ Members of this sesquiterpenoid family all contain a characteristic tricyclic *trans*-decalin skeleton with varying degrees of oxygenation (Figure 9). The dihydroagarofuran family members are exclusively obtained from their natural sources as ester derivatives (Table 1).^{30,35} Over 200 members of this family have been characterized based on over 40 different oxygenation patterns. Prior to the early 1980's, the various members of the dihydroagarofuran family of molecules were not known to possess any novel chemical or biological activity.³⁶

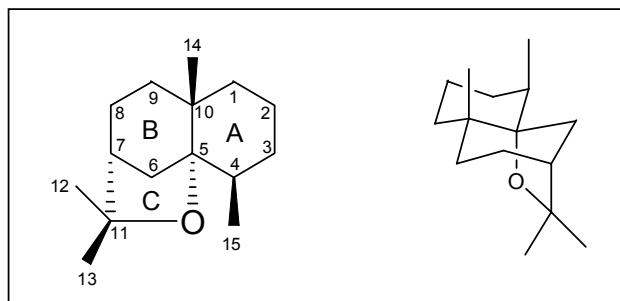


Figure 9 Dihydroagarofuran numbering

Then, in the mid to late 1980's, researchers began to discover these natural products contain a rich variety of bioactivity including anticancer, anti-bacterial, immunosuppressive, stimulant, and anti-HIV activity.^{35,37} In 1998, Lee and coworkers reported that several dihydroagarofuran natural products were able to reverse MDR in the vinblastine resistant KB-V1 cell line that over-expresses P-gp.³⁰ They also found that these natural products exhibited virtually no *in vivo*

cytotoxicity. The following year, the same group reported six new dihydroagarofuran MDR modulators.³¹ The IC₅₀ and MDR reversing properties of **1-12** are summarized in Table 1.

Compounds	IC ₅₀ (μM) ^a			
	KB-3-1	KB-V1	KB-V1 (+VLB)	EF ^b
1	268.0 ± 26.7	246.0 ± 32.3	19.6 ± 0.7	12.5
2	8.6 ± 0.1	9.6 ± 0.3	1.0 ± 0.2	9.6
3	16.8 ± 1.4	17.8 ± 0.9	1.2 ± 0.2	14.8
4	28.3 ± 2.3	33.1 ± 1.9	0.5 ± 0.2	66.2
5	32.4 ± 6.3	39.3 ± 3.2	1.1 ± 0.1	35.7
6	26.4 ± 1.5	28.6 ± 2.2	4.8 ± 0.1	5.9
7	41.3 ± 2.0	34.8 ± 1.2	0.4 ± 0.0	87.0
8	85.3 ± 6.2	79.4 ± 8.1	1.0 ± 0.1	79.4
9	27.3 ± 2.5	28.6 ± 2.2	0.5 ± 0.0	57.2
10	10.5 ± 0.4	12.3 ± 0.3	1.9 ± 0.0	6.4
11	12.4 ± 0.4	12.4 ± 0.2	0.7 ± 0.0	17.7
12	31.6 ± 0.8	32.0 ± 0.6	0.4 ± 0.0	80.0
VRP	45.2 ± 0.3	39.2 ± 0.5	1.6 ± 0.0	24.5

Table 1 MDR reversing dihydroagarofurans

Reprinted with permission from Lee, J. J. *et. al. J. Nat. Prod.* **1999**, *62*, 697.
Copyright 1999 American Chemical Society

From examination of Table 1, it can be seen that several trends appear. The tri-ester compounds **1-3**, **10**, and **11** all show weaker activity than the tetra-ester compounds, except **6**, which contains a C-2 benzoate. The tetra-esters **4**, **5**, **7**, **8**, and **12**, all having a C-2 acetate group, are exceptional in their ability to reverse MDR compared to other members of this family. Many have IC₅₀ values lower than verapamil and half of the species **1-12** were more effective.

Another recent study by Ravelo and coworkers has shown that dihydroagarofurans can reverse MDR in a P-gp-like transporter present in multidrug resistant *Leishmania tropica*, a protozoan parasite.³⁸ The authors found that the *Leishmania* P-gp expressing cells, resistant to

verapamil, responded to dihydroagarofuran inhibitors. In this work, the authors screened thirty dihydroagarofuran derivatives by *in vivo* assays and QSAR modeling. Their study concluded that electrostatic interactions, hydrogen-bonding donor and acceptor capability, and lipophilicity were essential requirements for good inhibitors. The authors also suggest that the C-2 and C-6 esters are crucial hydrogen-bonding elements, similar to results found with human P-gp by Lee and coworkers.³⁰⁻³¹

2.1. A Model for the Structural Basis of MDR Modulation

The purpose of this project is to develop a structural basis for P-gp inhibition. It is anticipated that this project will allow for the discovery of improved P-gp inhibitors. In addition to the discovery of new P-gp inhibitors, the results of this study will also aid in the design of new drugs that are not recognized by P-gp. In order to study the elements required for P-gp inhibition by dihydroagarofuran natural products, various analogs of celafolin A-1 (**11**) and orbiculin A

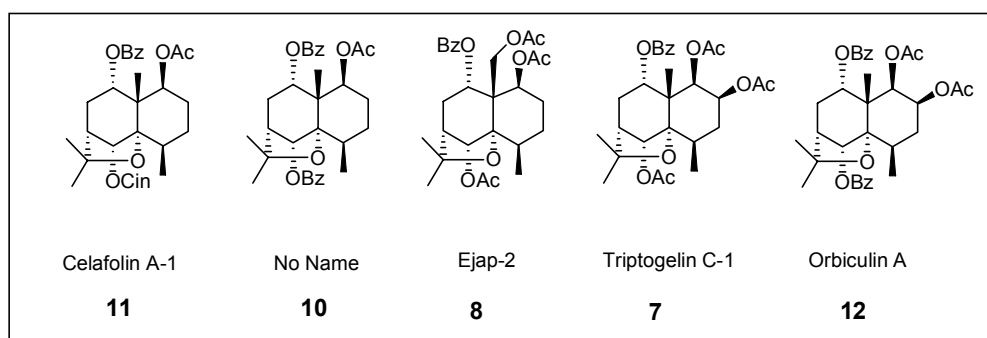


Figure 10 Representative dihydroagarofuran natural products

(**12**) will be prepared and evaluated for both P-gp binding and inhibition. Celafolin A-1 and orbiculin A were chosen as initial targets because they represent the simplest members of the

dihydroagarofuran family that have been shown to reverse MDR (Table 1).³⁰⁻³¹ Accordingly, the first goal of this project will be to develop a versatile and enantioselective route to orbiculins A and celafolin A-1.

2.2. Advantages of Using Dihydroagarofurans

There are multiple attractive features associated with using the dihydroagarofuran ring system for studying P-gp inhibition. For example, the syntheses of celafolin A-1 (**11**) and orbiculins A (**12**) can begin from (*R*)-(-)-carvone, an inexpensive chiral terpene available in high

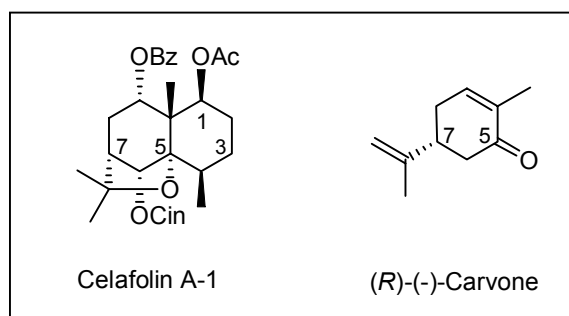


Figure 11 Comparison of carvone and the dihydroagarofuran skeleton

enantiomeric excess. The core skeletal features of celafolin A-1 (**11**) (Figure 11) consist of fifteen carbon atoms and seven chiral centers. Carvone already contains ten of the required carbons and one of the chiral centers.

The rigid tricyclic core of the dihydroagarofuran ring system represents an ideal system for studying P-gp inhibition. Unlike other inhibitors (Figure 12) such as verapamil³⁹ and stipiamide⁴⁰ whose solution structures are conformationally mobile, the rigid core of the dihydroagarofuran imparts a well-defined spatial relationship between the functional groups on

the tricyclic ring system. This rigidity will allow for a predictable solution conformation, making the data obtained from structure activity studies easier to interpret.

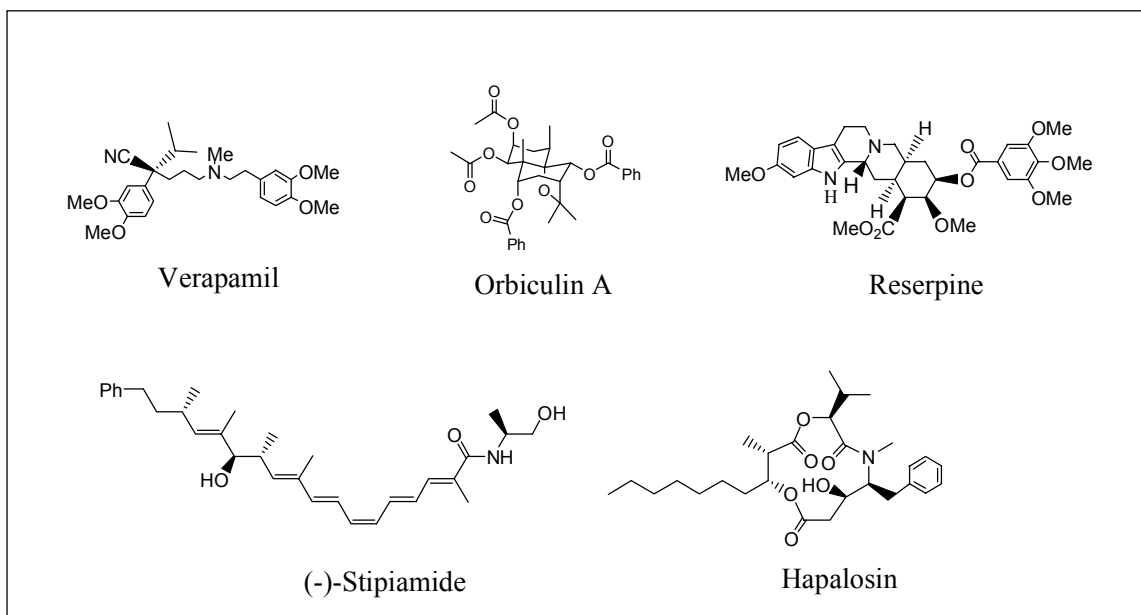


Figure 12 Structurally diverse MDR reversing agents

The syntheses of celafolin A-1 (**11**) and orbiculin A (**12**) should be relatively short, efficient, and capable of providing ample material for biological assays. The planned route should also be flexible enough to allow for the incorporation of new functional groups, this would facilitate the preparation of analogs with minimal synthetic changes. For example, an ideal synthetic scheme would allow for the multiple ester moieties present in Table 1 to be easily manipulated and selectively installed. This would provide access to other members of the dihydroagarofuran family of natural products.

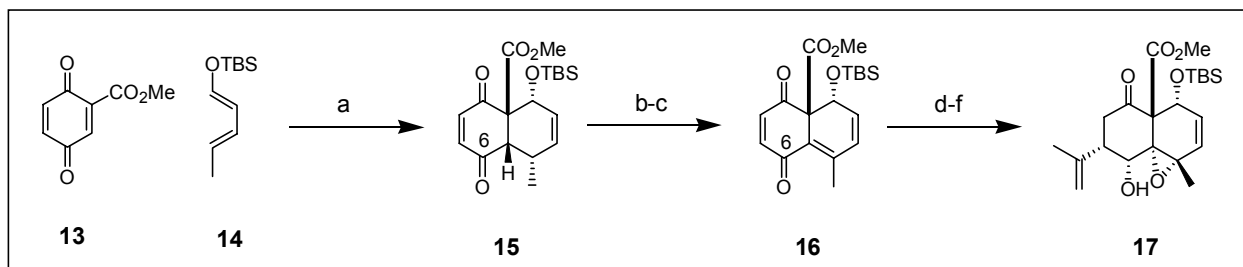
2.3. Previous Dihydroagarofuran Syntheses

A survey of the literature shows there are only a few racemic syntheses of dihydroagarofuran ring systems that have been published. The first reported synthesis of a dihydroagarofuran was published by Büchi and Barret in 1967.⁴¹ One year later Marshall⁴² and then Deslongchamps⁴³ published similar methods. In 1979, Büchi and Wüest reported the first stereocontrolled synthesis of a dihydroagarofuran.⁴⁴ Although carvone seems to be an obvious starting material, it was not utilized until 1986 when Huffmann introduced the first synthesis of a dihydroagarofuran starting from (*R*)-carvone.³⁶ It should be noted that even though Huffman used enantiomerically pure carvone, the synthesis was racemic due to an oxidation which transformed carvone into a C₂ symmetrical molecule.

Li and coworker have only recently reported the first asymmetric total synthesis of a dihydroagarofuran sesquiterpenoid in 2001.³⁷ Li and coworkers' approach utilized a modification of Huffmann's method³⁶ to synthesize (-)-isocelorbicol. To date, however, no one has prepared an enantiopure dihydroagarofuran capable of reversing P-gp induced multidrug resistance. Two particularly noteworthy syntheses, White and coworkers' synthesis of (±)-euonyminol⁴⁵ along with Li and coworkers' enantioselective synthesis of (-)-isocelorbicol³⁷ are briefly outlined below.

White and coworkers have demonstrated that the dihydroagarofuran ring system can be constructed in a racemic fashion by utilizing a Diels-Alder reaction (Figures 13 and 14). In order to construct the decalin core of (±)-euonyminol, White and coworkers began their synthesis with the readily available dienophile (**13**) and diene (**14**). When the diene (**14**) and dienophile (**13**) were heated to reflux in toluene a single cycloadduct was formed. The stereochemistry of the fused ring system was established by examination of the C-4 to C-5 coupling constant in the ¹H NMR spectrum, and was determined to be the desired *endo* product (**15**). The cycloadduct (**15**) was then subjected to an allylic bromination, followed by treatment with triethylamine to afford

HBr elimination providing the desired diene (**16**). The stereocenter at C-6 was selectively installed by a Luche reduction to give the required enone (**16**). A directed *m*-CPBA epoxidation followed by a γ -alkoxy substituent directed Michael addition of isopropenyl-magnesium bromide generated the desired product (**17**) in good yield.

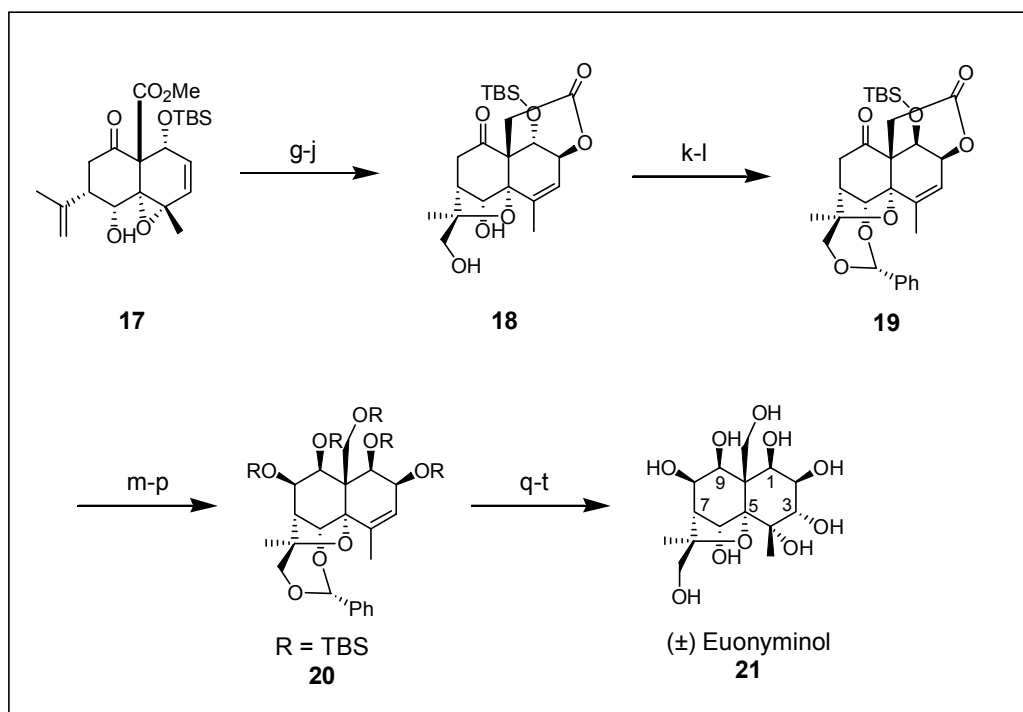


Reagents and conditions: a) benzene, heat, 88%. b) NBS, (PhCO)₂O₂, CCl₄. c) Et₃N, 95% over 2-steps. d) NaBH₄, CeCl₃·7H₂O, MeOH, 90%. e) *m*-CPBA, NaH₂PO₄, CH₂Cl₂, 88%. f) i. LDA, 15-crown-5, ii. isopropenylmagnesium bromide, THF, -78 °C to 25 °C, 63%.

Figure 13 White and coworkers (\pm)-euonyminol synthesis

The C-7 isopropenyl group was then selectively epoxidized using the Sharpless asymmetric epoxidation protocol, which set up an epoxide opening cascade cyclization (Figure 14). Treatment of the epoxide derivative of the cyclic ketone (**17**) with trifluoroacetic acid resulted in an S_N2' epoxide opening to produce a trifluoroacetate ester at C-2 and the desired tetrahydrofuran ring system. Mild hydrolysis conditions were used to selectively cleave the C-2 trifluoroacetate ester in the presence of a methyl ester. Treatment of this newly formed allylic alcohol with imidazole cleanly produced the C-2 to C-5 lactone. The C-1 axial silyl ether was converted to the required equatorial silyl ether by a retro aldol reaction and subsequent benzylidene acetal protection provided the desired product (**19**). The C-8 hydroxyl group was

stereoselectively incorporated by oxidation of the kinetic enolate of the C-10 ketone (**19**) using Davis' oxaziridine.



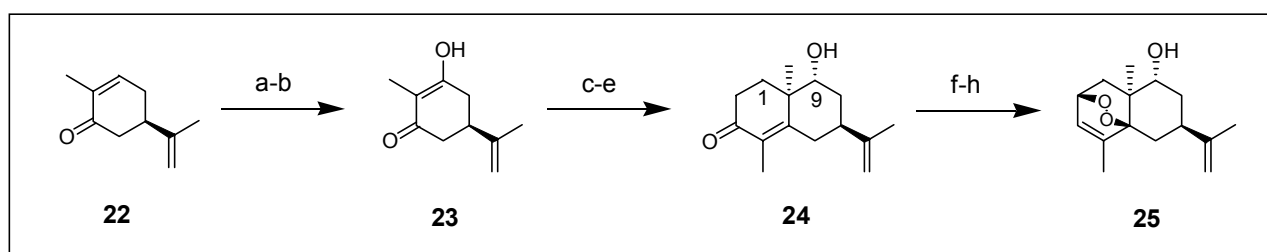
Reagents and conditions: g) *t*-BuOOH, VO(acac)₂, 2,6-lutidine, 55%. h) TFA, CHCl₃. i) pyridine, H₂O, THF. j) imidazole, CH₃CN, 76% over 3-steps. k) PhCH(OMe)₂, PPTS, toluene, heat, 83%. l) TBAF, THF, 96%. m) KHMDS, THF, then Davis' oxaziridine, 83%. n) AlMe₃, THF, 100%. o) LiAlH₄, THF, then 0.5 M HCl. p) TBSOTf, Et₃N, CH₂Cl₂. q) OsO₄, pyridine. r) HOAc, H₂O, heat. s) Ac₂O, pyridine, 30% over 5-steps. t) NaOMe, MeOH, then purification using amberlite IR 120 resin, 100%.

Figure 14 Completion of (±)-euonyminol

The newly formed hydroxy-ketone was then subjected to excess trimethylaluminum and undergoes a variant of the Lobry deBruyn-Alberda van Eckenstein transformation in which the C-8 ketone and C-9 alcohol groups are transposed. This rearrangement, which is believed to occur through an aluminum enediol species, gave the desired C-9 equatorial alcohol in

quantitative yields. A simple lithium aluminum hydride reduction, followed by global silyl protection produced the fully protected poly-hydroxyl derivative (**20**). The required oxidation states at C-3 and C-4 were introduced using a facially biased osmylation. The poly-silyl ether (**20**) was then subjected to global deprotection using acetic acid in water and then transformed into an octa-acetate species to facilitate purification. The octa-acetate derivative of (±)-euonyminol (**21**) was cleanly saponified using sodium methoxide to provide (±)-euonyminol in 20 steps with an overall yield of 3.5%.

Li and coworkers have only recently reported the first enantioselective route to a dihydroagarofuran (Figures 15 and 16). Their route to (-)-isocolorbicol (**27**) utilizes a modification of Huffmann's method³⁶ using (*R*)-(-)-carvone (**22**) as a starting material. A House epoxidation procedure was used to oxidize the enone of carvone. Exposure of this epoxy-ketone to sodium hydroxide provided the achiral di-ketone tautomer (**23**) of carvone. An asymmetric Robinson annulation, using ethyl vinyl ketone and a catalytic amount of D-(+)-phenylalanine, gave the desired bicyclic enone in 51% yield with an enantiomeric excess of only 54%.

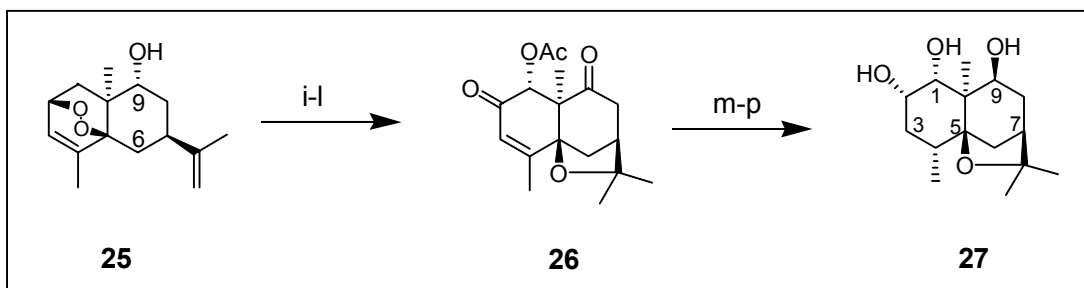


Reagents and conditions: a) 30% H₂O₂, KOH, MeOH, H₂O, 0 °C. b) 1M NaOH, H₂O, reflux, 25% over 2-steps. c) ethyl vinyl ketone, KOH, MeOH, reflux, 85%. d) D-(+)-phenylalanine, D-(+)-CSA, 70 °C, 6 days, 51%. e) NaBH₄, MeOH, 0 °C, 75%. f) TsNHNH₂, BF₃·Et₂O, 25 °C, 95%. g) *n*-BuLi, THF, -78 °C to 0 °C, 90%. h) O₃, P(OPh)₃, CH₂Cl₂, -78 °C to 0 °C, 81%.

Figure 15 Li and coworkers (-)-isocolorbicol synthesis

Following the Robinson annulation, the C-9 carbonyl group was selectively reduced with sodium borohydride to give the C-9 equatorial alcohol derivative (**24**). This intermediate was recrystallized twice, in an overall yield of 67%, from ether and hexane to increase the enantiomeric purity to greater than 98%. The C-3 to C-5 enone was converted to an α,β -unsaturated tosyl hydrazone and then treated with *n*-butyl lithium to generate a *cis*-diene. Treatment of this diene at $-78\text{ }^{\circ}\text{C}$ with ozone and triphenylphosphite, a recipe for generating singlet oxygen, produced the *endo*-cycloadduct (**25**) and also generated the *trans*-decalin ring fusion in one step.

When this cycloadduct (**25**) was exposed to potassium carbonate in tetrahydrofuran, the peroxide underwent a rearrangement to afford the enone precursor to (**26**). The C-1 acetate group



Reagents and conditions: i) K_2CO_3 , THF, $40\text{ }^{\circ}\text{C}$, 78%. j) $\text{Mn}(\text{OAc})_3$, benzene, reflux, 53%. k) TfOH, THF, $25\text{ }^{\circ}\text{C}$, 5 min., 95%. l) Dess-Martin periodinane, CH_2Cl_2 , $25\text{ }^{\circ}\text{C}$, 90%. m) LiAlH_4 , Et_2O , $0\text{ }^{\circ}\text{C}$, 62%. n) TBSOTf, Et_3N , CH_2Cl_2 , $25\text{ }^{\circ}\text{C}$, 68%. o) H_2 , 10% Pd-C, EtOH, $25\text{ }^{\circ}\text{C}$, 85%. p) TBAF, THF, H_2O , $25\text{ }^{\circ}\text{C}$, 47%.

Figure 16 Completion of (-)-isocolorbicol

was installed by using a regioselective acetoxylation with $\text{Mn}(\text{OAc})_3$. The C-5 β -hydroxyl group and the C-7 isopropenyl group then underwent a facile etherification in the presence of TfOH to afford the tetrahydrofuran C ring (**26**) and complete the tricyclic core of (-)-isocolorbicol (**27**).

The next transformation to address was the selective reduction of the C-9 and C-2 ketones to provide the required axial hydroxyl groups at these two positions. Instead of using a step-wise procedure, the authors found that both ketones could be simultaneously reduced using LiAlH₄. This reducing agent removed the C-1 acetate and provided the triol precursor to (-)-isocelorbicol (**27**) in 62% yield as a 3:1 mixture of epimers at C-2. The authors did not report any attempts to optimize this process. The last remaining step to complete (-)-isocelorbicol (**27**) was to selectively reduce the endocyclic C-3 / C-4 olefin. When the authors tried to directly convert the LiAlH₄ adduct to (-)-isocelorbicol (**27**) using H₂ and palladium on carbon, the reaction produced the incorrect β -methyl isomer (Figure 16). To circumvent this selectivity problem, the triol was converted to the tri-TBS ether derivative. Hydrogenation of this silyl ether species using H₂ and palladium on carbon gave the desired α -methyl stereocenter and a minor amount of the β -methyl epimer as a 10:1 mixture in 27% yield. Finally, global TBS ether deprotection gave (-)-isocelorbicol (**27**) in a total of 16 steps, 0.2% overall yield, from (*R*)-(-)-carvone. Although this route illustrates the first asymmetric synthesis of dihydroagarofuran, the overall yield is extremely low. Additionally, this sequence would not allow for the introduction of a C-6 ester, which has been shown to be a crucial moiety for P-gp inhibition.³⁰

While neither of these two syntheses are directly applicable to celafolin A-1 (**11**) or orbiculin A (**12**), they do establish precedent for multiple transformations on similar ring systems. In the chapters to follow, it will become apparent how our celafolin A-1 (**11**) and orbiculin A (**12**) syntheses have been designed to incorporate the particularly efficient transformations utilized by the Huffmann,³⁶ White,⁴⁵ and Li³⁷ groups.

3. Work Towards the Construction of the Dihydroagarofuran Ring System

One of the most important aspects of our synthetic plan was to design a synthesis that would allow for the simple preparation of analogs. During the course of these investigations, three distinct routes emerged as promising strategies. These routes will be presented in this chapter.

3.1. Orbiculin A as an Initial Target

When this project was initiated, orbiculin A (**12**) was chosen as our first target molecule. This dihydroagarofuran family member was selected since it possessed the most potent activity towards reversing P-gp MDR in a previous study (Table 1).³¹ Our retrosynthetic analysis for orbiculin A is highlighted in Figure 17. We decided to construct the tetrahydrofuran C ring and to establish the C-4 methyl stereocenter at the end of our synthesis. The C ring would be formed by an oxidative etherification protocol and the C-4 methyl group could be generated by a directed hydrogenation using the C-6 ester group. A directed epoxidation would be used to introduce the C-5 oxygen and establish the *trans*-decalin ring fusion. The subsequent opening of this epoxide would be brought about by a cleverly designed S_N2' epoxide opening reaction utilizing the C-1 acetate group. This acetoxy-assisted epoxide opening would also generate the desired C-2 acetate group in the same step. Alkylation of the C-5 alcohol with *para*-nitrobenzenesulfonyl chloride will induce a 2,3-sigmatropic rearrangement to create the allylic alcohol precursor for the C-4 to C-5 epoxide. The required bond connectivity for the *trans*-decalin ring will be constructed using an intramolecular addition of a (*Z*)-vinyl iodide into the

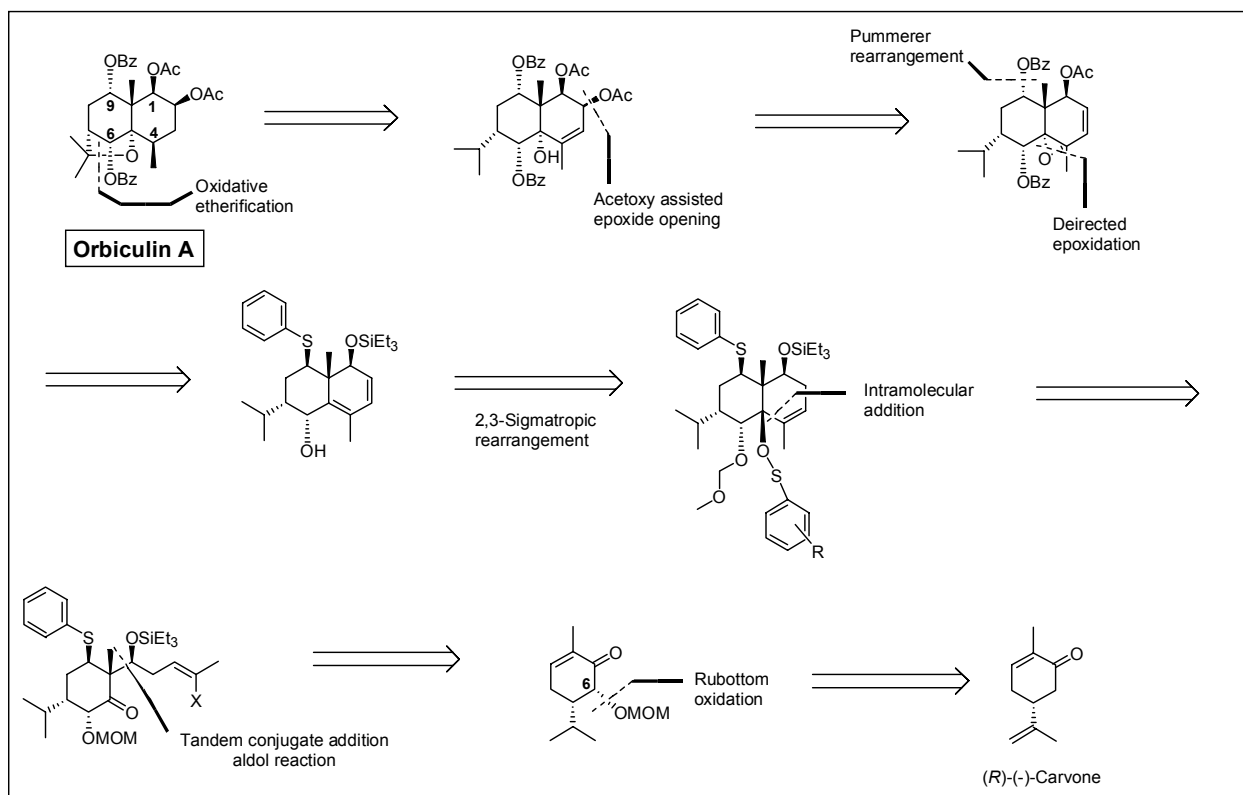


Figure 17 Retrosynthesis for orbiculin A

C-5 carbonyl group. We then planned to generate the C-1, C-9, and C-10 stereocenters and the C-1 to C-10 carbon-carbon bond in one step using a tandem conjugate addition-aldol reaction. Finally, the enone precursor to the aldol addition can be made from (*R*)-(-)-carvone in a three-step process using an enolate oxidation to install the C-6 oxygen, then methoxymethyl ether (MOM) protection, and Wilkinson's catalyst to selectively hydrogenate the C-7 isopropenyl group.

One of our initial synthetic approaches to orbiculin A (**12**) (Figure 18) began with addressing the problematic introduction of oxygen at C-6. At the time this work began, there was no literature precedent for an efficient method to prepare the required enone derivative (**31a**) of carvone. Early work had shown that oxidation of the kinetic enolate of carvone, using Davis'

oxaziridine (**28**), resulted in an inseparable mixture of the desired products (**31a** and **31b**) and oxaziridine byproducts. After chromatographic purification to separate the two diastereomeric products, analysis of the ^1H NMR revealed that two major impurities were present. These impurities were determined to be benzaldehyde and the di-phenyl sulfonimine byproduct from oxaziridine. The benzaldehyde formed is the result of slow sulfonimine hydrolysis during silica gel chromatography.

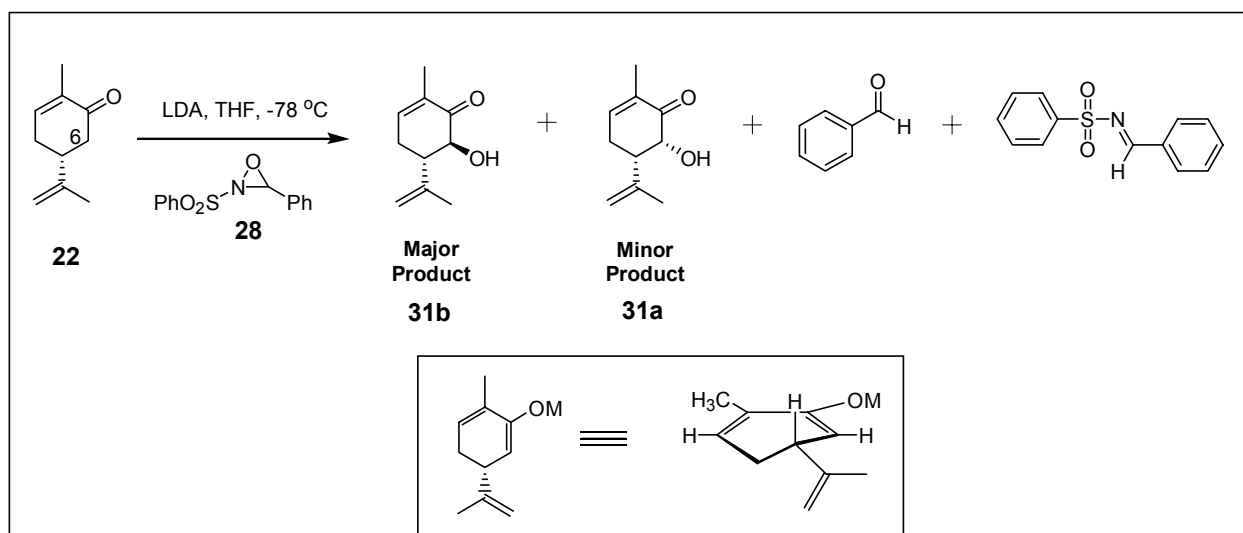
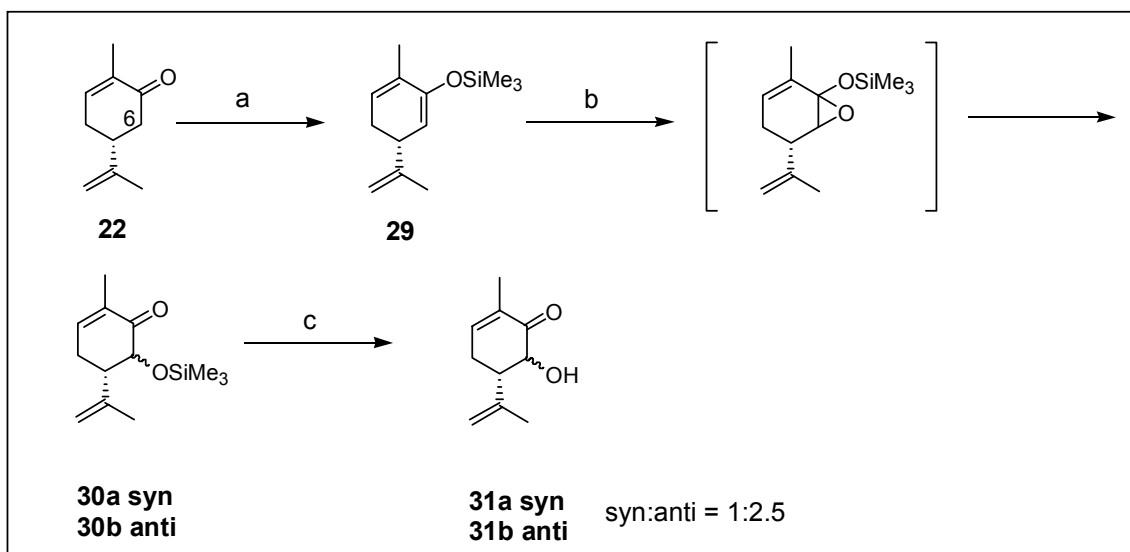


Figure 18 Oxidation of (*R*)-(-)-carvone using Davis' oxaziridine (**28**)

Additionally, we determined that the oxaziridine oxidation yielded predominantly the incorrect *trans*-stereoisomer at C-6 (**31b**). The preferential formation of the incorrect isomer (**31b**) can be rationalized by examining the geometry of the kinetic enolate of (*R*)-(-)-carvone (Figure 18). In the lowest energy conformation, the isopropenyl group will be in the pseudo-equatorial position. In this conformation, the isopropenyl group projects slightly downward, partially blocking the α -face of the enolate. When the oxaziridine reagent approaches the β -face

of the enolate this interaction is avoided and results in the formation of the undesired diastereomer (**31b**).

After a number of additional conditions were screened and we found that a Rubottom oxidation⁴⁶ gave superior results (Figure 19). Exposure of the trimethylsilyl (TMS) enol ether of (*R*)-(-)-carvone (**29**) to *m*-CPBA selectively oxidized the electron rich TMS enol ether in the presence of a 1,1-disubstituted olefin and a trisubstituted olefin. The resulting TMS ethers (**30a** and **30b**) could be cleaved using a number of reagents. We found that acetic acid, ammonium fluoride, and TBAF worked well for this purpose, but HF in methanol gave the best results. Using HF in methanol the desired products (**31a**) and (**31b**) were isolated as a 1:2.5 mixture in 63% yield from carvone. While this process still favored the formation of the undesired stereochemistry at C-6, the diastereomers were easily separated.

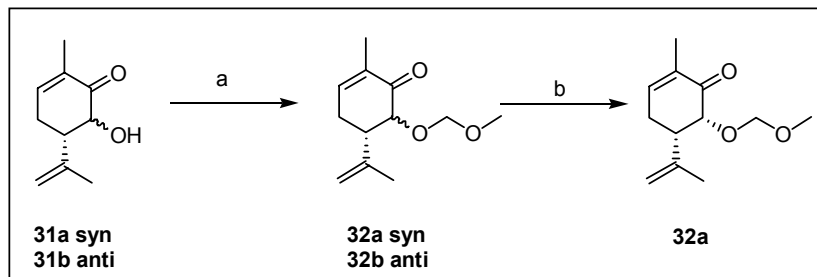


Reagents and conditions: a) LDA, THF, -78 °C then TMSCl. b) *m*-CPBA, NaHCO₃, CH₂Cl₂, 0 °C. c) HF (aq)

MeOH, syn:anti = 1:2.5, 63% from carvone.

Figure 19 Rubottom oxidation of (*R*)-(-)-carvone

Fortunately, conditions were developed to convert the undesired C-6 (*S*) stereocenter (**31b**) into the desired (*R*) isomer by a simple epimerization process. The C-6 alcohol was first protected as a methoxymethyl ether (MOM) and then epimerizing with lithium diisopropylamide (LDA) followed by an acetic acid quench (Figure 20). Experimentally, the easiest route to the desired *syn*-alkoxy enone (**32a**) was to carry both isomers (**31a** and **31b**) through as a mixture and then separate the two following MOM ether formation. This method minimized chromatographic separations and greatly facilitated the preparation of large quantities of material. We have found that this Rubottom oxidation procedure can be reproducibly performed on a 30-gram scale without any difficulties.



Reagents and conditions: a) MOMCl, DIPEA, CH₂Cl₂, DMAP, 45 °C, 99%. b) LDA, THF, -78 °C, then HOAc, anti:syn= 1:1.5, 92%.

Figure 20 Epimerization at C-6

Once a reliable route to the enone component (**32a**) was established, the next step was to synthesize the required aldehyde (**34**) for an aldol addition. The aldehyde coupling partner (**34**) was prepared by a Dess-Martin periodinane⁴⁷ oxidation of the corresponding primary alcohol (**33**) (Figure 21). Several attempts were made to purify this aldehyde, however this species was found to be both acid and base sensitive. Column chromatography using silica gel, silica gel deactivated with 3% triethylamine, basic alumina, and neutral alumina each caused the β,γ -

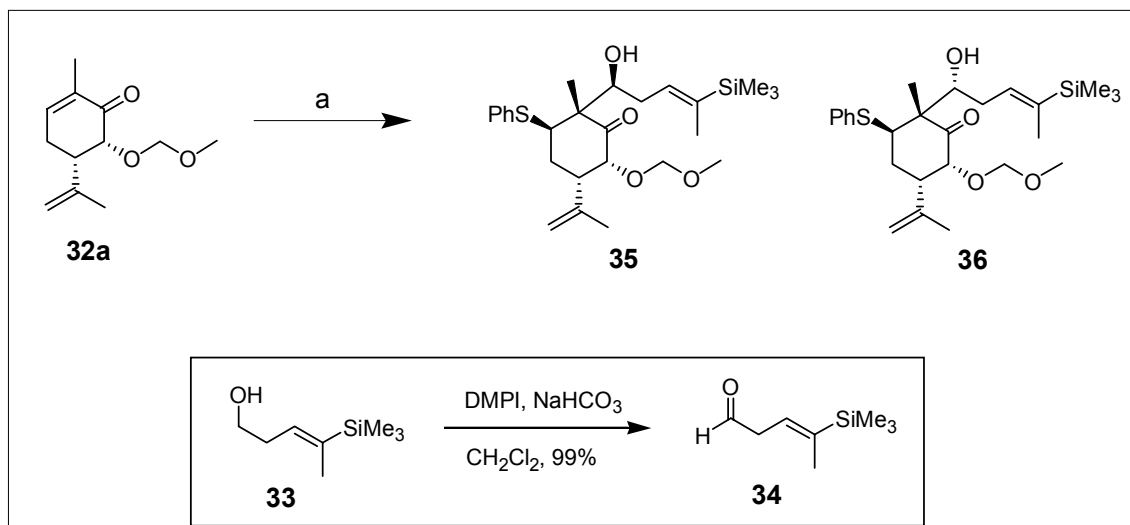
unsaturated aldehyde to rearrange to the more stable α,β -unsaturated isomer. The only way to avoid this undesired isomerization was to use the aldehyde crude.

At this point in the synthesis, we have established a reliable route to both the enone (**32a**) and the aldehyde (**34**) components. The next step was to evaluate the potential utility of a tandem conjugate addition-aldol reaction process (Figure 21). The tandem conjugate addition-aldol reaction procedure that we utilized was designed by adapting a method originally reported by Itoh and coworkers.⁴⁸ Itoh's method was an attractive alternative to a typical aldol addition, since the conjugate addition process introduces an oxygen atom precursor at C-9. Additionally, we recognized the potential for this reaction to generate three new chiral centers, including two neopentyl centers and one quaternary center. This process would also generate the C-1 to C-10 carbon-carbon bond.

Initial experiments using this method were carried out as follows (Figure 21): The chloromethylaluminum benzenethiolate reagent was prepared *in situ* by adding thiophenol to dimethylaluminum chloride at 0 °C in methylene chloride. This mixture was then cooled to -78 °C and a solution of the enone (**32a**) in tetrahydrofuran was added. The addition of the aldehyde (**34**) to the aluminum enolate resulted in the formation of two aldol diastereomers (**35** and **36**) in a 3:1 ratio and 25% overall yield. Even though the yield was low, it was encouraging to find that more than 70% of the enone (**32a**) could be recovered. A substantial amount of the aldehyde (**34**) was also present before aqueous work-up, but did not survive silica gel chromatography.

After repeating this experiment multiple times, we found that the conjugate addition reaction step always appeared to proceed slowly. In an attempt to optimize this aldol process, several experiments were evaluated. Different solvents were tried. The use of only methylene chloride or only tetrahydrofuran did not seem to improve the conversion of the conjugate

addition step. Different Lewis acids, such as trimethylaluminum, methylaluminum dichloride, and tetrakis(dimethylamino) titanium, were also screened.



Reagents and conditions: a) PhSAlMeCl, AlMe₂Cl, CH₂Cl₂, -78 °C to -50 °C, then **34** in THF, -50 °C, 25%.

Figure 21 A tandem conjugate addition-aldol reaction

The use of trimethylaluminum lowered the yield, but the use of the stronger Lewis acid, methylaluminum dichloride, simply caused quantitative cleavage of the C-6 MOM ether group. We also found that the Lewis acid tetrakis(dimethylamino) titanium resulted in the formation of a thick black slurry when the enone (**32a**) was added, and no identifiable products were isolated. Experiments using excess dimethylaluminum chloride and thiophenol also failed to improve the conversion of the conjugate addition step.

One important observation that was discovered during this process was that the use of two equivalents of a Lewis acid was usually necessary to obtain the best yields. This result is consistent with an open transition state. In our proposed open transition state model (Figure 22) one equivalent of an aluminum species is utilized in forming the five-membered ring aluminum

chelate with the C-6 MOM ether. This intramolecular chelate disfavors the intermolecular chelate required for a Zimmerman-Traxler type transition state. Unlike the Zimmerman-Traxler

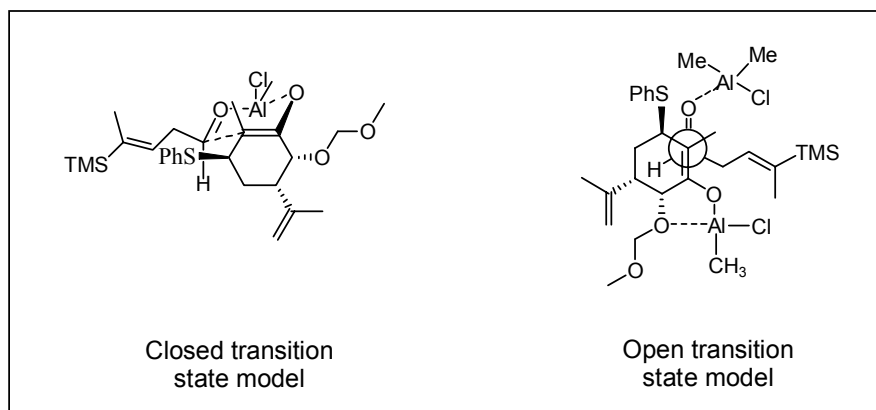


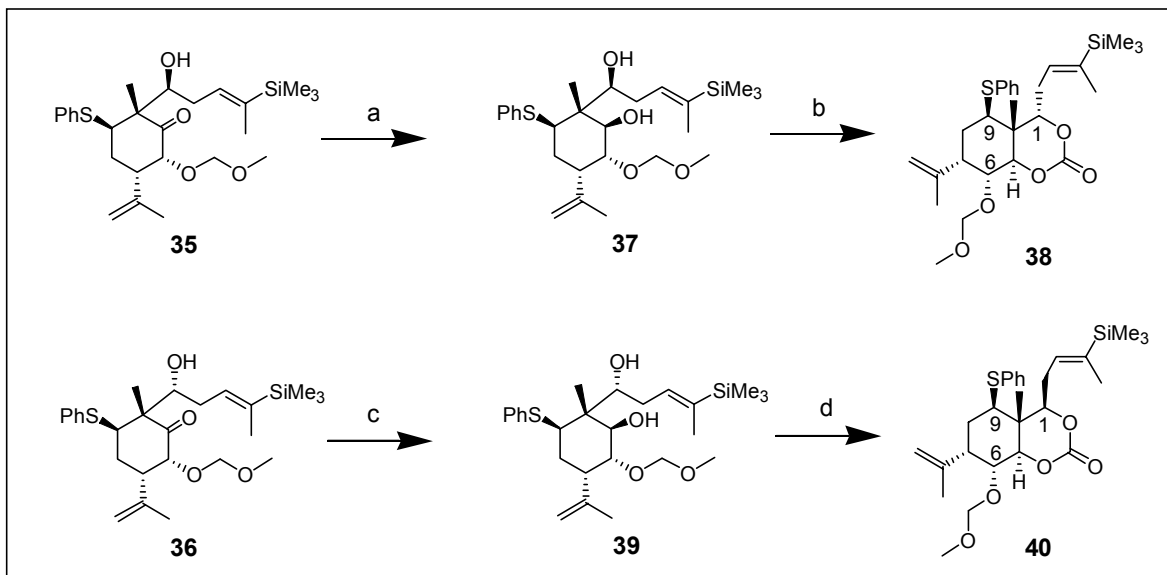
Figure 22 Closed and open transition state models

model, where the metal atom coordinated to the enolate activates the aldehyde carbonyl group, an open transition state requires the presence of a second equivalent of a Lewis acid to activate the aldehyde. This observation supports an open transition state model.

We also evaluated the use of other nucleophiles. Reactions were screened using both 4-methoxythiophenol and 4-nitrothiophenol, however these nucleophiles did not perform any better than thiophenol. Eventually longer reaction times, typically five to six hours at $-50\text{ }^{\circ}\text{C}$, were found to be required for the conjugate addition process to reach an optimal conversion, however the conversions were still low.

In order to determine if either of the aldol diastereomers (**35**) or (**36**) possessed the desired stereochemistry at C-1, C-9, or C-10, the rigid cyclic carbonate analogs (**38**) and (**40**) were prepared using a two-step sequence (Figure 23). The first step involved a directed reduction using sodium acetoxyborohydride. This reagent will only reduce a ketone if it is coordinated to an electron-rich group, such as a hydroxyl group.⁴⁹ The stereochemical outcome of this reaction

is controlled by the neopentyl C-1 alcohol group, which delivers the hydride to the α -face of the ketone. The diol species (**37** and **39**) were then converted into cyclic carbonates (**38** and **40**) using triphosgene and pyridine. The stereochemistry of both cyclic carbonates was determined based on analysis of H,H-COSY and 1D NOE experiments (Figures 24 and 25).



Reagents and conditions: a) $\text{NaBH}(\text{OAc})_3$, HOAc, 35%. b) Triphosgene ($\text{Cl}_3\text{CO}(\text{CO})\text{OCCl}_3$), pyridine, CH_2Cl_2 , $-78\text{ }^\circ\text{C}$ to $25\text{ }^\circ\text{C}$, 97%. c) $\text{NaBH}(\text{OAc})_3$, HOAc, 94%. d) Triphosgene, pyridine, CH_2Cl_2 , $-78\text{ }^\circ\text{C}$ to $25\text{ }^\circ\text{C}$, 58%.

Figure 23 Cyclic carbonate NOE analogs

In order to determine the stereochemistry of the cyclic carbonate derivative (**38**) from the major aldol product (**35**), each hydrogen atom was unambiguously assigned using a H,H-COSY experiment. 1D NOE experiments were then performed to determine the absolute stereochemistry. The first NOE experiment irradiated the C-1 methine. This produced NOE enhancements at the C-10 quaternary methyl group (4.2%). This confirmed that both of these groups were on the same face of the fused ring system. The next NOE experiment irradiated the

C-6 methine, producing an enhancement at the neighboring C-7 methine (4.2%) and at the C-10 methyl group (3.5%). Since the absolute configuration at C-7 is known, this experiment proved that the C-10 methyl, the C-1 methine, and the C-6 methine groups are all on the same face of the bicyclic ring system.

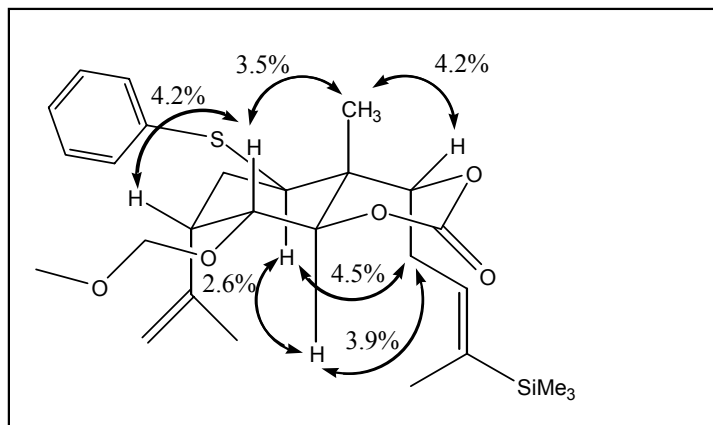


Figure 24 1D NOE results for carbonate (38) of the aldol reaction major product

When the C-5 methine was irradiated there were two enhancements observed, one with the C-9 methine (2.6%) and one with the methylene group once removed from the C-1 position (3.9%). The last NOE experiment on this substrate was to irradiate the C-9 methine. This irradiation produced enhancements at the C-5 methine (2.6%) and also at the methylene group mentioned in the last experiment (4.5%). These last two NOE experiments suggest that the C-5 and C-9 methine groups and the alkyl chain from the aldehyde are all positioned on the same face of the ring. These experiments support all of the stereochemical assignments for the cyclic carbonate (**38**) and show that the major product of the aldol addition is the isomer required for orbiculin A (**12**).

The cyclic carbonate derivative (**40**) of the minor product (**36**) from the aldol addition was also subjected to a battery of NOE experiments. The first NOE experiment with the cyclic carbonate (**40**) irradiated the C-10 methyl group. This irradiation produced enhancements at the C-6 methine (2.5%) and at the methylene group once removed from the C-1 methine (1.0%). The second experiment irradiated the C-6 methine and enhancements were seen at the neighboring

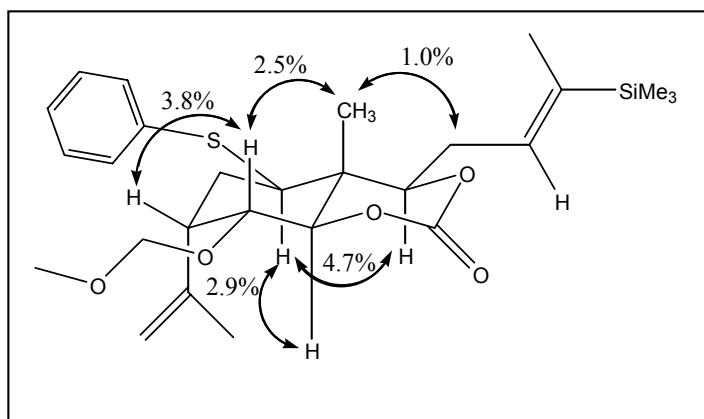


Figure 25 1D NOE results for carbonate (**40**) of the aldol reaction minor product

C-7 methine (3.8%) and also to the C-10 methyl group (2.5%). Since the absolute stereochemistry at C-7 is known, it can be assumed that all four of these groups are on the same face of the ring system. The final NOE experiment for this substrate irradiated the C-9 methine. This caused enhancements to appear at the C-1 methine (4.7%) and at the C-5 methine (2.9%). These three experiments confirm the configuration at all six stereocenters. The minor diastereomer (**36**) only differs from the major product (**35**) at the C-1 stereocenter.

Our NMR analysis reveals that the major product's (**35**) stereochemistry is not consistent with a closed Zimmerman-Traxler transition state model. This model predicts that the minor

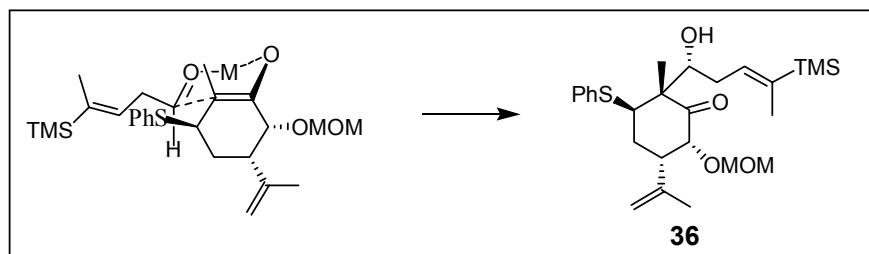


Figure 26 Zimmermann-Traxler model

product (**36**) should have been the major product. The major product is likely the result of an open transition state and the observed selectivity of this process can be attributed to several control elements. Conformational analysis reveals that prior to conjugate addition, the enone (**32a**) is most likely in a half chair conformation with the C-7 isopropenyl group in the pseudo-

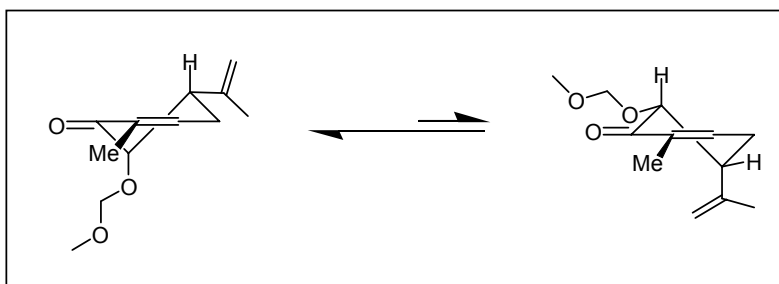


Figure 27 Half-chair conformations for enone (**32a**)

equatorial position (Figure 27). Axial addition of benzenethiolate into the enone (**32a**) gives the cyclic enolate (**41**) with the sulfide group in the pseudo-axial position, avoiding a potentially high energy A^{1,2} interaction with the C-10 methyl group. An open transition state (**42**) may be preferred to a closed, Zimmerman-Traxler type, transition state due to the formation of a stable five-membered ring aluminum chelate (**41**) with the C-6 MOM ether (Figure 28).

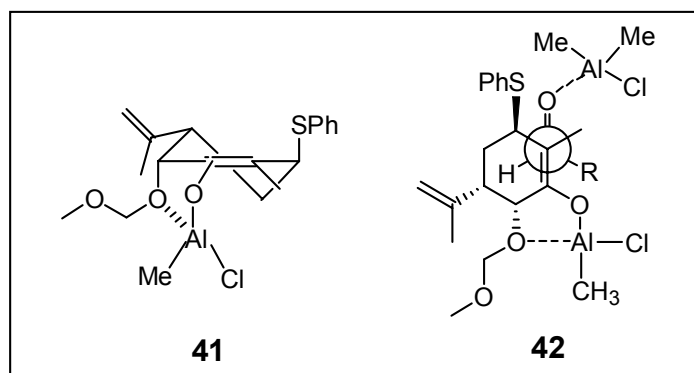


Figure 28 Aluminum chelate and open transition state models

In the open transition state model (**42**), the selectivity observed for the major product (**35**) presumably arises from the preference of the aldehyde to approach the enolate with the oxygen atoms anti-periplanar and the smaller hydrogen atom substituent under the enolate ring. The minor product (**36**) may arise from a similar approach, but with the alkyl chain of the aldehyde under the enolate ring instead. Another possibility is that a *syn*-clinal approach with respect to the aldehyde and enolate oxygen atoms, placing the smaller hydrogen atom under the enolate ring, also would produce the minor diastereomer. Although no direct evidence supporting the formation of a chelate species (**41**) was obtained, alkyl aluminum reagents have previously been recognized for their exceptional chelating ability in asymmetric synthesis.⁵⁰

Continuing on with the synthesis of orbiculic acid, the major product from the aldol addition (**35**) was protected as an acetate ester (**43**) using acetic anhydride and pyridine. The next step was to convert the (*E*)-vinyl silane (**43**) into the required (*Z*)-vinyl iodide (**44**). In the planning of this synthetic route, it was realized that a (*Z*)-vinyl iodide would be prone to elimination under basic conditions. Therefore it was decided to minimize the number of steps through which to carry this sensitive group. We chose to use an (*E*)-vinyl silane as a surrogate for a (*Z*)-vinyl iodide (Figure 29). When the (*E*)-vinyl silane (**43**) was exposed to iodine

monochloride in DMF, followed by Al₂O₃, multiple products were found. Following an aqueous work-up, analysis of the crude ¹H NMR showed no sign of the expected product (**44**).

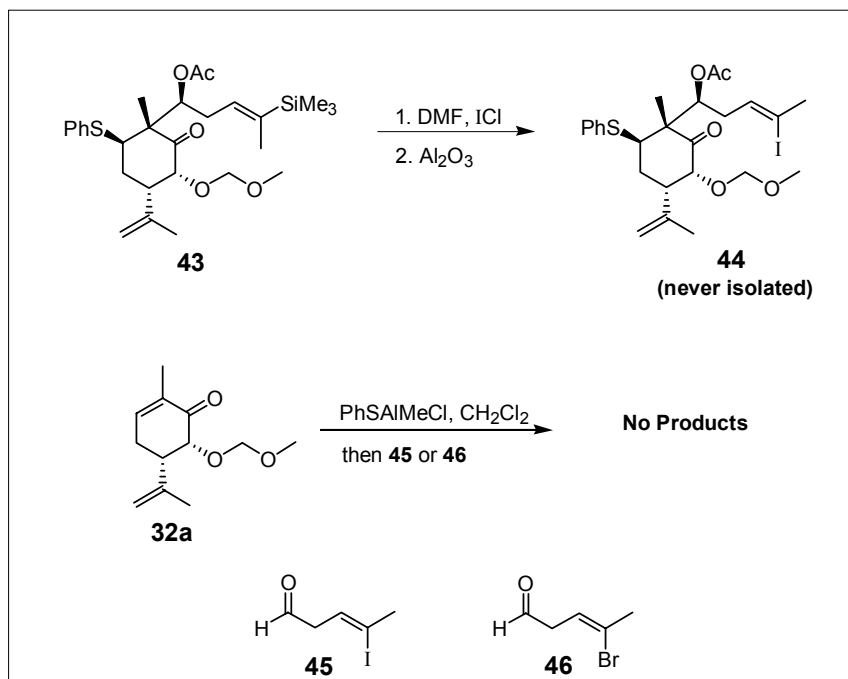


Figure 29 Attempted (Z)-vinyl iodide synthesis

In retrospect, this reaction probably failed because iodine monochloride is a potent oxidant. The C-9 phenyl sulfide most likely underwent oxidation to the sulfoxide or sulfone and this process consumed the iodine monochloride before it could react with the hindered tri-substituted vinyl silane.

In an attempt to circumvent this problem, the β,γ-unsaturated aldehydes (**45**) and (**46**) were prepared from (**34**) using procedures analogous to the iodine monochloride method shown in Figure 29. However, the aldehydes (**45**) and (**46**) were discovered to be incompatible with the conditions of the aldol reaction. Exposure of either aldehyde to the conditions of the tandem conjugate addition-aldol reaction produced no aldol products.

When we discovered that generating the (*Z*)-vinyl halide group was proving to be a difficult task, alternative routes were examined. One solution was to use a 1,1-disubstituted-vinyl iodide. This change would give an exocyclic olefin instead of an endocyclic olefin, but we were confident that conditions could be found to isomerize the exocyclic olefin (**47**) to the required endocyclic species (**48**).

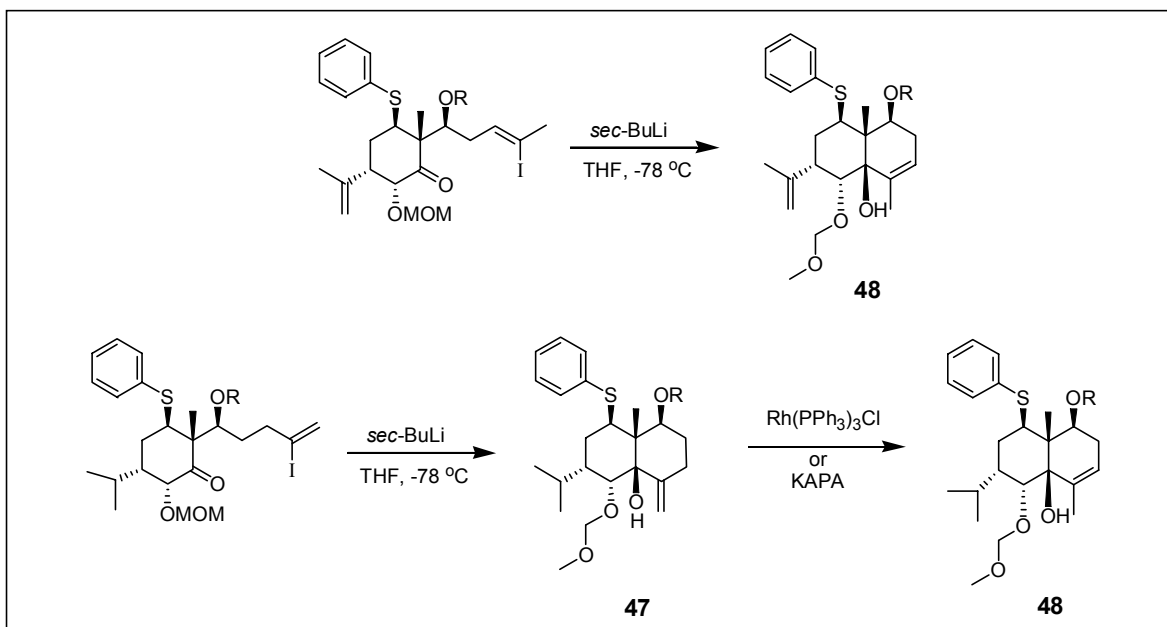


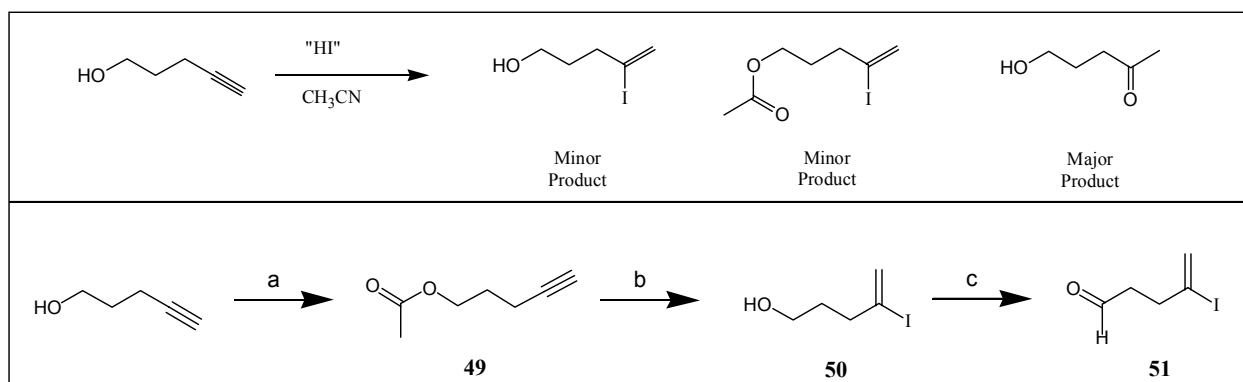
Figure 30 A comparison of the original route (top) and the new route (bottom)

In our revised route, the isopropenyl group of the carvone derivative (**32a**) was selectively reduced (Figure 32) by adapting the procedure of Ireland and coworkers using Wilkinson's catalyst and H₂.⁵¹ The isopropenyl group present in the enone (**32a**) was reduced at this stage simply due to a reordering of steps. The required aldehyde, 4-iodopent-4-enal (**51**), was synthesized in four steps from commercially available 4-pentyn-1-ol. The first step was to protect the primary alcohol as an acetate ester. We found that if the free alcohol was not protected prior to exposure to HI in acetonitrile, the desired product was obtained in low yield.⁵²

Analysis of several byproducts from this failed reaction by ^1H NMR revealed that a substantial amount of material underwent alkyne hydration, giving a methyl ketone species (Figure 31).

Another byproduct isolated from this reaction was consistent with acetate incorporation at the primary alcohol. The discovery of an acetate derivative was surprising. We presume that the formation of this species can be attributed to nucleophilic attack at the nitrile group of acetonitrile by the alcohol, followed by hydrolysis. To circumvent this problem, we discovered that protection of the primary alcohol as an acetate ester (**49**) before treatment with HI dramatically improved the yield.

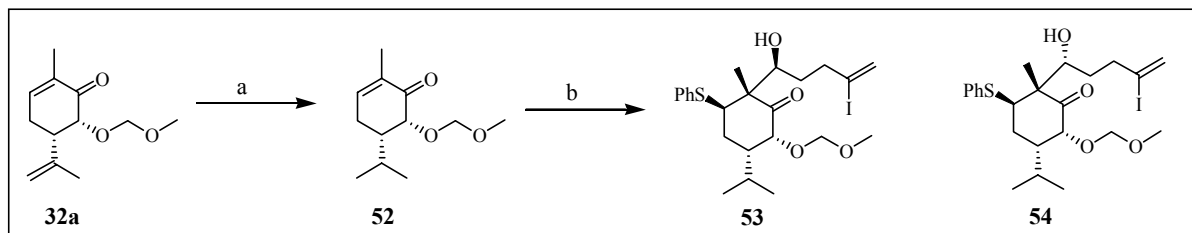
The procedure for generating HI *in situ* involved the slow addition of water to a solution of trimethylsilyl chloride and sodium iodide in acetonitrile (Figure 31).⁵² Following HI addition, the crude vinyl iodide was subjected to potassium carbonate in methanol, providing 4-iodopent-4-enol (**50**) in 83% yield. The final step utilized a Dess-Martin periodinane oxidation⁴⁷ that provided 4-iodopent-4-enal (**51**) in 93% yield.



Reagents and conditions: a) Ac₂O, DMAP, Et₃N, CH₂Cl₂, 99%. b) i) TMSCl, NaI, CH₃CN, then H₂O, then (**49**). ii) K₂CO₃, MeOH, 83% over 2 steps. c) DMPI, NaHCO₃, CH₂Cl₂, 93%.

Figure 31 An improved preparation of 4-iodopent-4-enal

When our new enone derivative (**52**) was subjected to the benzenethiolate aldol reaction conditions, the conjugate addition process was still quite slow (Figure 32). After stirring for five hours at -50 °C, 4-iodopent-4-enal (**51**) was added. This produced the desired products (**53** and **54**) in 28 % yield as a 6:1 ratio of diastereomers, presumably at C-1.



Reagents and conditions: a) $(\text{PPh}_3)_3\text{RhCl}$, H_2 , C_6H_6 , 25 °C, 98%. b) PhSAlMeCl , CH_2Cl_2 , -50 °C, then 4-iodopent-4-enal, **53:54**= 6:1, 28%.

Figure 32 A selective tandem conjugate addition-aldol reaction

Although the yield was low, the reaction seemed to favor the formation of the correct diastereomer (**53**). This was determined empirically by examining two diagnostic peaks in the ^1H NMR spectra. We had discovered that a fairly reliable way to differentiate the two C-1 diastereomers from this aldol reaction involved simply examining the coupling constants of the MOM ether methylene protons and the chemical shift values of the C-1 methine protons. This method suited or needs for exploratory work, since it did not involve the time consuming process of preparing analogs and acquiring NOE data. The assignments based on this method were never considered conclusive, only suggestive.

Examination of the data in Table 2 illustrates this trend. The first four entries in Table 2 are from diastereomers whose relative configurations were established using the aid of H,H-COSY and 1D NOE experiments. The stereochemistry in the last two entries, aldol adducts (**53**

and **54**), were tentatively assigned by comparison to the first four entries. Although this assignment was not rigorously tested with 1D NOE experiments, we were confident that the open transition state model (Figure 28) was still operative in this system and our assignment was reliable for the aldol adducts (**53** and **54**).

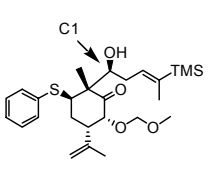
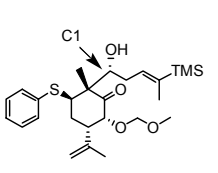
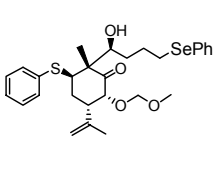
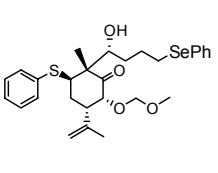
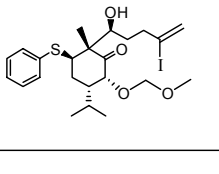
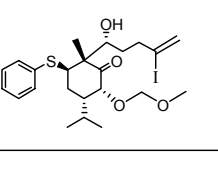
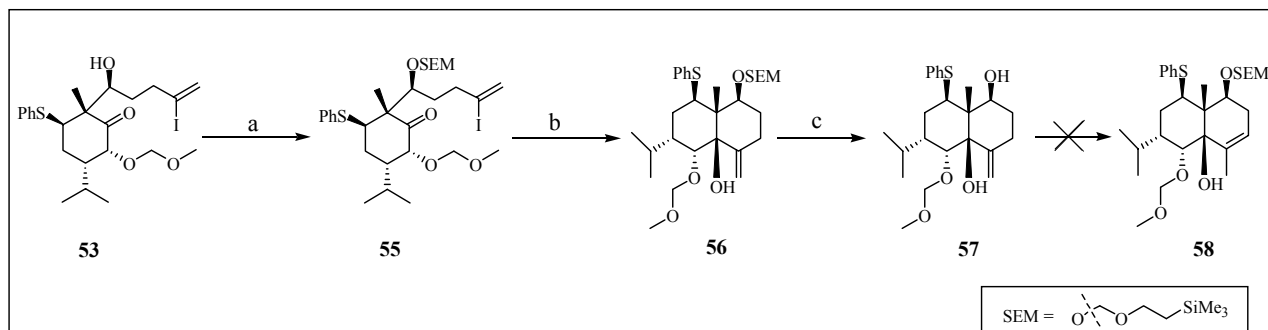
	C-1 Methine	MOM Methylene		C-1 Methine	MOM Methylene
	3.99 ppm	4.66 ppm, s, 2H		4.35 ppm	4.74 ppm, d, $J = 6.9$ Hz, 1H 4.66 ppm, d, $J = 6.9$ Hz, 1H
	3.89 ppm	4.67 ppm, s, 2H		4.11 ppm	4.65 ppm, d, $J = 6.8$ Hz, 1H 4.59 ppm, d, $J = 6.8$ Hz, 1H
	3.99 ppm	4.61 ppm, s, 2H		4.35 ppm	4.74 ppm, d, $J = 6.0$ Hz, 1H 4.51 ppm, d, $J = 6.0$ Hz, 1H

Table 2 A comparison of the ^1H NMR data from six aldol diastereomers

Table 2 shows that when the desired (*S*) stereocenter (left-hand side of Table 2) is present at the C-1 center, the C-1 methine signal is always shifted upfield compared to the opposite C-1 (*R*) isomer (right-hand side of Table 2). This indicates that the C-1 hydrogen in the undesired C-1 (*R*) isomer is in a slightly more electron deficient environment. The second diagnostic signal is the peak shape and splitting pattern observed at the MOM ether methylene group. The ^1H NMR peak(s) associated with this methylene group always show up as a slightly broadened singlet when the desired C-1 (*S*) isomer is present. When the opposite C-1 (*R*) isomer is present this methylene group shows up as two doublets in the ^1H NMR spectrum. This apparent broadened

singlet is the result of incidental chemical shift equivalence of the two diastereotopic MOM ether methylene protons in the desired product (**53**).

Before the *cis*-decalin ring system could be constructed, the C-1 hydroxy group required protection. Protection of the C-1 alcohol was necessary for two reasons. First, it would be difficult to avoid quenching the vinyl lithium precursor to the decalin ring (**55**) in the presence of an alcohol. Secondly, we suspected that strongly basic conditions might cause a retro-aldol reaction to occur. The major aldol isomer (**53**) was protected as a trimethylsilylethylmethoxy (SEM) ether (**55**) in good yield (Figure 33). Treatment of this vinyl iodide with one equivalent of *sec*-butyl lithium gave the desired *cis*-decalin ring system (**56**). This reaction represents our first successful synthesis of a decalin ring system.



Reagents and conditions: a) SEMCl, DIPEA, DMAP, CH₂Cl₂, 80%. b) *sec*-BuLi, 73%. c). KAPA, THF, 75%

Figure 33 A successful *cis*-decalin synthesis

In order to convert the *cis*-decalin ring (**56**) to the desired *trans*-decalin ring, the di-substituted exocyclic olefin would require isomerization to an endocyclic tri-substituted olefin (**58**). This conversion was first attempted using potassium aminopropyl amide (KAPA), a reagent designed for olefin isomerization.⁵³ Exposure of the exocyclic olefin (**56**) to KAPA gave the diol

derivative of the starting material (**57**) as the sole product. The strongly basic reagent had simply cleaved the SEM ether and no olefin isomerization was detected. We then recognized that in the absence of the SEM ether this isomerization process would need to generate three anions in one molecule (Figure 34). The formation of two anions in one molecule is reasonable, but forming three anions would give a fairly high-energy species and would be quite difficult. The KAPA reagent was a poor choice for our application due to our protecting group selection.

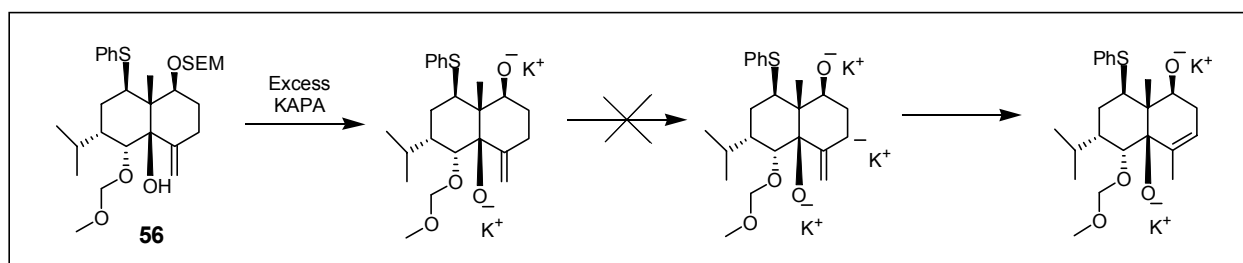


Figure 34 The KAPA mediated olefin isomerization

Olefin isomerization was also attempted using Wilkinson's catalyst.⁵⁴ We found that these conditions also failed to isomerize the exocyclic olefin. This result was not surprising since rhodium catalysts normally exhibit a higher affinity for sulfide groups than olefins. Coordination of the catalyst to the olefin pi system was likely disfavored due to the soft nature of the sulfide group.

Although these two synthetic routes did not yield a natural product, they did succeed in providing us with a substantial amount of information for planning future routes. We had found optimal conditions for the conjugate addition initiated aldol reaction and had determined a reliable method for establishing the stereochemistry of the aldol products. We had also constructed a transition state model for predicting the stereochemical outcome of this process

and discovered the chemical incompatibility and limitations associated with the phenyl sulfide group. Using this knowledge, we designed a new system that would avoid the problems encountered in the first two attempts.

3.2. A Ring Closing Metathesis Route to Celafolin A-1

Celafolin A-1 (**11**) is one of the simplest members of the dihydroagarofuran family of natural products that is known to reverse MDR in cancers over-expressing P-gp.³⁰⁻³¹ Since the chemistry developed to synthesize celafolin A-1 would be directly applicable to orbiculins, we

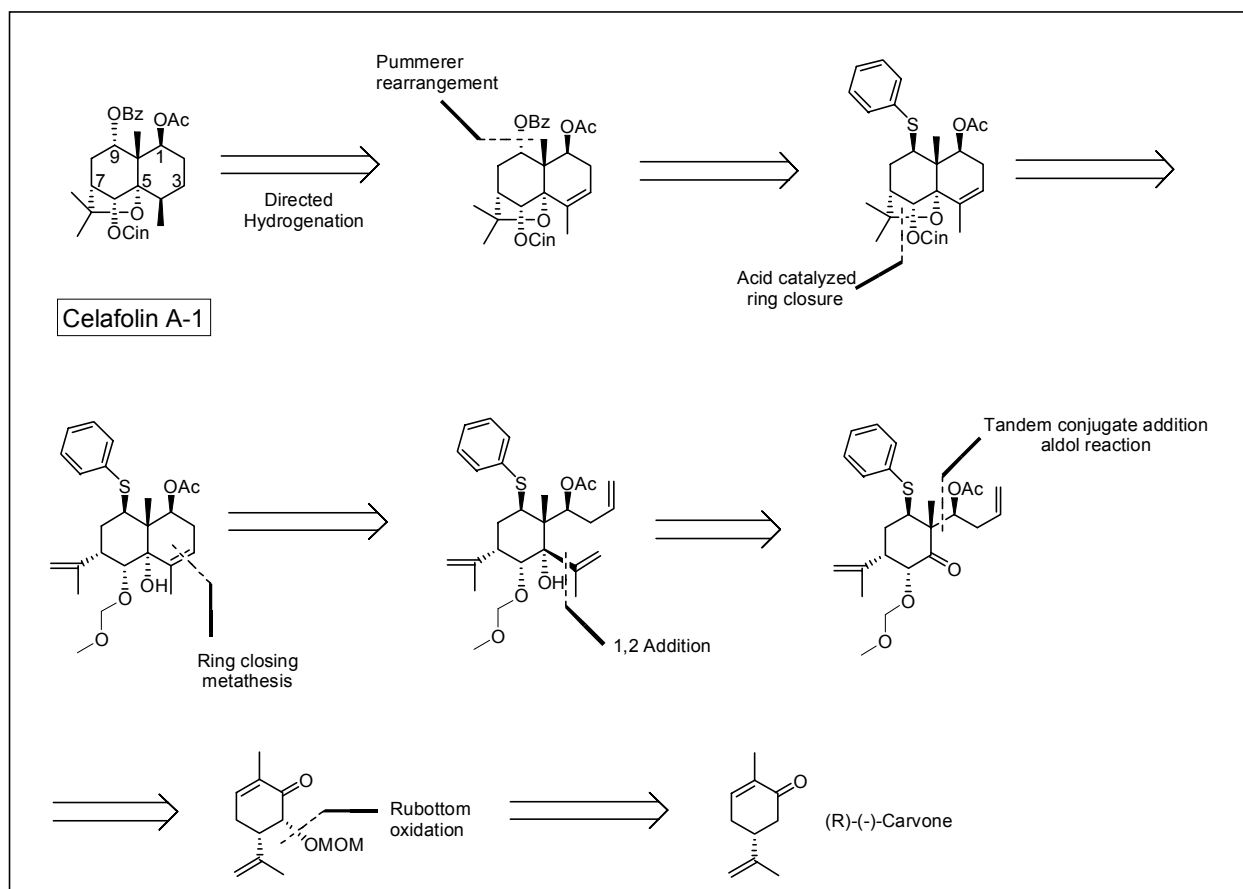


Figure 35 Retrosynthesis of celafolin A-1

decided to pursue this simpler natural product first. The selected disconnections for celafolin A-1 (Figure 35) closely resemble our initial route to orbiculin A. The major change in our new route was the use of a ring closing metathesis (RCM) reaction to generate the *trans*-decalin ring.

In an earlier experiment, we discovered that Grignard reagents could add easily into the hindered C-5 carvone carbonyl group. Our idea for using a ring closing metathesis approach for constructing the dihydroagarofuran ring system originated from the experiment shown in Figure 36. While investigating a model system for orbiculin A, it was discovered that isopropenyl magnesium bromide readily added to the neopentyl C-5 carbonyl group. Although the model system in Figure 36 exhibited no facial selectivity, this result was encouraging since many of our attempts to add alkyl lithium nucleophiles, during intramolecular reactions, into the C-5 carbonyl group had previously failed. The success of this addition initiated our investigation of a ring closing metathesis route to celafolin A-1 (**11**).

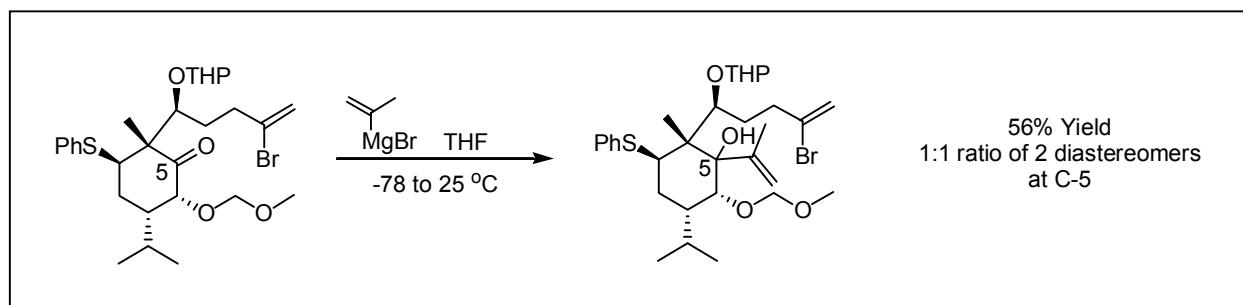


Figure 36 Grignard addition into a neopentyl ketone

The first transformation to address was the selection of a coupling partner for the C-5 isopropenyl group. We reasoned that this group could be installed using a tandem conjugate addition-aldol reaction (Figure 35) with an aldehyde similar to 3-butenal.⁵⁵ Following protection of the resulting aldol adduct, isopropenyl-magnesium bromide could be added into the C-5

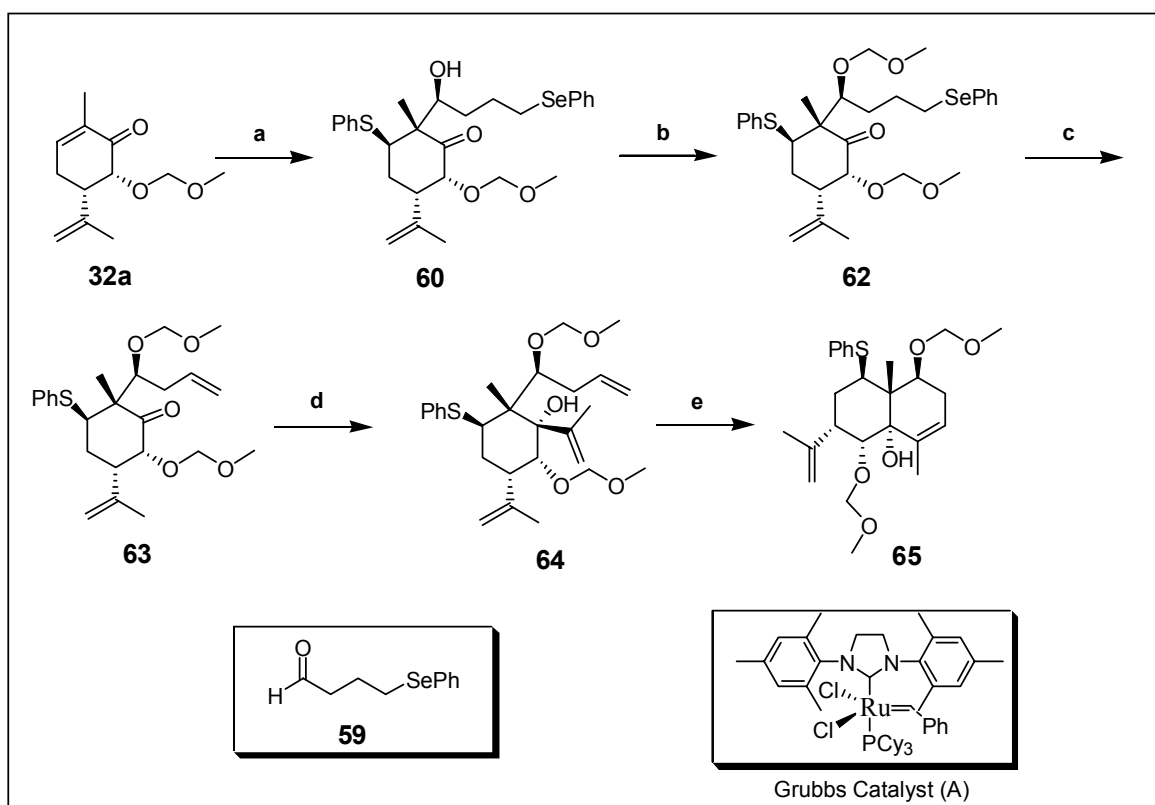
ketone, giving the second coupling partner for the ring closing metathesis.⁵⁶ This plan would yield a *trans*-decalin ring system in fewer steps than initially proposed for orbiculin A (**12**) (Figure 17).

Our initial attempts using 3-butenal gave discouraging results. This aldehyde was difficult to prepare, gave poor yields, and produced mixtures of undesired products when subjected to the conditions of our aldol reaction. The major problems seemed to be due to the propensity of 3-butenal to isomerize to the more stable α,β -unsaturated isomer, crotonaldehyde. Fortunately, we found that 4-phenylselenobutanal (**59**)⁵⁷⁻⁵⁸ could be used as a substitute for 3-butenal since selenium oxidation and elimination⁵⁹ affords the required terminal olefin.

When 4-phenylselenobutanal (**59**), a known species prepared in one step from 4-phenylselenyl-butyric acid methyl ester, was subjected to the conjugate addition initiated aldol with the enone (**32a**), it was found to be both reactive toward the aluminum enolate and remarkably robust. This aldehyde reacted with the aluminum enolate to give the desired aldol products as two diastereomers. Following purification of these two C-1 diastereomers (**60** and **61**), the yield for the reaction, based solely on product obtained, was found to be 22% in a 6.3:1 ratio of diastereomers favoring the desired isomer (**60**). An additional 58% of the enone (**32a**) and 78% of the aldehyde (**59**) were also recovered. The major aldol diastereomer (**60**), which we believed contained the required stereochemistry for celafolin A-1, was then carried through the remaining synthesis and the stereochemistry was determined at a later point.

Before isopropenylmagnesium bromide could be added into the C-5 carbonyl group, the neopentyl C-1 alcohol of the aldol adduct (**60**) required protection to prevent a possible retro-aldol reaction. The MOM ether protecting group was selected based on the high, reproducible yields during its formation and the simplicity of its removal. We also elected to perform the

selenoxide elimination prior to the Grignard addition. Oxidative elimination of the phenylselenide group (**62**) was accomplished by a chemoselective *m*-CPBA oxidation to generate the selenoxide in the presence of a phenyl sulfide.⁶⁰ Oxidation of the sulfide was avoided by slowly adding one equivalent of *m*-CPBA to the phenylselenide substrate (**62**) in methylene chloride at -78 °C. The crude selenoxide was allowed to slowly warm to room temperature and then pyridine and dihydropyran were added. Dihydropyran was added since elimination of the selenoxide produces phenylselenenic acid, a potent electrophile. In the absence



Reagents and conditions: a) PhSAlMeCl, CH₂Cl₂, then **59**, -50 °C, 6.3:1 ratio, 22%. b) MOMCl, DMAP, DIPEA, CH₂Cl₂, 40 °C, 99%. c) *m*-CPBA, CH₂Cl₂, -78 °C, then pyridine, DHP, reflux, 97%. d) Isopropenylmagnesium bromide, THF, 25 °C, 20%, (80% based on recovered SM). e) Grubb's catalyst (A), CH₂Cl₂, reflux, 94%.

Figure 37 Construction of the A and B ring of celafolin A-1

of the electrophile scavenger dihydropyran, the phenylselenenic acid would react with either the newly formed terminal olefin or the C-7 isopropenyl group. The desired elimination was achieved by gently refluxing the selenoxide, pyridine, and dihydropyran solution giving the desired olefin (**63**) in good yield.

The first conditions that were evaluated for the addition of isopropenyl magnesium bromide into the C-5 carbonyl group involved exposure of the ketone substrate (**63**) to excess isopropenyl magnesium bromide in THF at $-78\text{ }^{\circ}\text{C}$, followed by slow warming to ambient temperature. These conditions gave the RCM substrate (**64**) as a single isomer in 20% yield. The isolation of a single isomer was a surprising result, considering that no facial selectivity was observed in the model substrate in Figure 36. Although the yield was low, most of the starting material (**63**) was recovered. The stereochemical outcome of this addition can be explained by examining the chair conformation of the starting material (**63**) (Figure 38). From this conformation, the Felkin-Ahn model accounts for the observed selectivity and formation of the desired isomer for celafolin A-1 (**11**).

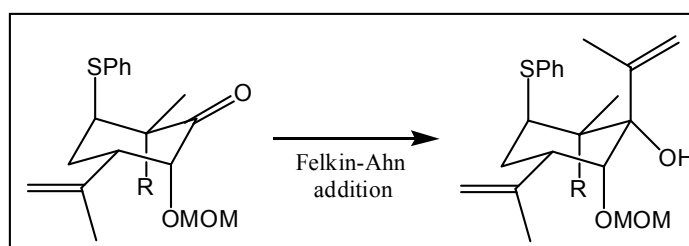


Figure 38 Substrate controlled addition into the C-5 ketone (**63**)

Although selectivity for this Grignard addition process was excellent, the yield needed to be further optimized. The first experiment tried was to replace the solvent tetrahydrofuran with diethyl ether. This solvent change produced no increase in yield. Since this Grignard addition

seemed to be a slow reaction, other competing processes, such as a Wurtz coupling, could be consuming the Grignard reagent before it could react with the hindered ketone (**63**). In an attempt to circumvent this competing reaction, an experiment was evaluated where fresh Grignard reagent was periodically added. This experiment failed to improve the yield. Since periodic addition of fresh Grignard reagent did not improve product conversion, perhaps the sluggish reactivity can be attributed to the ketone.

Grignard reagents are both inherently nucleophilic and basic. We speculated that rather than adding into the ketone carbonyl group, the Grignard reagent may be acting as a base to deprotonate at C-6 giving a magnesium enolate. Formation of a magnesium enolate would certainly prevent Grignard addition.

Enolate formation was initially a concern, but since no epimerized ketone starting materials (**63**) were recovered, it was presumed to not occur. In order to verify this conclusion the Grignard addition reaction was quenched with deuterium oxide instead of dilute HCl. To our surprise, a deuterium label was incorporated at the C-6 carbon (Figure 39). Even more surprising was that the deuterium incorporation occurred with a high degree of facial selectivity causing no epimerization at C-6. This result showed that nucleophilic addition and enolate formation were two competing processes. Furthermore, selective protonation of the enolate during an aqueous quench does not allow for enolate formation to be detected under normal reaction conditions.

In an attempt to prevent enolate formation the cerium derived reagent, isopropenylcerium dichloride, was prepared using 2-lithiopropene and anhydrous CeCl_3 . The use of this nucleophilic cerium reagent, which is a substantially weaker base than a Grignard reagent, also failed to improve product conversion. We speculate that the sterically demanding neopentyl ketone may be too hindered to react with the larger cerium reagent. Since our initial attempts to

optimize this reaction were not improving the yield of product, a temporary solution was to continually re-subject recovered starting material in order to explore new chemistry in subsequent steps.

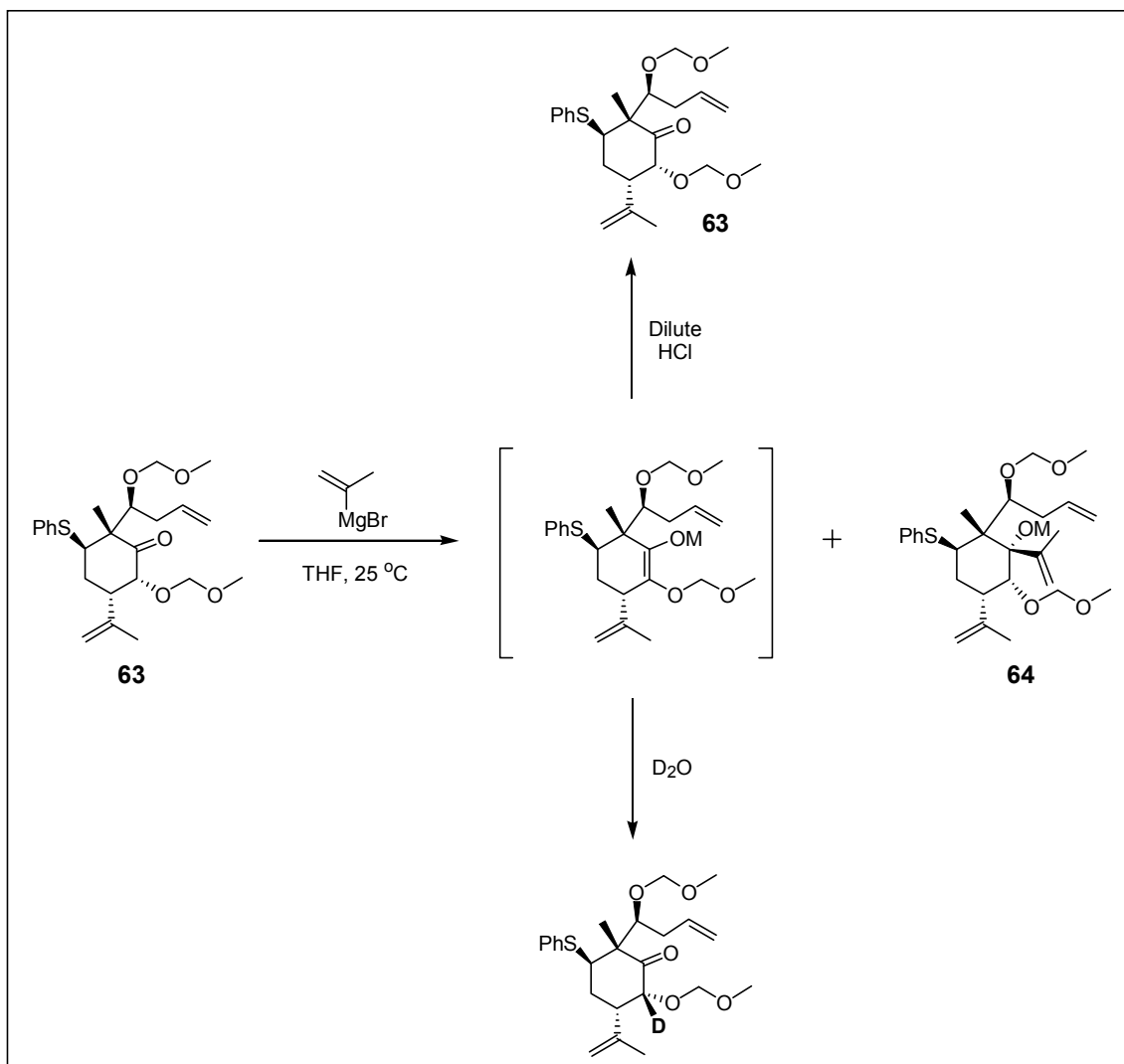


Figure 39 Deuterium labeling experiment

The next step in our sequence was the anticipated ring closing metathesis reaction to construct the *trans*-decalin ring system (Figure 37). The outcome of the ring closing metathesis reaction in the presence of a phenyl sulfide was dependent largely upon the catalyst's affinity for

sulfur. Our previous experience with transition metal catalysts and sulfides taught us that sulfides are typically better ligands for transition metal complexes than olefins. Literature precedent has previously demonstrated that the first generation Grubbs' catalyst is inactive in the presence of sulfide groups.^{56, 61} However, in a recent paper by Danishefsky and coworkers, it was reported that the 2nd generation Grubbs' catalyst⁵⁶ was able to function in the presence of a thioacetal protecting group.⁶² Encouraged by this result, we opted to try this procedure in the presence of the phenyl sulfide (**64**). The reaction that ensued was very fast, even at 0.04 M concentration, with a catalyst loading of 2.5 mol%. After a silica gel filtration to remove the catalyst, the crude ¹H NMR revealed the presence of a single product (**65**).

Prior to the ring closing metathesis reaction, the stereochemistry at C-5 and the stereochemistry of the ring fusion for the newly formed bicyclic ring were unknown. Examination of the coupling constants in the ¹H NMR of the RCM product (**65**) suggested a *trans*-ring fusion with the molecule in a half chair-boat conformation (Figure 40). To provide

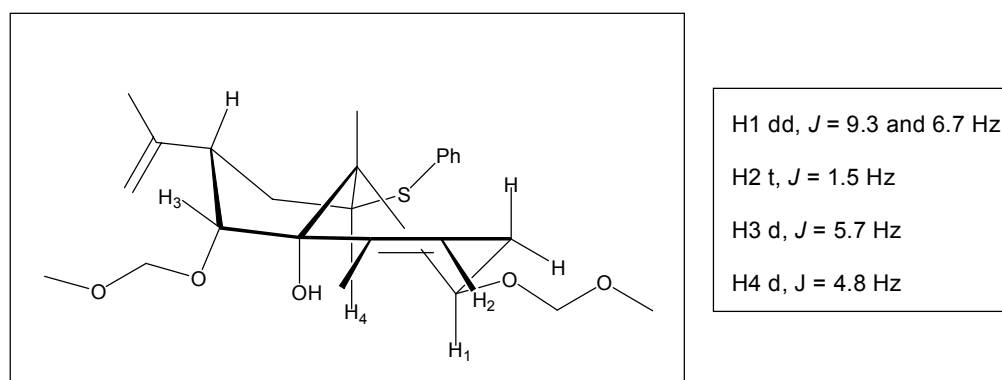


Figure 40 ¹H NMR coupling constant analysis for the RCM product (**65**)

additional evidence supporting the assigned ring system, a 1D NOE experiment was performed.

The result of this experiment showed that when the C-10 quaternary methyl group was

irradiated, an enhancement was seen at the C-2 methylene (1.0%) and the C-7 methine (1.2%) positions. Unfortunately, additional NOE experiments were not possible since many of the diagnostic hydrogen signals could not be irradiated without also irradiating nearby signals. Furthermore, this experiment did not provide additional support for the assigned stereochemistry at C-1, but we were confident in our assignment based on results from similar substrates using the thiophenol tandem conjugate addition-aldol reaction.

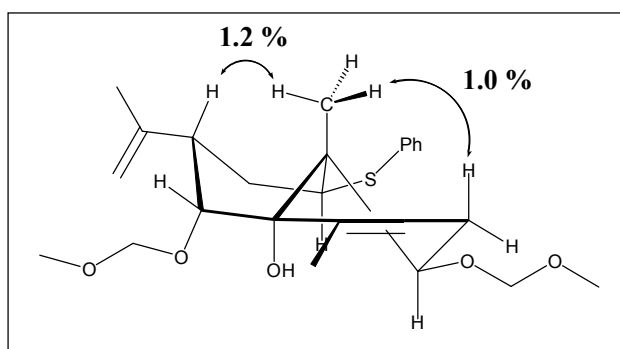
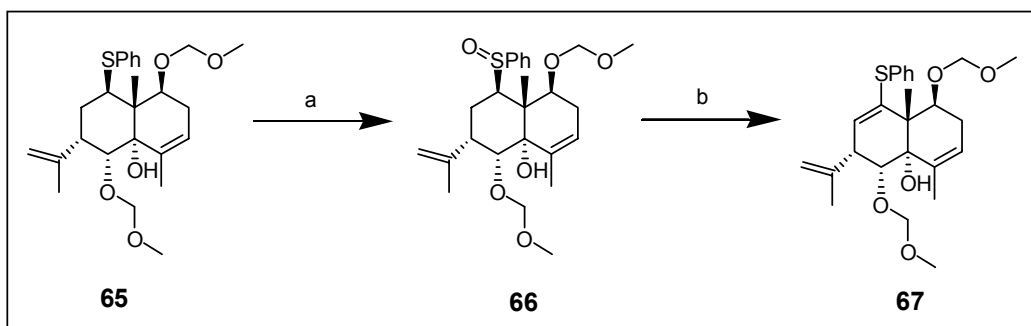


Figure 41 C-10 NOE enhancements

With the *trans*-decalin bicyclic substrate (**65**) in hand, the conversion of the C-9 phenyl sulfide into a carbonyl group was attempted via a Pummerer rearrangement⁶³ (Figure 42). Clean oxidation of the phenyl sulfide (**65**) to the corresponding sulfoxide (**66**) was achieved using *m*-CPBA at -78 °C. The sulfoxide (**66**) was then treated with trifluoroacetic anhydride (TFAA) and pyridine, which led to the exclusive formation of a vinyl sulfide (**67**) in 87% yield.



Reagents and conditions: a) *m*-CPBA, CH₂Cl₂, -78 to 25 °C, 100%. b) TFAA, Pyridine, CH₂Cl₂, 25 °C, 87%.

Figure 42 Attempted Pummerer rearrangement

In order for a successful Pummerer rearrangement to occur, trifluoroacetate has to attack the C-9 carbon center of the activated sulfide (Figure 43). Since the sulfide is attached to a neopentyl carbon, nucleophilic attack is slow. A competing reaction, elimination, can then occur which explains the formation of observed vinyl sulfide (**67**). This Pummerer rearrangement

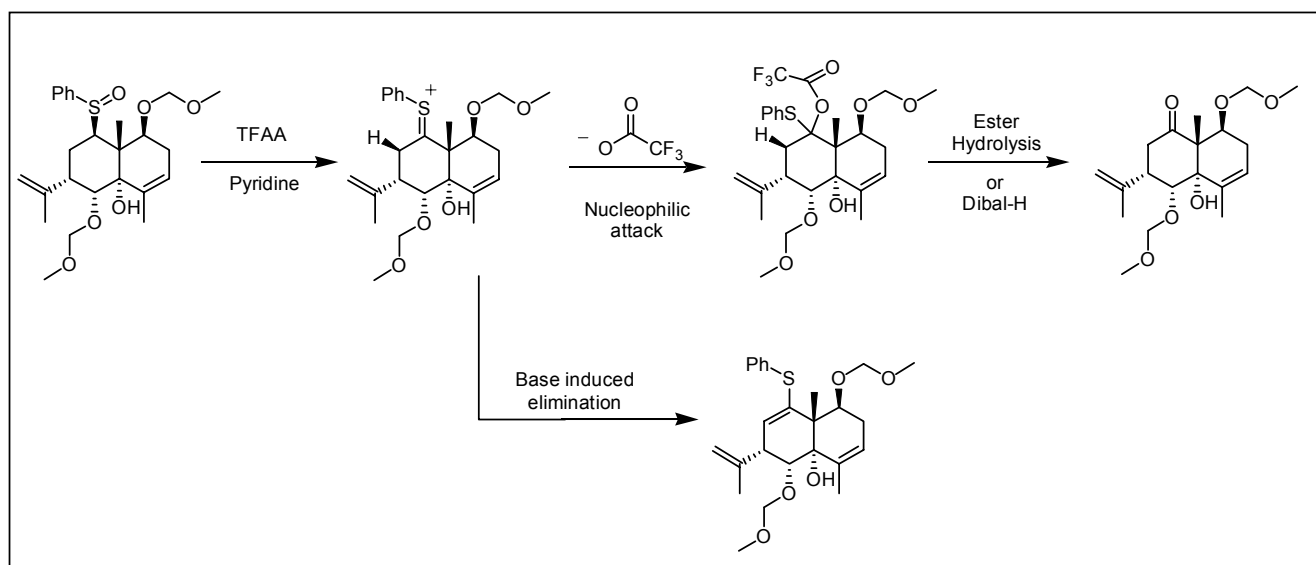
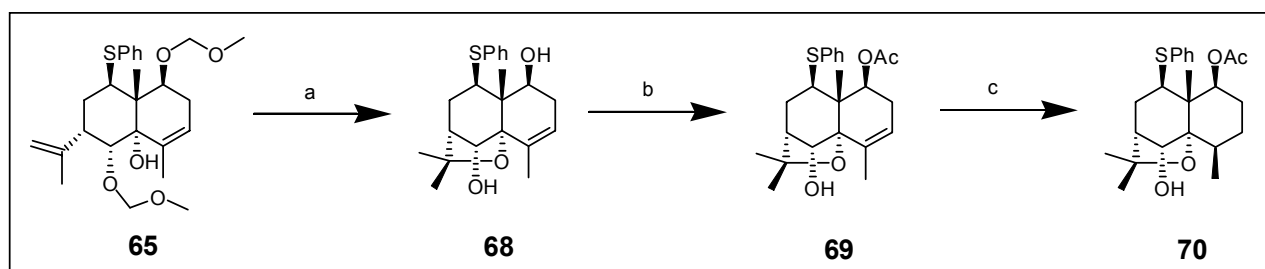


Figure 43 The Pummerer rearrangement and a competing elimination process

strategy was tested on other celafolin A-1 intermediates, (**64**) and (**68**), but these also failed to give the desired C-9 ketones. These initial results prompted a change in the synthetic scheme that would address this conversion at a later point.

Our attention then turned to the construction of the tetrahydrofuran C ring. The tricyclic tetrahydrofuran ring system (**68**) was constructed using a trifluoromethanesulfonic acid (TfOH) mediated etherification protocol. This method has been successfully used to close the C ring of



Reagents and conditions: a) TfOH, THF, 25 °C, 30%. b) Ac₂O, pyridine, DMAP, CH₂Cl₂, 25 °C, 56%. c) [Ir(cod)py(PCy₃)]PF₆, H₂, CH₂Cl₂, 65% based on recovered SM.

Figure 44 Completion of the celafolin A-1 ring system

similar natural products.^{37,45} The TfOH cyclization proceeded with the loss of both MOM ether protecting groups to give a diol (**68**) in modest yield (Figure 44). The success of this cyclization confirmed stereochemistry of the *trans*-ring junction, since the incorrect isomer at C-5 would have not undergone cyclization. NMR analysis, including H,H-COSY and 1D NOE experiments, were utilized to assign all of stereocenters in the tricyclic ring system (**68**). The data from the 1D NOE experiments for this diol (**68**) provided additional evidence supporting the *trans*-ring junction and previous stereochemical assignments (Figure 45). When the C-6 methine was irradiated, NOE enhancements were observed at the neighboring C-7 methine (5.5%) and also at the C-10 quaternary methyl group (5.7%). Even more satisfying, irradiation of the C-9 sulfide

methine provided a NOE enhancement to the C-1 methine (2.0%) suggesting the stereochemistry at C-1 is the desired (*S*) configuration required for celafolin A-1. Irradiation of the C-9 methine also produced an enhancement at one of the tetrahydrofuran ring quaternary methyl groups (3.7%), providing additional evidence for our assignments.

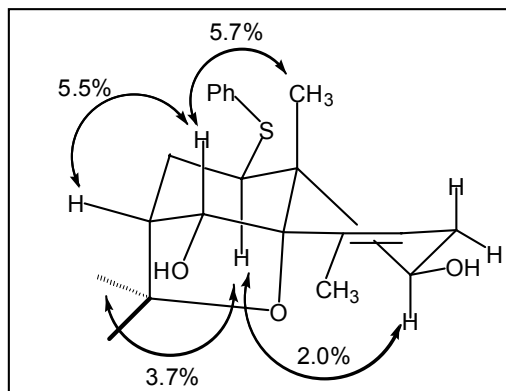


Figure 45 NOE results for diol (**68**)

The next challenge was to determine if the C-1 and C-6 hydroxyl groups could be selectively manipulated. Our analysis of the tricyclic ring system in Figure 45 shows that both alcohols are equatorial and adjacent to quaternary centers. The C-1 alcohol may be slightly more accessible since the C-2 carbon is di-substituted, whereas the C-7 carbon is tri-substituted. When the diol (**68**) was treated with acetic anhydride, pyridine, and DMAP in methylene chloride two products were isolated. One product was consistent with mono-acylation at the C-1 hydroxyl group (**69**) and was isolated in 56% yield (Figure 44). This was determined by the downfield shift observed at the C-1 methine in the ¹H NMR. The second product was consistent with acylation at both C-1 and C-6 hydroxyl groups. This *bis*-acylated byproduct was isolated in 11% yield and the starting material (**68**) was recovered in 33% yield. An interesting observation was that no product with *mono*-acylation at C-6 was found. This result indicates that the selectivity

for acylation at C-1 could be improved if a less-reactive acylating reagent was employed. For example, by excluding DMAP in the above reaction conditions the selectivity might improve.

The C-6 hydroxyl group was then utilized to perform a directed reduction of the C-3 olefin. This step involved using a directed hydrogenation to set the C-4 methyl stereocenter. Treatment of the homoallylic alcohol (**69**) with Crabtree's catalyst⁶⁴ under 1 atm of H₂ gave the desired product (**70**) in 65% yield based on recovered starting material. Examination of the ¹H NMR revealed a single diastereomer and the absolute configuration of this product (**70**) was assigned by a 1D NOE experiment (Figure 46). Irradiation of the C-6 methine showed a strong enhancement at the C-4 methyl group (3.1%). This enhancement would not be observed if the opposite stereocenter was formed. The presence of additional NOE enhancements at the C-7 methine (3.8%) and the C-10 methyl group (6.4%) provided further evidence supporting our stereochemical assignments.

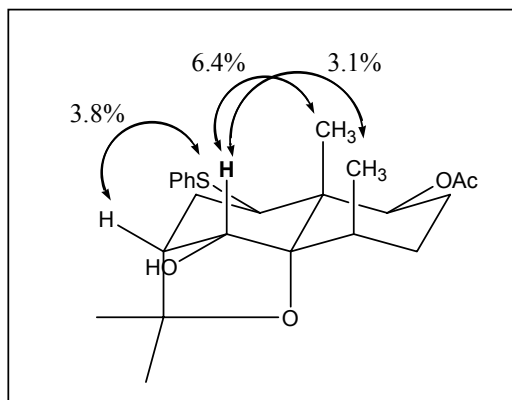


Figure 46 Acetate (**70**) NOE experiment

At this point, the skeleton of the dihydroagarofuran ring system was complete. Additional experiments showed that the C-6 hydroxyl group could be acylated with benzoyl triflate,⁶⁵ however insufficient quantities of the starting material (**70**) made complete characterization of this advanced intermediate difficult. Conversion of the C-9 phenyl sulfide into a carbonyl group

also proved difficult, as multiple Pummerer reaction conditions were explored but the neopentyl sulfide proved resistant to the desired reactivity. Overall, this synthesis represents a concise route to the *trans*-decalin core of the dihydroagarofuran natural products. Although this RCM route did not allow us to complete celafolin A-1, we were closer than ever to our goal.

The RCM sequence allowed us to test four new transformations, a ring closing metathesis reaction for constructing the *trans*-decalin core, a TfOH mediated etherification, C-1 and C-6 ester formation and differentiation, and a directed hydrogenation to set the C-4 stereocenter selectively. When we began to run out of options at the end of this sequence, we decided to evaluate how to improve the troublesome steps in this route.

Despite multiple attempts to optimize the tandem conjugate addition-aldol reaction, the isopropenyl Grignard addition, and the TfOH mediated etherification steps, no efficient conditions were found. These problems prevented the preparation of larger quantities of material and ultimately lead us to investigate alternative routes that would avoid these bottleneck steps.

3.3. A Revised Route to Celafolin A-1

Due to the difficulty encountered in multiple steps of the previous route, a completely new approach was designed. The ring closing metathesis route to celafolin A-1 (**11**) contained three troublesome elements that needed to be addressed. First, the yield of the aldol addition to construct the C-1 to C-10 carbon-carbon bond was low. Designing a system that will undergo an intramolecular aldol addition instead of a tandem conjugate addition-aldol process should improve the efficiency of the aldol reaction. Secondly, this new route would avoid the difficulties associated with nucleophilic additions at neopentyl centers, since the required C-1 and C-9 oxygen atoms are installed earlier in the synthesis. The conversion of the C-9 sulfide into a

ketone was a major problem encountered in earlier routes utilizing Pummerer⁶³ rearrangements. Finally, a better method for constructing the tetrahydrofuran C ring of the dihydroagarofuran skeleton needed to be found. Acid catalyzed etherification^{37, 45} was an impractical route, as demonstrated earlier, due to the presence of multiple acid labile groups incorporated as intermediates during the planned synthesis.

Our planned disconnections for a new aldol-based route to celafolin A-1 (**11**) are outlined in Figure 47. In a substantial change from our previous syntheses, we decided to investigate whether an intramolecular aldol addition could be used to generate the thermodynamically preferred *trans*-decalin ring junction. The C-5 stereocenter of the aldol precursor can be selectively constructed by an organolithium addition into the C-5 carbonyl group. This addition, as shown previously (Figure 36), should proceed through a Felkin-Ahn type process to give the desired C-5 stereoisomer for celafolin A-1. The required epoxide for this addition can be stereoselectively constructed from the known enone (**32a**) by treatment with alkaline hydrogen peroxide. This analysis then leads back to (*R*)-(-)-carvone as the preferred chiral starting material.

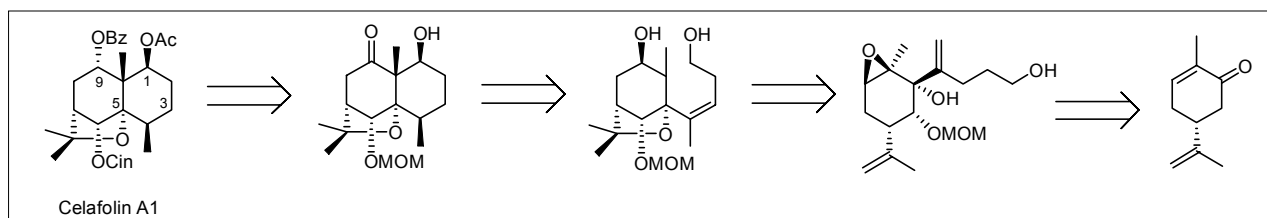
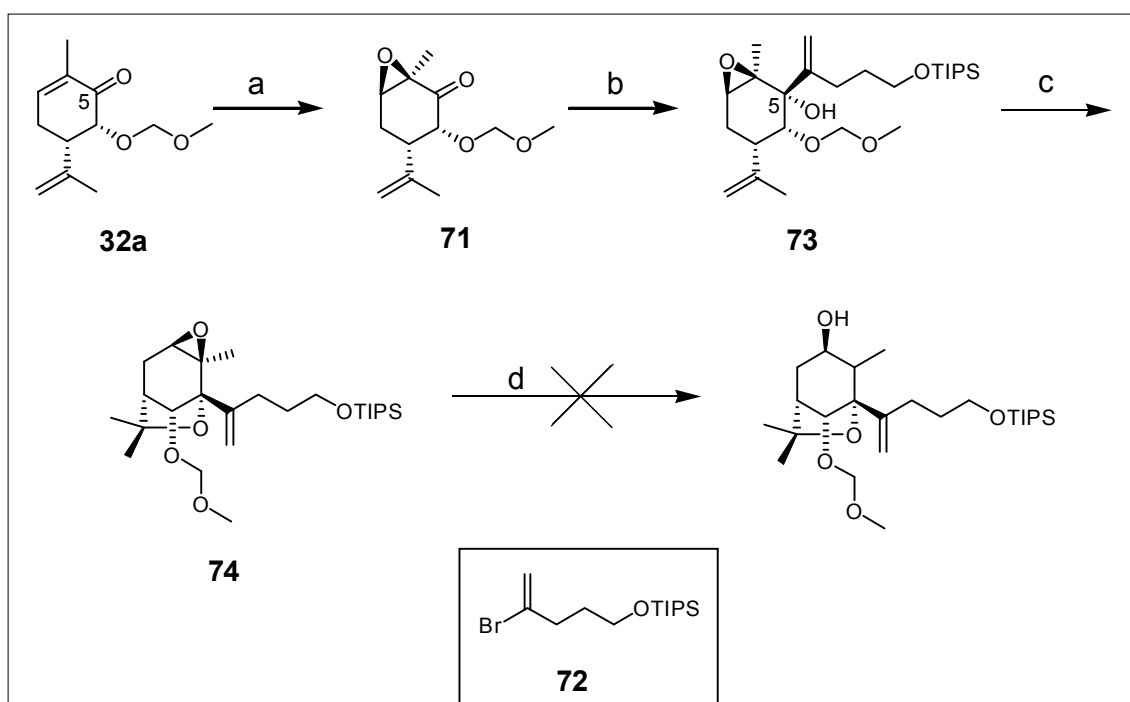


Figure 47 Revised retrosynthesis of celafolin A-1

Our intramolecular aldol addition route to celafolin A-1 (**11**) began with the known enone (**32a**) that was used in the three previous routes. The first new step in this sequence was to

epoxidize the enone using the conditions developed by House and coworkers.⁶⁶ We found that subjection of the enone (**32a**) to hydrogen peroxide and sodium hydroxide in methanol and water caused C-6 epimerization and extensive decomposition. Using a modification of the House epoxidation method, the enone (**32a**) was cleanly epoxidized with hydrogen peroxide and potassium carbonate in a mixture of methanol, water, and tetrahydrofuran.⁶⁷ These conditions provided the desired epoxy ketone (**71**) in good yield with no C-6 epimerization (Figure 48).



Reagents and conditions: a) K₂CO₃, H₂O₂, H₂O, THF, 25 °C, 77%. b) (4-bromo-pent-4-enyloxy)-triisopropylsilane (**72**), *t*-BuLi, THF, -78 °C, β:α= 12:1, 58%. c) i. I₂, pyridine, CH₂Cl₂, 25 °C, ii. AIBN, Bu₃SnH, toluene, reflux, 87% (2 steps), d) Cp₂TiCl₂, 1,4-cyclohexadiene, Mn, collidine-HCl, THF, 25 °C.

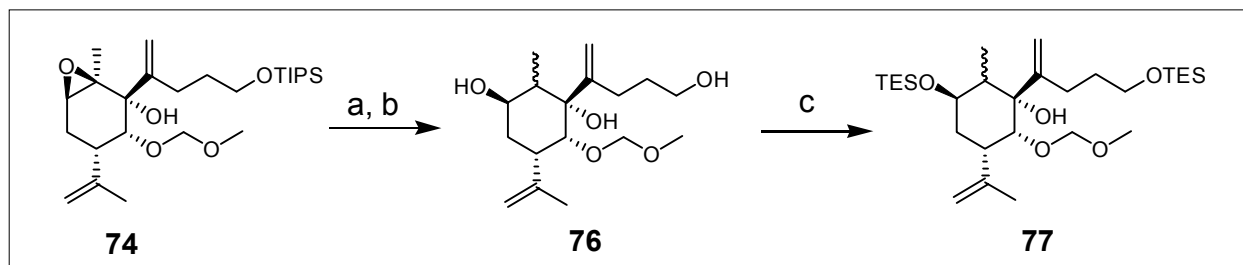
Figure 48 Construction of the tetrahydrofuran C ring

The next step required the addition of a vinyl lithium reagent into the C-5 carbonyl to construct the C-4 to C-5 carbon-carbon bond and generate the required (*R*)-stereocenter at C-5

for celafolin A-1 (**11**). The known vinyl bromide (**72**) was constructed by alkylation of the lithium enolate of *t*-butyl acetate with 2,3-dibromopropene, followed by a LiAlH₄ reduction and protection of the primary alcohol as a triisopropylsilyl (TIPS) ether. The vinyl bromide (**72**) was then treated with two equivalents of *t*-butyl lithium at -78 °C to cleanly generate the required vinyl lithium reagent. This vinyl lithium derivative of (**72**) was then added to a solution of the epoxy-ketone (**71**) in tetrahydrofuran at -78 °C. The resulting regioselective addition into the C-5 carbonyl group gave the expected allylic alcohol as a 12:1 ratio of diastereomers at C-5 in 58% yield, favoring the desired diastereomer (**73**).

Initially, the next step was to utilize an iodoetherification-dehalogenation procedure to close the tetrahydrofuran C ring (Figure 48). Exposure of the epoxy-alcohol (**73**) to iodine and pyridine in methylene chloride, followed by treatment with tributyltin hydride and AIBN gave the desired [3.2.1] bicyclic ring system (**74**) in 87% yield over two steps. However, we later found that this substrate would not undergo epoxide opening. Reagents that failed to open this epoxide include titanocene chloride, Red-Al, and sodium cyanoborohydride in the presence of boron trifluoride diethyl etherate.

The failure encountered in opening the epoxide at this stage led us to investigate this transformation at other points in this sequence. The silyl ether substrate (**73**) was subjected to the titanocene chloride and cyclohexadiene reductive epoxide opening conditions, but also failed to react. Eventually, a solution was found to this problem. When the TIPS ether in the epoxy-alcohol (**73**) was removed, the diol species (**75**) underwent reductive epoxide opening mediated by titanocene chloride⁶⁸ to give the triol product (**76**) in excellent yield. A second, minor product, isolated from this reaction was determined to be an allylic alcohol formed due to radical



Reagents and conditions: a) TBAF, THF, 93%. b) Cp_2TiCl_2 , 1,4-cyclohexadiene, Mn, collidine-HCl, THF, 25 °C, 80%. c) TESCl, pyridine, DMAP, CH_2Cl_2 , 55%.

Figure 49 A successful epoxide-opening route

disproportionation. The formation of this byproduct can be explained by examining the mechanism for this reductive epoxide opening process (Figure 50). The desired product is formed when the tertiary carbon radical abstracts a hydrogen atom from 1,4-cyclohexadiene or from 1,4-cyclohexadiene radical. The undesired allylic alcohol byproduct results from radical disproportionation. This disproportionation process occurs when the tertiary radical encounters another radical species before it can abstract a hydrogen atom from 1,4-cyclohexadiene. This process can be minimized, but not eliminated, by using excess 1,4-cyclohexadiene.

In order for this reductive epoxide opening to be catalytic, the titanocene chloride must be regenerated during the reaction. To complete the catalytic cycle in Figure 50, two steps need to occur before the titanium (IV) alkoxide can be converted back to the catalytically active titanium (III) species. One of the two steps requires protonation of the titanium bound oxygen atom and the second step requires manganese metal to reduce the titanium (IV) to titanium (III).

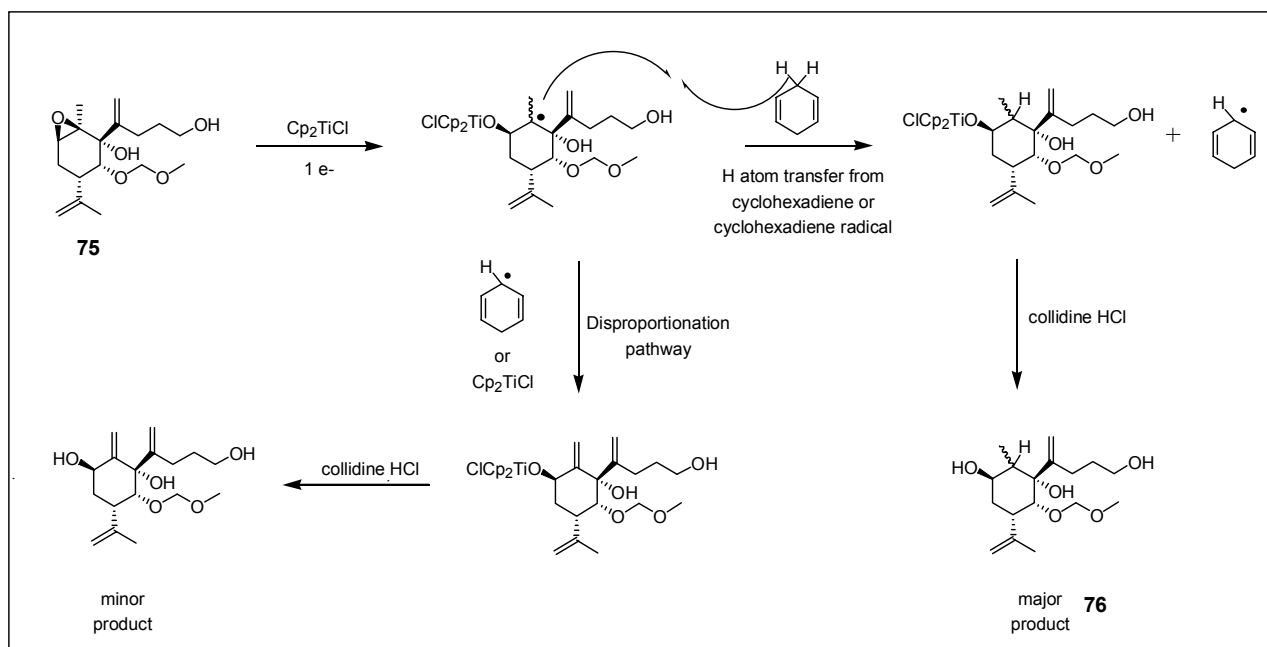
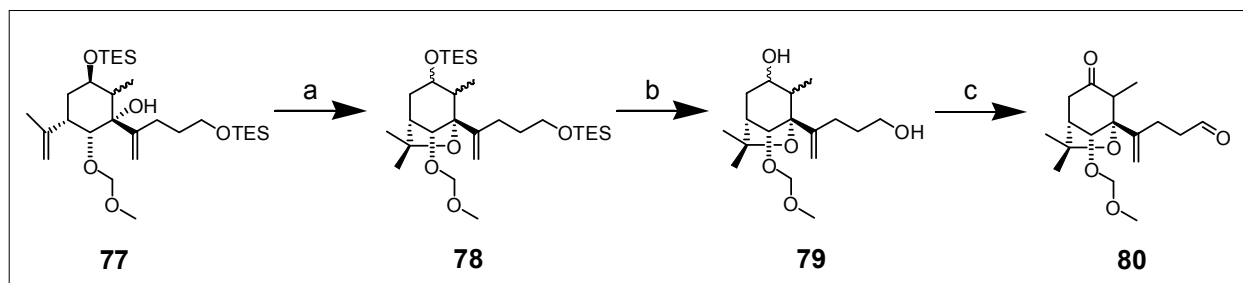


Figure 50 Titanocene chloride reductive epoxide opening

The titanium oxygen bond is a comparatively strong bond and therefore requires a relatively strong acid to facilitate cleavage. However, if a strong Bronsted acid were used, the manganese metal would oxidize when exposed to the acid and would not be able to regenerate the titanocene (III) chloride. To successfully complete the catalytic cycle, this reaction requires an acid that is strong enough to facilitate cleavage of the titanium oxygen bond, but weak enough to prevent manganese metal oxidation. This is the reason for the use of the fairly uncommon reagent, collidine hydrochloride, during this epoxide opening reaction.

In order to close the tetrahydrofuran ring, the primary and secondary hydroxyl groups in the triol substrate (**76**) required protection. Both hydroxyl groups were protected as triethylsilyl (TES) ethers using TESCl, DMAP, and pyridine to afford the *bis*-silyl ether (**77**) in an acceptable yield. A two-step iodoetherification-dehalogenation procedure (Figure 51) gave the expected tetrahydrofuran product (**78**) in 55% yield. After carefully analyzing the ^1H NMR data for the

tetrahydrofuran product (**78**), an interesting observation was made. We noticed that the stereochemistry at the C-9 TES ether had been partially epimerized. The presence of two



Reagents and conditions: a) i. I₂, pyridine, CH₂Cl₂, 25 °C, ii. AIBN, Bu₃SnH, toluene, reflux, 55% (2 steps). b) TBAF, THF, 25 °C, 92%. c) DMPI, NaHCO₃, CH₂Cl₂, 25 °C, 80%.

Figure 51 Formation of the tetrahydrofuran C ring

diastereomers was particularly noticeable in the region of the MOM ether proton signals. A probable mechanism for the epimerization that occurred during the dehalogenation process is shown in Figure 52.

The primary alkyl iodide precursor of the [3.2.1] bicyclic ring containing substrate (**78**) contains a mixture of four diastereomers resulting from the previous epoxide opening and the stereo-random etherification. When the primary alkyl iodide reacts with the tributyltin radical, a primary carbon radical is produced. If given the opportunity, this high-energy primary radical can abstract a hydrogen atom to form a lower energy radical. Figure 52 shows one of the two radical intermediates is within close proximity to the C-9 hydrogen atom. Hydrogen atom transfer results in the formation of an oxygen stabilized tertiary radical. Eventually this new radical is reduced with tributyltin hydride and during this process the C-9 center is epimerized. Fortunately, this process is inconsequential since the C-9 stereocenter will be oxidized to a ketone after the TES ethers are removed.

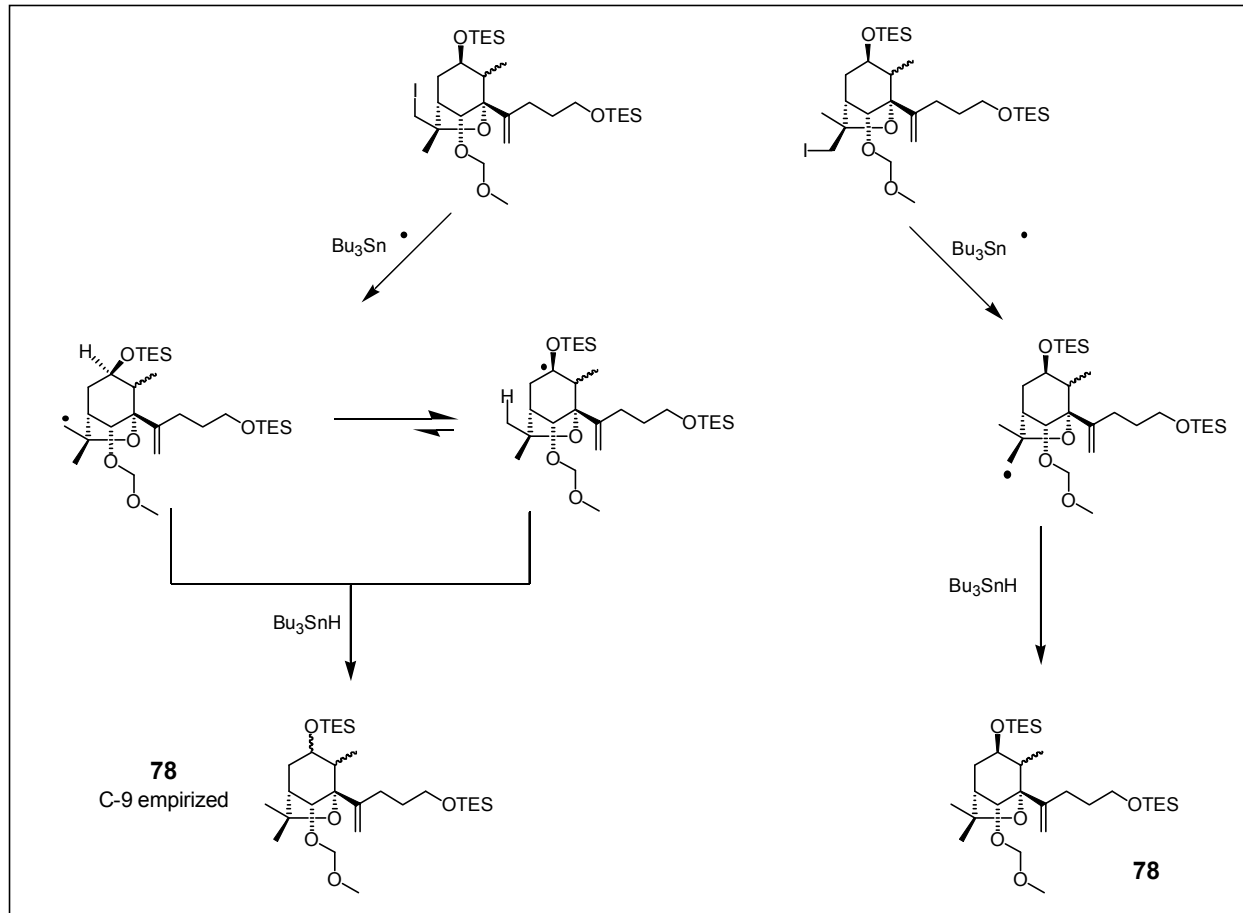


Figure 52 Mechanism for C-9 epimerization

This two-step iodoetherification-dehalogenation procedure (Figure 51) yields the desired tetrahydrofuran ring system in an overall yield of 55%. This represents a substantial improvement compared to a 30% yield from the previous TfOH catalyzed etherification method (Figure 44).⁶⁹ The TES ethers groups present in (**78**) were then removed by treatment with TBAF to give the desired diol (**79**). Dess-Martin periodinane (DMPI) oxidation⁴⁷ afforded the keto-aldehyde (**80**) as a single isomer.

In order to generate the required *trans*-decalin ring fusion, conditions for thermodynamic equilibrium needed to be determined. The *cis*-decalin ring system is the kinetically favored

product when an intramolecular aldol addition is utilized to construct a [4.4.0] fused bicyclic ring. The *trans*-decalin ring system, which is the thermodynamically favored product, can only be obtained if the conditions employed allow for equilibration to occur. For comparison purposes, the difference in energy between a *cis*-decalin and a *trans*-decalin ring is approximately 3 kcal/mol. The difference in energy between the *cis*- and *trans*-decalin ring junctions in the tricyclic ring systems of the potential aldol adducts in Figure 53 is unknown. In order to estimate the energy differences between the possible aldol products, molecular mechanics calculations were performed. Macromodel (v. 5.5) was utilized to perform a Monte Carlo conformational search using the MM2* force field.⁷⁰

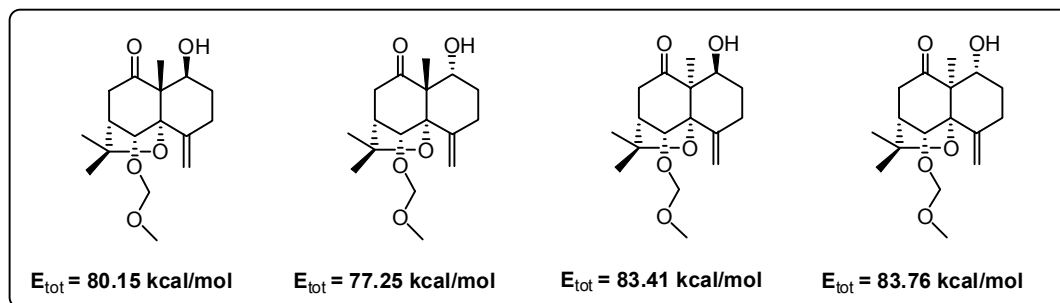


Figure 53 Macromodel Monte Carlo calculations

After minima for each of the possible products were found, it became apparent (Figure 53) that the *trans*-decalin products were the thermodynamically favored species. Both of the *cis*-decalin adducts were found to be at least 3-6 kcal/mol higher in energy than the corresponding *trans*-decalin isomers. This energy difference is in agreement with the energy difference between *cis*- and *trans*-decalin rings. Figure 53 shows that both *cis*-decalin aldol adducts are practically identical in energy. The *cis*-decalin adduct with the equatorial C-1 alcohol may be slightly lower in energy due to a hydrogen bonding interaction with the C-9 carbonyl group. The second *cis*-

decalin adduct has an axial C-1 alcohol that cannot participate in a hydrogen bond since it points away from the C-9 carbonyl group (see NOE Figure 56).

The interactions responsible for the larger energy difference between the two *trans*-decalin isomers cannot be attributed to only hydrogen bonding with the C-9 carbonyl group. In the *trans*-decalin ring system, each isomer has a hydroxyl group that is equally likely to participate in a hydrogen bond with the C-9 ketone (Figure 54). However, the axial isomer can participate with a second hydrogen bond acceptor group, the oxygen atom in the tetrahydrofuran ring. This interaction alone can still not explain the greater than 3 kcal/mol energy difference.

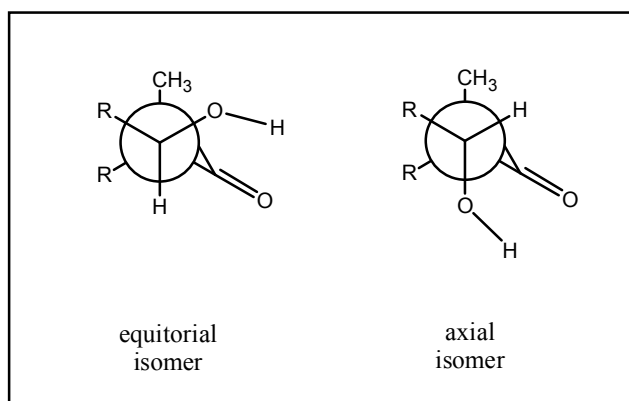


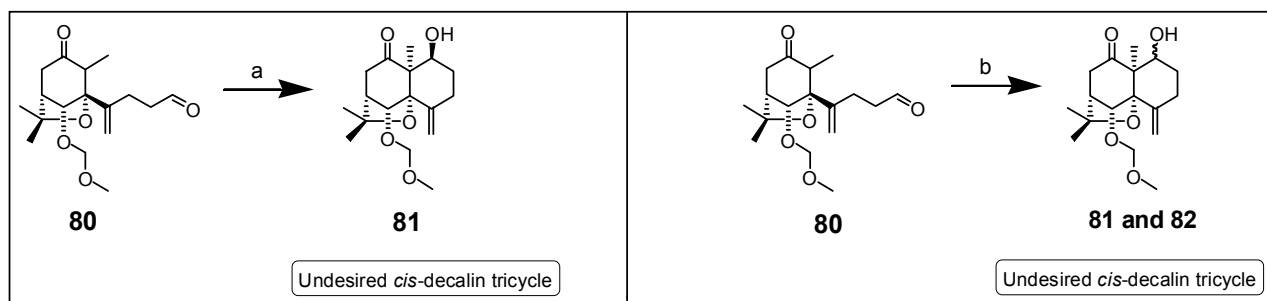
Figure 54 Hydrogen bonding interactions in the *trans*-decalin ring system

Further examination shows the equatorial alcohol in the *trans*-decalin ring has a higher energy interaction with the neighboring quaternary center methyl group. The axial alcohol isomer does not experience this gauche interaction with the C-10 quaternary center.

The results from our Macromodel calculations led to the conclusion that equilibration of the *cis*-decalin ring to the *trans*-decalin ring should be thermodynamically favorable, but the activation barrier for this conversion was still unknown. The Curtin-Hammett principle states that the product distribution is not dependent upon the energy difference of the products, but rather

the energy difference between the two transition states leading to the products. We anticipated that the use of non-equilibrating enolization conditions, such as LDA, would give the kinetically preferred *cis*-decalin ring fusion. The use of equilibrating conditions during the aldol addition should result in equilibration and favor formation of the *trans*-decalin products.

In order to test this theory, the amine base DBU was initially investigated (Figure 55). Treatment of keto-aldehyde (**80**) with DBU in methylene chloride at high dilution for 5 hours



Reagents and conditions: a) DBU, CH₂Cl₂, 25 °C, 5 hrs, 71%. b) DBU, CH₂Cl₂, 25 °C, 18 hrs, $\alpha:\beta= 3:1$, 80%.

Figure 55 DBU intramolecular aldol additions

resulted in clean conversion to the aldol adduct (**81**). The ¹H NMR was consistent with the desired product and the C-1 methine hydrogen appeared as a doublet with a coupling constant of 2.9 Hz. The multiplicity and coupling constant for this hydrogen suggested that the C-1 hydroxyl group was in the axial position. To verify the stereochemistry, H,H-COSY and 2D NOESY experiments were performed. The most noticeable cross peak in the NOESY spectrum (Figure 56) was between the C-10 methyl group and the C-1 methine hydrogen. Since we had established that the C-1 hydroxyl group was in an axial position, this NOESY result suggests a *cis*-decalin bicyclic ring with the B ring in a chair-like conformation. A second cross peak was observed between the C-6 methine and the axial hydrogen of the C-8 methylene group. This suggests that

the A ring is in a chair conformation. A third NOESY cross peak was also found between the C-10 methyl group and one of the C-4 olefin hydrogens, providing additional evidence for a

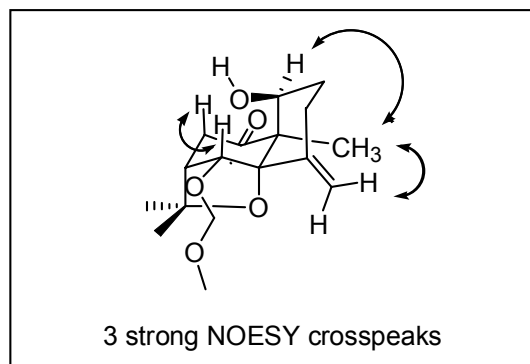


Figure 56 NOESY for *cis*-decalin (81**)**

chair-like conformation in the B ring. These results (Figure 56) clearly showed this species (**81**) was the undesired *cis*-decalin adduct.

In an identical experiment using DBU, the reaction duration was increased to 18 hours. These conditions produced two products, the initially isolated *cis*-decalin species (**81**) and a new isomer (**82**). Analysis of the ^1H NMR coupling constants revealed that the new product (**82**) contained an equatorial C-1 hydroxyl group. Our assignment was based on the appearance of the C-1 hydrogen as a doublet of doublet of doublets (ddd) with coupling constants of 12.4, 4.9, and 1.1 Hz. The unusual multiplicity of a ddd at this position can be attributed to long-range coupling to possibly the C-4 methylene group. After utilizing a H,H-COSY experiment to verify the identity of each proton, a 2D NOESY experiment was used to determine the stereochemistry (Figure 57). Four important cross peaks were observed in this experiment. The C-1 and C-6 methine groups and the C-8 axial methylene hydrogen each possessed cross peaks to one

another. The fourth cross peak found was between the C-10 methyl group and one of the C-4 olefin hydrogens. Since this identical cross peak was observed in the NOESY spectrum of other

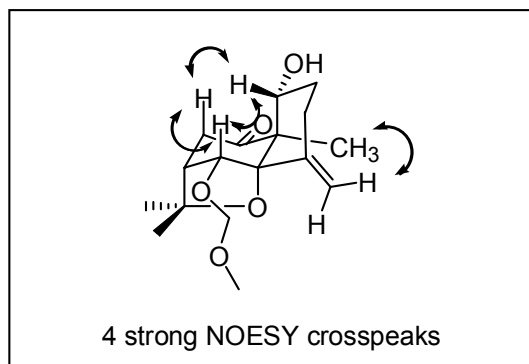


Figure 57 NOESY for *cis*-decalin (**82**)

aldol isomer (**81**), it can be reasoned that this new species (**82**) is also not a *trans*-decalin adduct. All four of these cross peaks are consistent with another *cis*-decalin ring system.

Isomerization of the *cis*-decalin ring to the *trans*-decalin ring was proving to be a difficult conversion. The equilibration of the *cis*-axial isomer (**81**) to the *cis*-equatorial isomer (**82**) corresponds to Macromodel calculations and experimental observations, but *cis*- to *trans*-decalin conversion does not. Thermodynamic equilibration of the *cis*-decalin kinetic product to the *trans*-decalin product may require longer reaction times. We tested this theory by subjecting the keto-aldehyde (**80**) to DBU in methylene chloride for 72 hours. When this reaction was checked using ^1H NMR analysis, only *cis*-decalin products were observed. The keto-aldehyde (**80**) was also exposed to potassium carbonate in methanol, since a protic solvent may disrupt the hydrogen bonding network in the aldol products (**81** and **82**) and possibly promote *cis*- to *trans*-decalin conversion. After stirring for 72 hours, the crude ^1H NMR spectrum still showed only *cis*-decalin aldol adducts (**81**) and (**82**).

Figure 58 illustrates why isomerization of the *cis*-decalin ring to the *trans*-decalin ring is not occurring. Analysis of either the chair or the boat transition state leading to the *cis*-decalin ring system shows that the exocyclic C-4 olefin is in a staggered conformation with respect to the

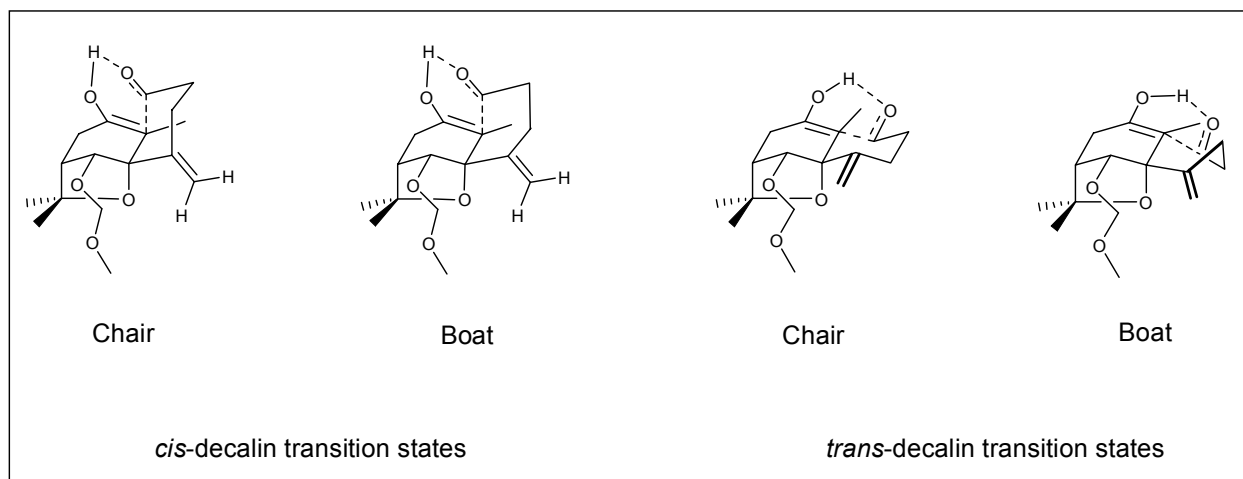


Figure 58 Transition states for *cis*- and *trans*-decalin ring forming aldol reactions

C-5 tetrahydrofuran oxygen and the C-6 MOM ether. In order to achieve a conformation that will access the transition states required for the *trans*-decalin product, the C-4 olefin has to either eclipse the C-6 MOM ether (chair) or rotate counterclockwise moving closer to the C-6 MOM ether (boat). The methyl groups on the THF C-ring also partially block the approach of the aldehyde in the *trans*-decalin transition states. Although the experiment was not attempted, heating this reaction may provide enough energy to allow rotation around the C-4 / C-5 bond and could provide access to the transition states leading to the *trans*-decalin products.

The principle of least motion can also be invoked to explain our inability to convert the *cis*-decalin products (**81** and **82**) to the desired *trans*-decalin species. Even if the aldol reaction is reversible, and we have shown that it is, the formation of the *trans*-decalin ring requires the

aldehyde to wrap around to the opposite face of the ring. If bond rotation is somewhat slow, this reorganization process is difficult during an intramolecular reaction.

Although initial experiments failed to obtain the desired *trans*-decalin ring system, this method has successfully circumvented three problems encountered in the previous routes. The yield of the intramolecular aldol reaction utilized to construct the C-1 to C-10 bond is substantially higher than the conjugate addition aldol. The incorporation of oxygen was achieved at C-9 prior to the formation of the quaternary C-10 stereocenter. This early transformation eliminates the need for a Pummerer rearrangement, which is a difficult transformation at a neopentyl carbon with β -hydrogens present. This route has also demonstrated that the use of an iodoetherification reaction to close the tetrahydrofuran C ring gives a better yield than the corresponding triflic acid procedure used in earlier routes. Additionally, the intramolecular aldol route can quickly build up a complex ring system and is flexible enough to allow for the preparation of analogs with no changes other than ester groups at the end of the synthesis. Further experimentation should allow for a means to obtain the desired *trans*-decalin ring fusion.

When conditions are found which generate the *trans*-decalin ring system this route will be an exceptionally facile route to the dihydroagarofuran tricyclic ring system. The remaining steps for the total synthesis consist of a directed reduction of the C-9 ketone and removal of the C-6 MOM ether. This sequence gives the triol analog of celafolin A-1. The remaining ester groups can be selectively installed, similar to previous work, since each hydroxyl group is in a unique steric environment.⁶⁹

3.4. Summary

This body of work has shown that the *trans*-decalin skeleton (**68**) of the dihydroagarofuran natural products can be quickly synthesized from (*R*)-carvone in eight steps.⁶⁹ A key aspect of the RCM route to the celafolin A-1 intermediate (**68**) is the tandem conjugate addition-aldol reaction. This reaction creates the C-1 to C-10 bond and sets the C-1, C-9, and C-10 stereocenters with excellent control. Although the overall yield is low, 7% for eight steps, this route is substantially shorter than previously published routes. In fact only two of the eight steps, the aldol addition and TfOH catalyzed etherification, are problematic.

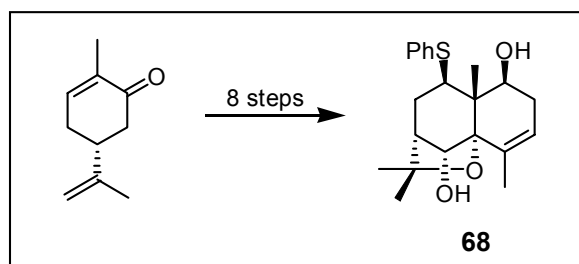


Figure 59 RCM route to celafolin A-1

In order to improve these two steps an intramolecular aldol route was designed. A four-step sequence was used to construct the tetrahydrofuran precursor (**77**) in an acceptable 24% yield. There are two advantages associated with avoiding the thiophenol conjugate addition process. First, the oxygen at C-9 was already installed using this new route, since Pummerer reactions failed to provide this functional group previously. Secondly, an iodoetherification method was used to close the tetrahydrofuran C-ring. This reaction is milder than TfOH, but

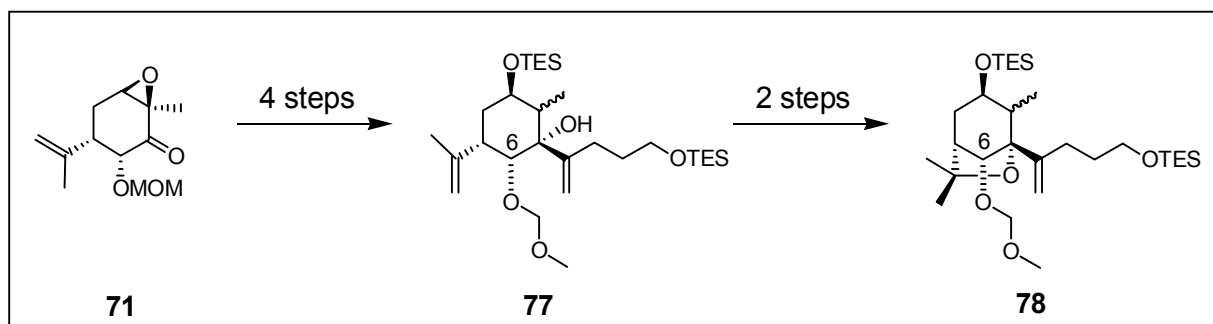


Figure 60 The intramolecular aldol addition route

could not be used in the two earlier routes due to the presence of the phenyl sulfide group. The phenyl sulfide group would readily oxidize in the presence of iodine. This two-step procedure utilized iodine and pyridine to close the tetrahydrofuran ring, then tributyltin hydride and AIBN to reduce the primary alkyl iodide. This sequence produced the desired [3.2.1] bicyclic ring system (**78**) in superior yield.

The last challenge to address was how to improve the C1 to C10 bond forming aldol process. Our results have demonstrated that an intramolecular aldol reaction can substantially improve this process. The chemical efficiency of the intramolecular aldol process was excellent. Macromodel calculations (Figure 53) show that the *trans*-ring junction should be the thermodynamically preferred product, but initial experiments gave exclusively the kinetically preferred *cis*-decalin adducts. More conditions need to be explored for this step. If this conversion is possible, this may be the preferred route to the dihydroagarofuran natural products.

4. Studies Directed Toward Bryostatin 1: A MDR Modulating Natural Product

Tetrahydropyran (THP) rings are common structural elements present in numerous biologically active molecules such as: polyether antibiotics, marine toxins, pheromones, C-glycosides⁷¹ and anti-tumor species such as bryostatin⁷² and phorboxazole⁷³ (Figure 61). A variety of methods have emerged recently⁷⁴⁻⁸⁹ for the non-racemic construction of 2,6-*cis*-THP rings contained in these natural products.

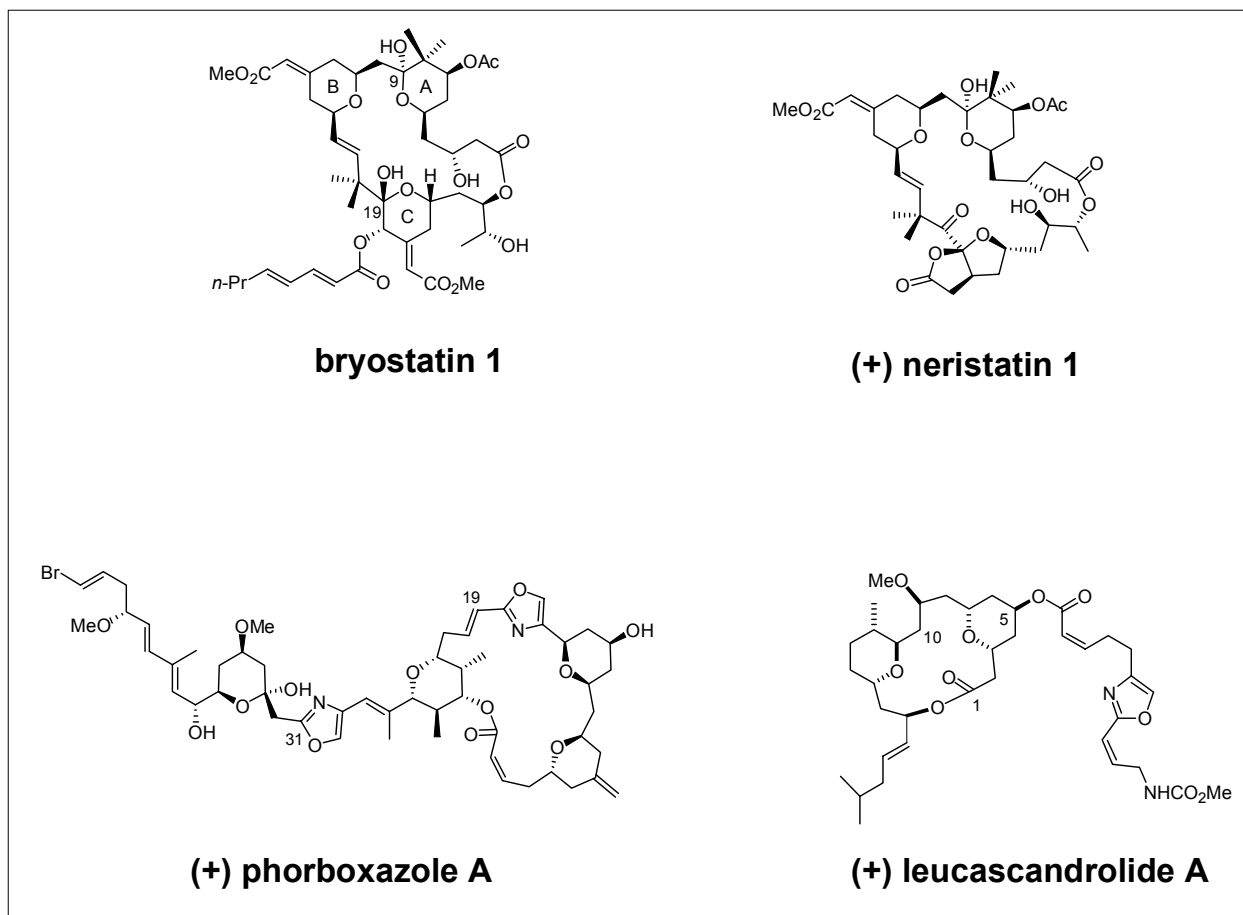


Figure 61 Bioactive THP ring containing natural products

A survey of recent publications shows that there are at least five common routes to 2,6-*cis*-THP ring systems: hetero Diels-Alder reactions,⁷⁴ S_N2 type cyclizations,⁷⁵ Claisen rearrangements,⁷⁶ ring closing metathesis,⁷⁷ and Prins cyclizations.⁷⁸⁻⁸⁴ Prins reactions have become a popular method for this transformation. However, many of these recent Prins methods require the use of strong acids to generate oxocarbenium ions via condensation of an alcohol and an aldehyde.⁸⁰⁻⁸⁴ Few examples exist where non-racemic THP ring systems are formed under mild conditions using relatively weak Lewis acids.

A selection of recent methods for constructing non-racemic THP rings is shown in Figure 62. The first method in Figure 62 is from Evans and coworkers synthesis of bryostatin 2.⁸⁵ Evans' route to the bryostatin THP B ring utilized a sequence of aldol reactions to construct a β,δ -dihydroxy ester. When this substrate was exposed to trifluoroacetic acid (TFA), the desired lactone was formed in high yield. Evans then used a two-step sequence, organolithium addition and elimination, to convert this lactone into a 2,6-*cis*-THP ring. One year after Evans method was disclosed, Smith⁸⁶ reported that the Petasis-Ferrier rearrangement⁸⁷ could be used to synthesize chiral 2,6-*cis*-THP rings. Smith's method utilizes dimethylaluminum chloride to ionize a vinyl acetal into an oxocarbenium ion and an aluminum enolate. The recombination of these two groups, via a chair transition state, results in the selective formation of a 2,6-*cis*-THP ring. Rychnovsky has also demonstrated that α -acetoxy ethers can be used to regioselectively generate oxocarbenium ions for Prins reactions.⁸⁸ The major drawback associated with these three methods is that a strong Lewis acid is required to initiate THP ring formation.

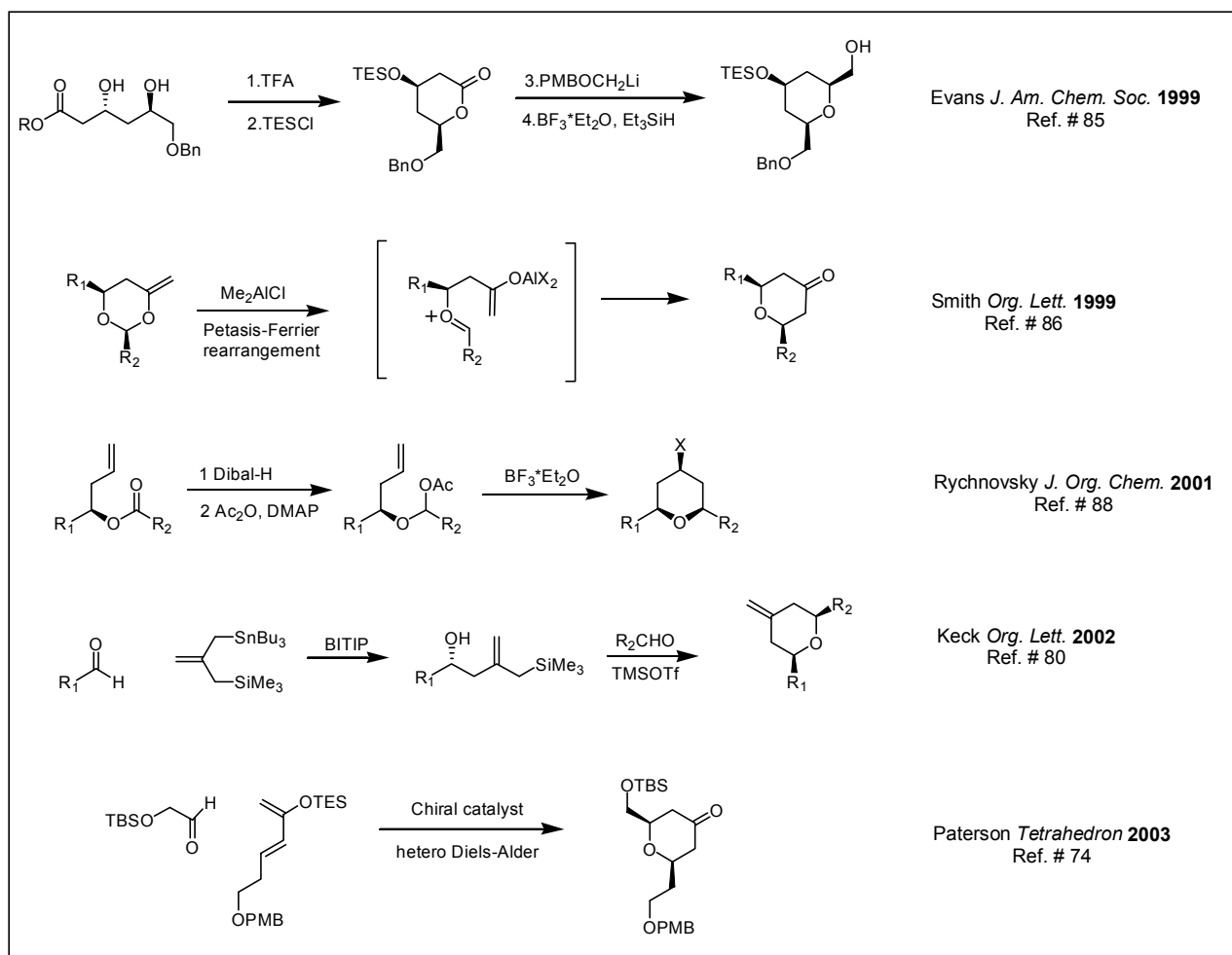


Figure 62 Five routes to non-racemic 2,6-*cis*-THP rings

In 2002, Keck reported a new catalytic asymmetric method for constructing allyl silane substrates for intramolecular Prins reactions.⁸⁰ Keck's method is attractive since it utilizes achiral starting materials and a chiral titanium binol catalyst (BITIP) to generate hydroxy-allyl silanes with high enantioselectivity. Finally, the hetero Diels-Alder reaction is also an important method for synthesizing chiral THP rings. A recent example is from Paterson's total synthesis of (+)-leucascandrolide A.⁷⁴ Paterson was able to construct the C-1 to C-10 subunit of (+)-leucascandrolide A in greater than 95% enantiomeric purity using a hetero Diels-Alder reaction

with a Jacobsen's catalyst. This method is perhaps the mildest of the reactions shown in Figure 62.

4.1. A Mild Method for Constructing 2,6-*cis*-THP Rings

During the course of our studies toward the synthesis of MDR modulating natural products, a new and exceptionally mild method for constructing 2,6-*cis*-THP rings was developed. Previous work in our laboratory (Figure 63) has shown that an intramolecular Prins reaction between an acetal and an allylic silane can be used to synthesize 2,6-*cis*-THP rings in high yield.^{79, 89} While it is well known that allylic silanes are excellent nucleophiles for trapping oxocarbenium ions,⁹⁰⁻⁹⁴ we have found that Prins reactions with allylic silanes can be carried out in aqueous media utilizing the Lewis acid surfactant catalysts Sc(SDS)₃⁹⁵ or Ce(NO₃)₃ / SDS.⁷⁹ Our new method utilizes a cyclic acetal as an oxocarbenium ion precursor. This unique process generates a highly reactive oxocarbenium ion in an aqueous system under very mild conditions.

While we were developing new substrates for this method, we observed that silyl enol ethers were not as reactive towards cyclization compared to allylic silanes. Silyl enol ethers, under identical reaction conditions, routinely produced low yields of the desired Mukaiyama aldol⁹⁶ products (Figure 63). Several experiments were attempted in order to optimize this reaction. Our observation was that conversion of *tert*-butyldimethylsilyl enol ethers to tetrahydropyranones was slow. Since prolonging the reaction time resulted in slow hydrolysis of the *tert*-butyldimethylsilyl enol ether, we predicted that a triisopropylsilyl enol ether might prevent hydrolysis. The triisopropylsilyl enol ethers were effective in preventing hydrolysis, but were now not reactive toward cyclization. The addition of more Lewis acid or more SDS also failed to improve conversions. Eventually, we discovered that simply replacing the aqueous

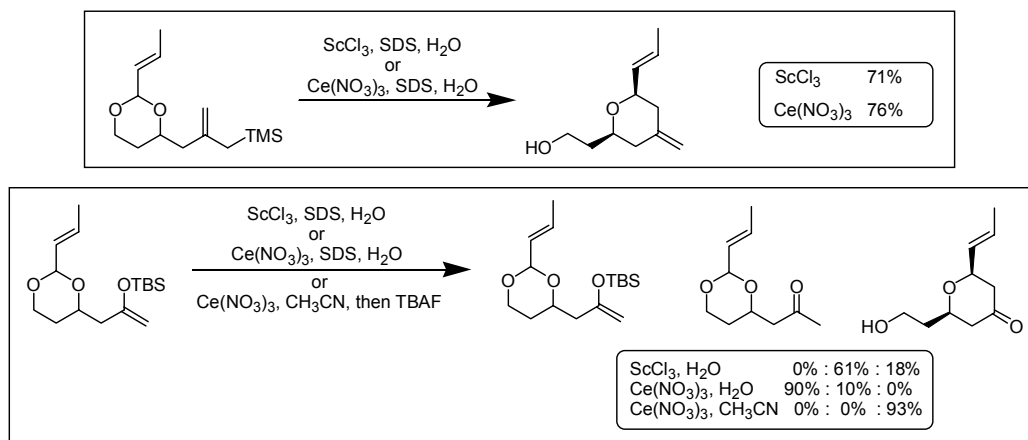


Figure 63 Aqueous Prins and Mukaiyama aldol conditions

media with acetonitrile produced superior results. The desired Mukaiyama aldol reaction⁹⁶ now proceeded to full conversion in one hour at ambient temperature using $\text{Ce}(\text{NO}_3)_3$, a very mild Lewis acid.

Before $\text{Ce}(\text{NO}_3)_3$ was evaluated, we had previously screened other Lewis acids, including TiCl_4 and TMSOTf , for this reaction but the lanthanide species $\text{Ce}(\text{NO}_3)_3$ produced the best results. There were also several other features associated with $\text{Ce}(\text{NO}_3)_3$ that made it a desirable Lewis acid. First, lanthanide metal complexes are known to undergo fast inner-sphere ligand exchange.⁹⁷ This aspect of $\text{Ce}(\text{NO}_3)_3$ promotes turnover and prevents product inhibition at the catalytic metal center. Secondly, $\text{Ce}(\text{NO}_3)_3$ is non-corrosive, non-toxic and easy to handle, unlike TiCl_4 , TMSOTf , or BF_3 etherate. Lastly, $\text{Ce}(\text{NO}_3)_3$ is easy to separate from the organic products and will not form troublesome emulsions.

An interesting aspect of our cyclization reaction was the observation that regardless of nucleophile and acetal structure, 2,6-*trans*-THP or tetrahydropyranone rings were never isolated. The exclusive selectivity for 2,6-*cis*-THP or tetrahydropyranone products can be explained by examining a chair transition state model (Figure 64). In the initial oxocarbenium ion

intermediate, and then in the Prins or Mukaiyama aldol reaction transition state, both substituents are preferentially in the pseudo-equatorial position. We believe this transition state produces the observed 2,6-*cis* stereochemical selectivity.

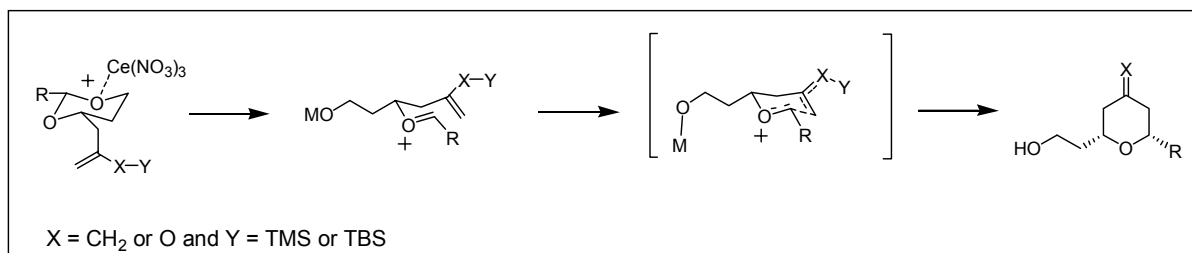


Figure 64 Chair transition state model

More importantly, side chain scrambling, which normally occurs during Prins reactions due to the troublesome oxonia-Cope rearrangement,^{82, 98} was not observed under our conditions (Figure 65). The oxonia-Cope rearrangement is less favorable in our substrates due to the stabilizing effect of the α,β -unsaturated acetal. Fragmentation of the acetal generates an oxocarbenium ion that will not easily undergo a [3,3] sigmatropic rearrangement. The rearrangement would produce a higher-energy oxocarbenium ion, preventing the formation

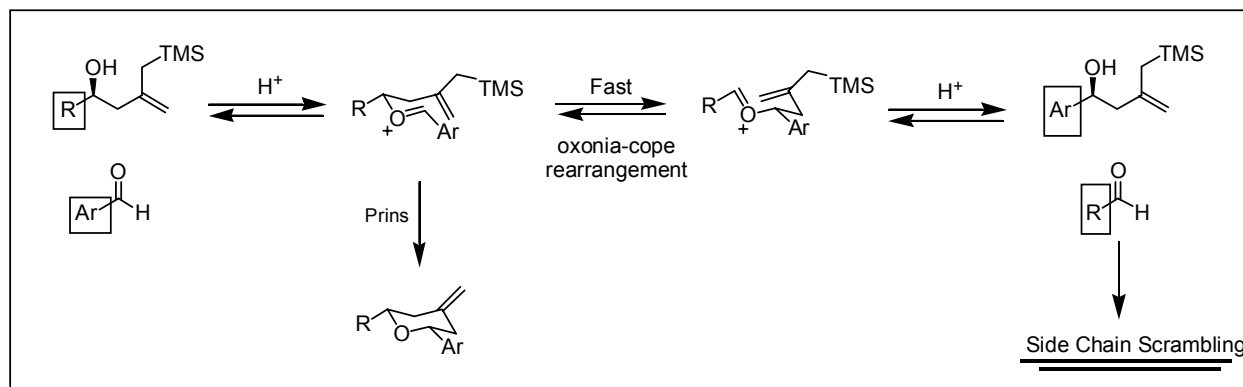


Figure 65 The oxonia-Cope rearrangement produces side chain scrambling

of the oxonia-Cope product (Figure 66). Encouraged by these results and our success with model systems (Figure 71), a new asymmetric route to the B-ring fragment (C-9 to C-19) of bryostatin 1 was pursued.

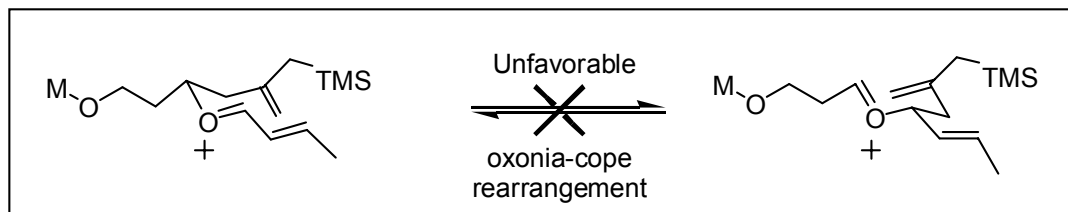


Figure 66 An unfavorable [3,3]-rearrangement

4.2. The Bryostatins: Isolation and Biological Activity

In 1968 the first bryostatin, bryostatin 1, was isolated from the marine bryozoa *Bugula neritina linnaeus*.⁹⁹ The structure of bryostatin 1 was first determined by Petit in 1982 using a combination of single crystal X-ray diffraction analysis, NMR, and high-resolution mass spectroscopy.¹⁰⁰ Since then, over twenty new bryostatins have been discovered and fully characterized.¹⁰¹

The bryostatins (Figure 67) are a family of potent anti-tumor agents. Bryostatin 1 exhibits powerful antineoplastic activity against murine P388 lymphocytic leukemia, B-cell lymphoma, reticulum cell sarcoma, ovarian carcinoma, and melanoma.¹⁰¹⁻¹⁰³ Bryostatins have also been shown to promote T-cell production, stimulate the immune system, and activate protein kinase C (PKC).¹⁰⁴ Bryostatin 1 has a remarkable affinity, in the picomolar range, for the phorbol ester binding site of PKC.¹⁰⁵

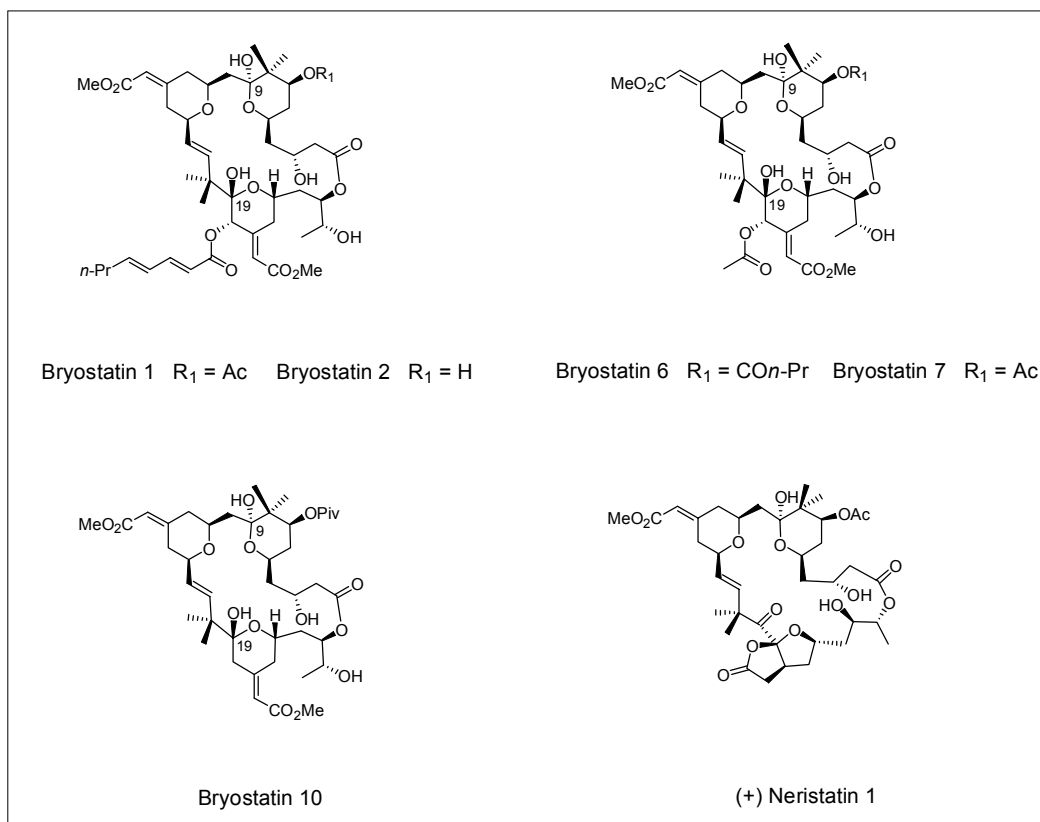


Figure 67 Bryostatin family members

Bryostatin 1 is capable of reversing P-gp dependent MDR in several human cancer cell lines.⁷² The exact mode of action for MDR reversal by bryostatin 1 is still unknown. Initially, bryostatin 1 was thought to reverse MDR by activating PKC. Researchers speculated that PKC activation reduces phosphorylation at P-gp, preventing P-gp pumping activity. However, recent studies have shown that bryostatin 1 does reduce phosphorylation of P-gp, but this does not cause MDR reversal.¹⁰⁵ The currently accepted theory is that bryostatin 1 directly interacts with P-gp and prevents its pumping activity.⁷²

4.3. Previous Bryostatin Syntheses

The first total synthesis of a bryostatin family member was reported in 1990 by Masamune and coworkers.¹⁰⁷ Their synthesis of bryostatin 7 was the only total synthesis published until eight years later when Evans and coworkers⁸⁵ reported their synthesis of bryostatin 2. Shortly thereafter, Nishiyama and Yamamura¹⁰⁸ completed another family member, bryostatin 3, in 2000. Each of these three syntheses are extraordinarily long. The shortest route is Evans bryostatin 2 synthesis, which is over 40 steps counting only the longest linear sequence.⁸⁵

Due to the complexity of these natural products, other groups have begun to synthesize simplified analogs of the bryostatin family. Most notable is the work of Wender and coworkers (Figure 68).¹⁰⁹⁻¹¹⁵ Their studies have led to the discovery of two simplified bryostatin-like macrolides. The activity of analog 1 is comparable to bryostatin 1 and analog 2 is significantly more potent than bryostatin 1 in binding to PKC and in inhibiting human cancer cell growth.¹¹³⁻¹¹⁵ These fully synthetic analogs are currently in pre-clinical trials.¹¹⁴

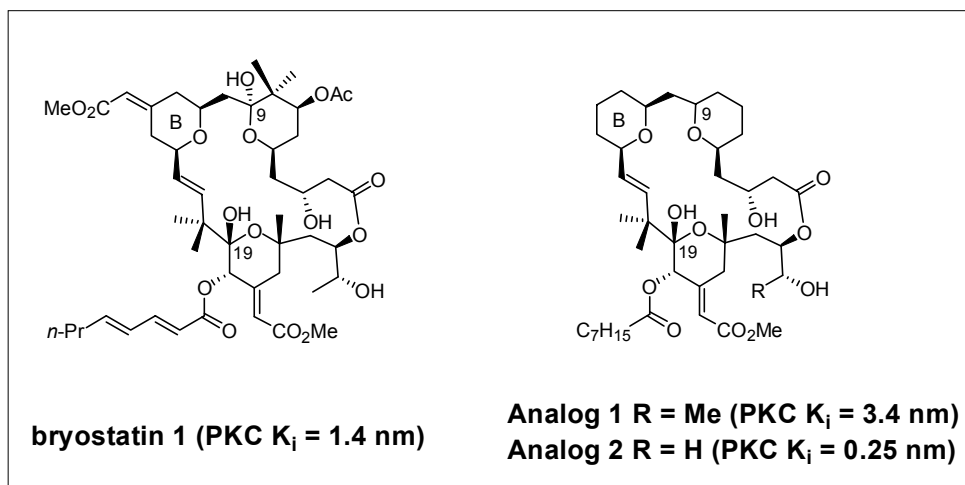


Figure 68 Wender and coworkers bryostatin analogs

4.4. A Model System for the Bryostatin B Ring

In preparation for our synthesis of the bryostatin 1 B-ring, two model systems (**90** and **91**) were created to study and optimize the Mukaiyama aldol process shown in Figure 69. These two

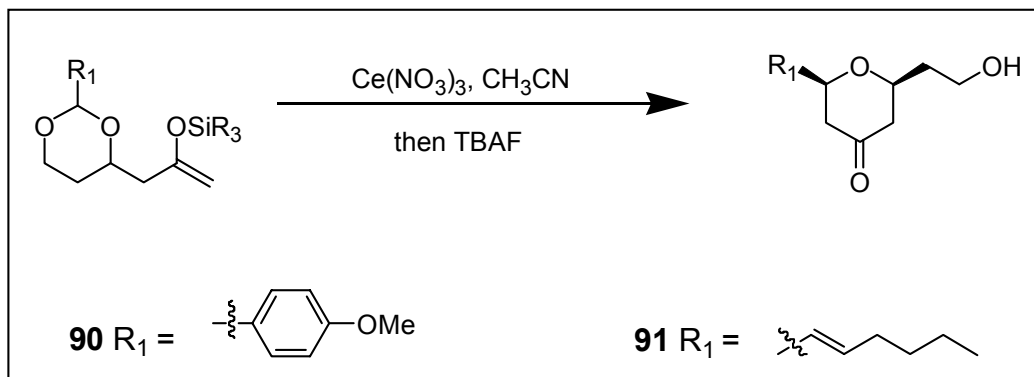
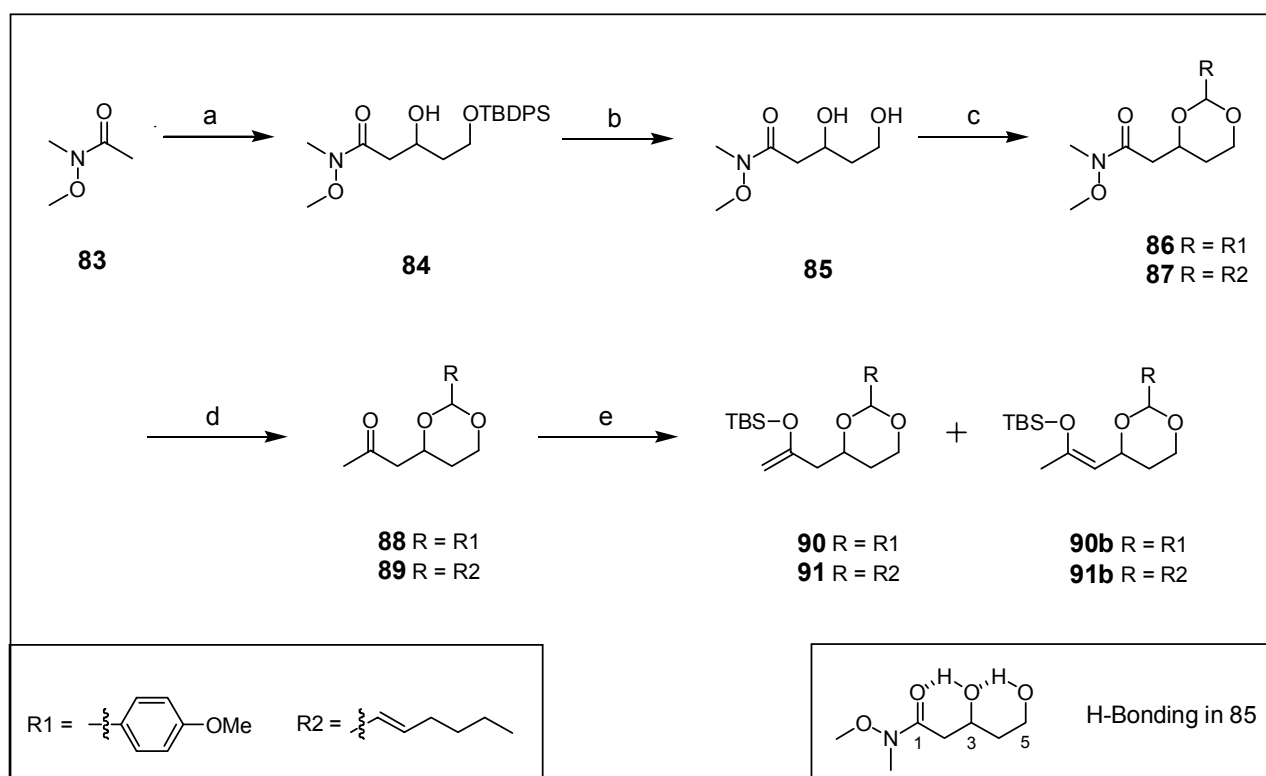


Figure 69 An intramolecular Mukaiyama aldol reaction

model systems (**90** and **91**) were utilized to investigate the role of the acetal group, the reactivity of the silyl enol ether, and also to test the effects of different solvents and additives. The syntheses of these two substrates are shown in Figure 70.

The first step in the preparation of our test substrates (**90** and **91**) was to construct the acetal portion of the model. The required 1,3-diol (**85**) was synthesized by an acetate aldol addition using the Weinreb amide¹¹⁶ of acetic acid (**83**). Treatment of the Weinreb amide at low temperature with LDA, followed by the addition of 3-(*tert*-butyldiphenylsilyl)-hydroxy propionaldehyde gave the β -hydroxy amide (**84**) in acceptable yield.⁷⁹ Subsequent removal of the *tert*-butyldiphenylsilyl (TBDPS) ether gave the expected diol (**85**) in excellent yield. Initially, we attempted to synthesize the cyclic acetals (**86** and **87**) using anisaldehyde and *trans*-2-heptenal. We found that when the diol (**85**), PPTS, and either of the two aldehydes were heated to reflux using a Dean-Stark trap, only a small amount of the desired products (**86** and **87**) were

formed. A similar experiment was attempted using the diethyl acetals of anisaldehyde and *trans*-2-heptenal. These experiments yielded only slightly better results. We suspect that the low reactivity of this diol (**85**) is due to the presence of the neighboring Weinreb amide group. There may be two strong hydrogen bonding interactions between the C-3 secondary alcohol and the Weinreb amide carbonyl oxygen, and also between the C-5 alcohol and the C-3 alcohol oxygen (Figure 70). This interaction may explain the difficulty encountered during cyclic acetal formation.



Reagents and conditions: a) LDA, THF, -78 °C, then 3-(*t*-butyldiphenylsilyl)-hydroxy propionaldehyde, 47%. b) TBAF, THF, 25 °C, 97%. c) anisaldehyde diethylacetal (R=1) or *trans*-2-heptenal diethylacetal (R=2), C₆H₆, PPTS, reflux, (R=1) 71%, (R=2) 64%. d) MeLi, THF, -78 °C, (R=1) 97%, (R=2) 92%. e) TBSOTf, Et₃N, CH₂Cl₂, -78 to 0 °C, (R=1) 56% (**90**) and 19% (**90b**), (R=2) 66% (**91**) and 20% (**91b**).

Figure 70 Mukaiyama aldol substrates

Ultimately, we found the best way to synthesize the cyclic acetals (**86** and **87**) was to dissolve the diol (**85**), PPTS, and the corresponding diethylacetal in benzene, and then heat the mixture until no further liquids distilled. We did not attempt to heat the diol (**85**) and a diethylacetal of an aldehyde in the absence of a solvent, since azeotropic distillation with benzene gave good results.

A two-step process was then used to introduce the second element of our model, the silyl enol ether groups. Treatment of the Weinreb amides (**86** and **87**) with methyl lithium at low temperature provided the methyl ketones (**88** and **89**) in high yield.¹¹⁶ The remaining step was to convert the methyl ketones (**88** and **89**) to the desired silyl enol ethers (**90** and **91**). Exposure of the methyl ketones to *tert*-butyldimethylsilyl triflate (TBSOTf) and triethylamine gave the desired silyl enol ethers (**90** and **91**) in acceptable yield. The undesired tri-substituted regioisomers (**90b** and **91b**), resulting from trapping the thermodynamically more stable enol ethers, were also isolated as major byproducts. There was no attempt was made to optimize this process since we were only interest in testing the Mukaiyama aldol reaction.

The first cyclization conditions which we explored with the Mukaiyama aldol substrate (**91**) utilized two equivalents of Ce(NO₃)₃ and acetonitrile as solvent (conditions C in Figure 71). These conditions produced a white biphasic mixture due to the partial insolubility of Ce(NO₃)₃ in acetonitrile. We observed that this method produced very slow product conversion. After 16 hours at 25 °C the reaction was quenched with a small amount of water and the desired product (**93**) was isolated in 53% yield. A trace amount of starting material (**91**), 8%, was recovered, but the remaining 39% of material could not be accounted for. We presumed that this missing material had undergone acetal cleavage and silyl enol ether hydrolysis to give the water-soluble

byproduct, 4,6-dihydroxy-2-hexanone. This byproduct could have been easily lost during an aqueous workup.

R ¹	R ²	Conditions/ Solvent	S.M.	Yield 1	Yield 2
	TBS-	A / CH ₃ CN	0%	93%	0%
	TBS-	B / CH ₃ CN	5%	77%	0%
	TBS-	C / CH ₃ CN	8%	53%	0%
	TBS-	B / CH ₂ Cl ₂	93%	0%	0%
	TBS-	A / CH ₃ CN	0%	81%	0%
	TBS-	B / CH ₃ CN	10%	44%	0%
	TBS-	C / CH ₃ CN	0%	23%	0%

Figure 71 Mukaiyama aldol optimization

We suspected that during the Mukaiyama aldol cyclization there were competing processes occurring. One likely decomposition pathway could certainly be due to hydrolysis. This undesired process was likely due to the presence of trace amounts of water or nitric acid and prolonged reaction times. In an attempt to prevent hydrolysis, two additives were evaluated. First, an identical reaction was run using the heptenal acetal model (**91**) and solid NaHCO₃ as a buffer. This additive had little effect on the conversion rate and the yield did not change appreciably. The second experiment was to try molecular sieves as an additive (conditions B in Figure 71). The use of molecular sieves resulted in an increase in yield, but the reaction conversion was still relatively slow. Next, we tried replacing the solvent acetonitrile with

methylene chloride. This change completely inhibited all reactivity and only the starting material (**91**) was recovered after stirring for sixteen hours. This result suggested that a solvent with a high dielectric constant might be required to facilitate oxocarbenium ion formation.

The second anisaldehyde acetal test substrate (**90**) was also subjected to a similar series of experiments. We found that when this aromatic acetal (**90**) was treated with $\text{Ce}(\text{NO}_3)_3$ in acetonitrile only 23% of the desired product was isolated. The addition of NaHCO_3 had little effect. When molecular sieves were added, the yield increased to 44% and a small amount of starting material was recovered using these conditions. The low yields observed during both of these experiments with the anisaldehyde acetal (**91**) were definitely caused by acetal hydrolysis. In this case, acetal hydrolysis was confirmed by the presence of anisaldehyde during TLC analysis.

It became apparent to us that using additives to slow hydrolysis was probably not the most effective way to improve the yield of the Mukaiyama aldol reaction. We realized that if hydrolysis could not be slowed, we needed to find conditions that would increase the rate of the desired reaction instead. The simplest way to increase the rate of the Mukaiyama aldol addition was to use more $\text{Ce}(\text{NO}_3)_3$. This change produced excellent results (conditions A in Figure 71). When four equivalents of $\text{Ce}(\text{NO}_3)_3$ were used, the Mukaiyama aldol addition proceeded to 100% conversion in under one hour at room temperature. These conditions (Figure 71) gave the expected product (**93**) in 93 % yield, a substantial improvement. In a subsequent reaction, the less reactive anisaldehyde acetal substrate (**90**) was evaluated with these new conditions. When four equivalents of $\text{Ce}(\text{NO}_3)_3$ were used with the aromatic acetal (**90**), a dramatic increase in yield was also observed. The desired Mukaiyama aldol reaction now proceeded to 100% conversion, and the product (**92**) was isolated in 81% yield. This slightly lower yield was

acceptable considering the improvement from 44% yield using two equivalents of $\text{Ce}(\text{NO}_3)_3$ and molecular sieves.

Overall, we were quite satisfied with these results. Our optimized conditions substantially improved product conversions in both model systems (**90** and **91**) and dramatically decreased the reaction times as well, from sixteen hours to one hour (Figure 72).

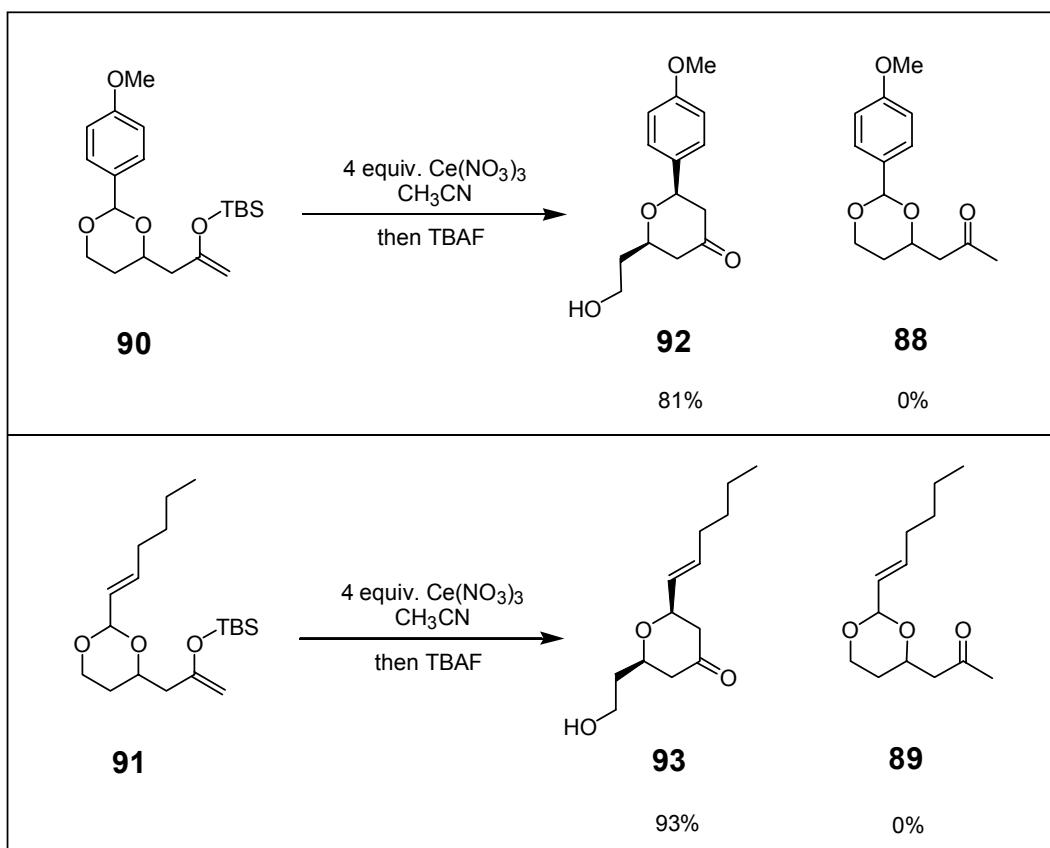


Figure 72 Optimized Mukaiyama aldol reactions

We had good reason to believe that the Mukaiyama aldol reaction would yield exclusively 2,6-*cis*-tetrahydropyranone products, based on our Prins reaction model (Figure 64). In order to confirm the 2,6-*cis*- relationship, the relative stereochemistry of the tetrahydropyranone ring was established using H,H COSY and 2D NOESY experiments.

The H,H-COSY experiment was not absolutely necessary for differentiating the C-2 and C-6 methine hydrogens. Coupling constant analysis alone could be used to confirm this. The purpose of the H,H-COSY was to distinguish normally coupled peaks from the peaks in the NOESY spectrum. This comparison revealed a strong cross peak in the NOESY spectrum corresponding to the methine hydrogens at C-2 and C-6 (Figure 73). This strong signal, which was also present in the NOESY spectrum of the 2,6-*cis*-THP Prins reaction products, supports the assigned 2,6-*cis*-tetrahydropyranone stereochemistry.

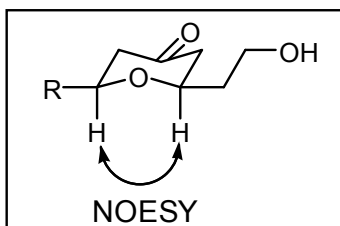


Figure 73 NOESY results for (93)

In addition to these two model systems (**90** and **91**), a saturated acetal and a phenyl acetal were also evaluated (Figure 74). We found that both of these substrates failed to react under all of our conditions. The lack of reactivity of the saturated acetal was not surprising, since there is no group to stabilize the oxocarbenium ion intermediate. The failure of the phenyl acetal was not expected, but also not surprising considering the lowered reactivity of the anisaldehyde acetal (**91**) compared to the heptenal acetal (**90**).

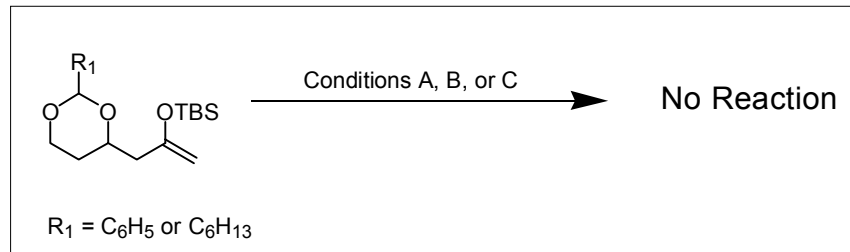


Figure 74 Failed Cyclization Reactions

Our model systems revealed that the nature of the acetal was a crucial component for reactivity. During our study we discovered that only electron rich aromatic or α,β -unsaturated acetals were reactive enough toward $\text{Ce}(\text{NO}_3)_3$ to generate the required oxocarbenium ion. We also observed a significant solvent dependence for this Mukaiyama aldol reaction. One interesting result showed that when methylene chloride was used as solvent, no reaction occurred and starting materials were recovered in near quantitative yield. This discovery corresponds to our previous result when this reaction was evaluated inside of a SDS micelle. The micelle and methylene chloride are both relatively non-polar environments, which do not promote oxocarbenium ion formation. Acetonitrile, having a substantially higher dielectric constant, must facilitate oxocarbenium ion formation. However, we can not rule out the possibility that the solubility of $\text{Ce}(\text{NO}_3)_3$ in methylene chloride compared to acetonitrile may also explain the difference in reactivity.

At this point in the project, we were satisfied with our optimized Mukaiyama aldol reaction conditions. Our next challenge was to apply this method, in an asymmetric manner, to the synthesis of the complex macrolide bryostatin 1. The following section of this chapter will demonstrate the utility of this method in preparing the B ring fragment of Bryostatin 1.

4.5. Enantioselective Preparation of the B Ring of Bryostatin 1

Our disconnections for the bryostatin 1 B ring (Figure 75) were chosen to allow for the construction of the C-14 to C-15 bond (bryostatin numbering) using our $\text{Ce}(\text{NO}_3)_3$ mediated Mukaiyama aldol process. Following this aldol reaction, we envisioned that the C-13 ketone could be converted to the required α,β -unsaturated methyl ester by utilizing a Horner-Emmons reaction. Our planned disconnections show that the tetrahydropyranone ring can be synthesized

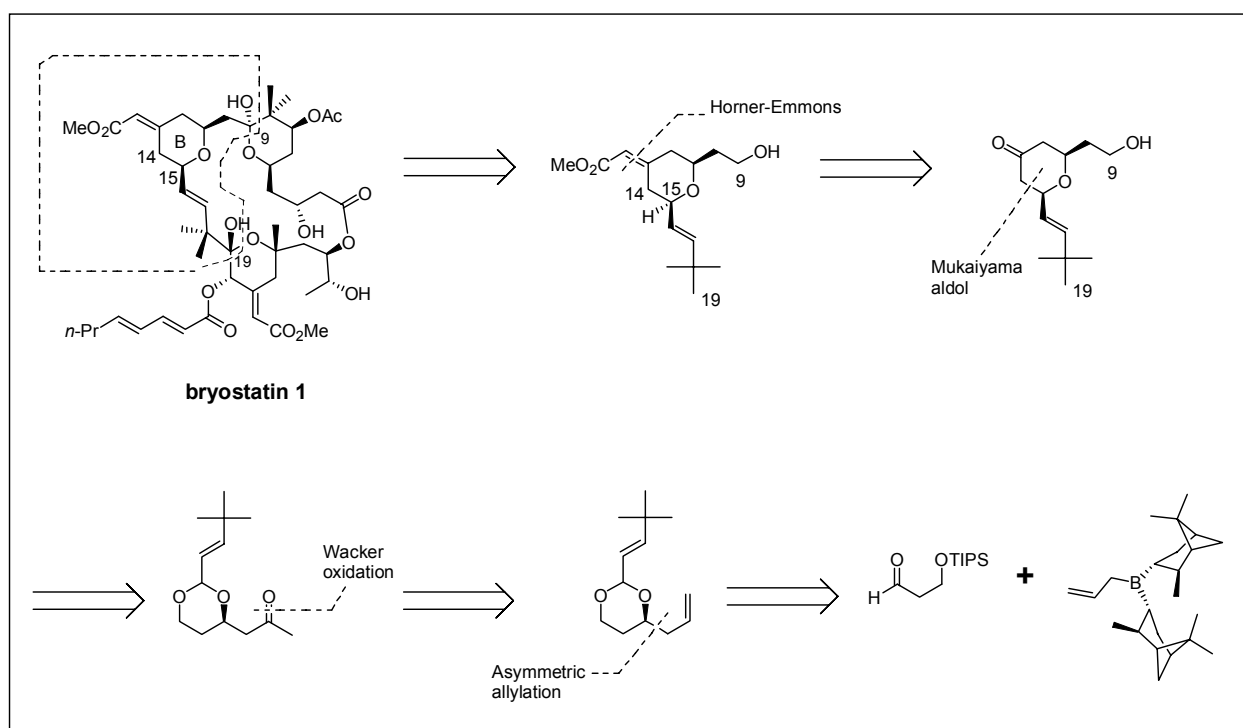
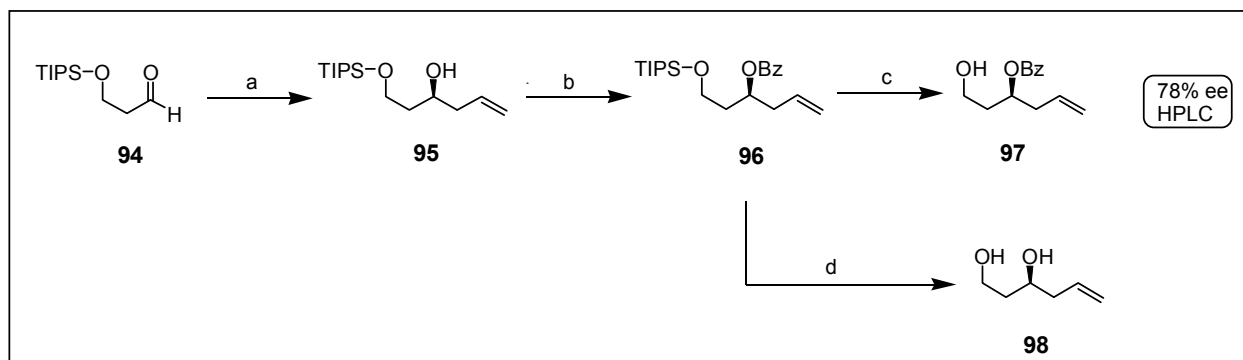


Figure 75 Retrosynthesis of the bryostatin 1 B ring

in two steps from an appropriate methyl ketone. In order to introduce this ketone, a Wacker oxidation¹¹⁷ can be used to regioselectively convert the terminal olefin into the required methyl ketone. The enantiomerically enriched 1,3-dioxane ring can be synthesized via an asymmetric

allylation of a propionaldehyde derivative using Brown's pinene derived chiral allyl borane reagent.¹¹⁸

Our synthesis of the bryostatin1 B ring began with the TIPS ether of 3-hydroxy propionaldehyde (**94**), which was synthesized by a modification of a known procedure for the corresponding TBDPS ether.⁷⁹ The (-)-allyl-B(Ipc)₂ reagent was prepared by Brown's method using (+)- α -pinene.¹¹⁹ We found that treatment of the propionaldehyde analog (**94**) with Brown's allyl borane reagent, followed by an alkaline oxidative workup provided the desired homoallylic alcohol (**95**) in excellent yield (Figure 76). The enantiomeric excess of the allylation product (**95**) was determined by preparing a UV-active benzoate ester (**96**). The benzoate ester chromophore was required since the enantiomers in question were to be separated using a chiral column and a HPLC instrument with a UV detector. A racemic sample, for comparison purposes, was prepared exactly as in Figure 76 by using allyl magnesium bromide instead of Brown's



Reagents and conditions: a) (-)-Allyl-B(Ipc)₂, Et₂O, -78 to 25 °C, then H₂O₂, NaOH, reflux, 90%. b) BzCl, pyridine, CH₂Cl₂, 2 hr, 85%. c) TBAF, THF, 1 hr, 70%. d) TBAF, THF, 90 min, 92%.

Figure 76 Asymmetric allylation

reagent. Multiple HPLC experiments were attempted using a Chiracel ODH column, but the benzoate ester enantiomers (**96**) could not be separated. This separation was difficult because the Chiracel ODH column is a normal phase HPLC column. The non-polar benzoate ester (**96**) traveled too quickly through the stationary phase and separation could not be achieved.

This problem was easily remedied by removing the TIPS protecting group using TBAF, providing the primary alcohol derivative (**97**). This time, the new benzoate ester enantiomers (**97**) separated into two resolved peaks using the same chiral HPLC column. Our HPLC experiment determined the enantiomeric excess to be 78%. This result is slightly low, but not surprising since the difference in size between the methylene group and the aldehyde hydrogen is not relatively large for this propionaldehyde derivative (**94**). The two possible transition states for the (-)-allyl-B(Ipc)₂ additions are shown in Figure 77. The low enantiomeric excess could be the result of the disfavored transition state or it could be due to the quality of the chiral borane reagent.

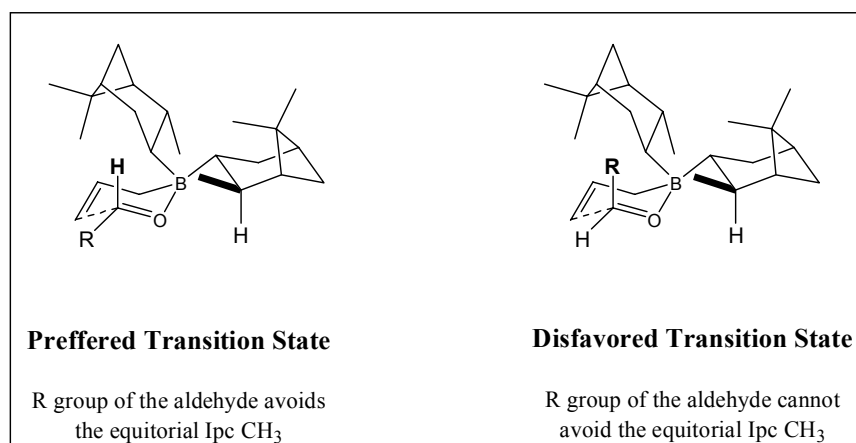
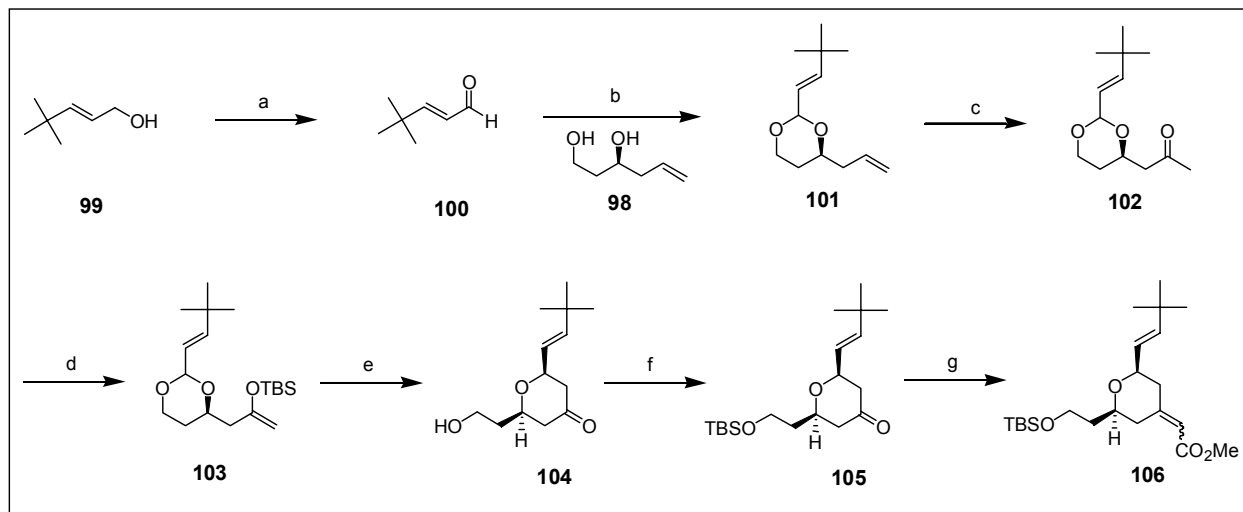


Figure 77 Asymmetric allylation transition states

The next step of our synthesis was to address the construction of the cyclic acetal. This required the synthesis of the known aldehyde, *trans*-4,4-dimethylpent-2-enal (**100**). We were able to prepare this aldehyde in one step, from the corresponding allylic alcohol precursor (**99**),¹²⁰ using a Dess-Martin periodinane oxidation⁴⁷ (Figure 78). When the chiral 1,3-diol (**98**) was exposed to *trans*-4,4-dimethylpent-2-enal (**100**) and catalytic PPTS, under reflux conditions, the desired cyclic acetal (**101**) was formed in excellent yield.

A Wacker oxidation¹¹⁷ was then employed to selectively oxidize the mono-substituted olefin in the presence of the newly introduced di-substituted olefin. We were not concerned with the selectivity of the Wacker oxidation for two reasons. First, Wacker oxidations with sterically



Reagents and conditions: a) DMPI, NaHCO₃, CH₂Cl₂, 25 °C, 99%. b) Diol **79**, PPTS, C₆H₆, 110 °C, 91%. c) PdCl₂, CuCl₂, Li₂CO₃, THF, H₂O, O₂, 25 °C, 79%. d) TBSOTf, Et₃N, CH₂Cl₂, -78 to 25 °C, 63% (**84**), 20% tri-substituted enol ether isomer. e) 4 equiv. Ce(NO₃)₃, CH₃CN, 25 °C; then TBAF, 70%. f) TBSCl, imidazole, CH₂Cl₂, 25 °C, 92%. g) trimethylphosphonoacetate, THF, NaHMDS, 0 °C; then (**86**), 90%, E:Z = 1:1.

Figure 78 Bryostatin 1 B ring synthesis

encumbered olefins are usually slow.¹¹⁷ This sensitivity arises from steric repulsions between the palladium complex and the olefin as the metal coordinates to the olefin's pi system. Palladium coordination with an olefin containing a *tert*-butyl group is not highly favorable. The second reason is that Wacker oxidations exhibit a high degree of regioselectivity, generally oxidizing the more electron rich carbon atom in the most electron rich olefin, if the option exists.¹¹⁷ The most electron rich carbon atom is preferentially oxidized since it bears more of the positive charge during complexation to the electrophilic palladium species. This method provides a convenient way to synthesize methyl ketones from terminal olefins in the presence of less reactive olefins.

However, a significant drawback to the Wacker oxidation is the generation of HCl from CuCl₂ and PdCl₂ during the reaction. When the standard Wacker conditions¹¹⁷ were employed, the acetal group (**101**) was cleaved quantitatively in less than 1 hour. We found that the addition of a buffer, such as Li₂CO₃, could alleviate this problem. However, buffering a Wacker oxidation raises the pH and can cause palladium metal to precipitate from the reaction, removing the catalyst and preventing oxidation. Conditions were eventually found, utilizing Li₂CO₃ and periodic additions of fresh PdCl₂, which minimized both problems associated with high and low pH.

The methyl ketone (**102**) was then converted to the silyl enol ether using TBSOTf and Et₃N at low temperature. This gave the desired product (**103**) in good yield along with a small amount of the undesired tri-substituted enol ether. Exposure of this silyl enol ether (**103**) to Ce(NO₃)₃ in acetonitrile, followed by a TBAF quench, and then an aqueous workup gave the tetrahydropyranone product (**104**) as a single isomer. The formation of a single product is consistent with the Zimmerman-Traxler transition state model (Figure 79). We attempted to verify the 2,6-*cis*-stereochemistry in the Mukaiyama aldol adduct (**104**), but the H,H-COSY

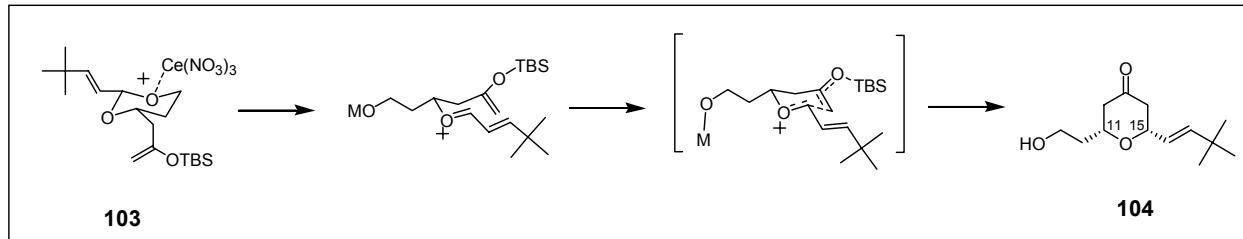


Figure 79 Transition state for the Mukaiyama aldol

spectrum did not provide enough information. We found that the C-10, C-12, and C-14 methylene groups (bryostatin numbering) could not be differentiated. This prevented us from positively identifying the C-11 and C-15 methine protons.

In an attempt to circumvent this problem, the C-9 primary hydroxyl group was protected as a TBS ether (**105**). This conversion produced a downfield shift at the C-9 methine and the C-10 methylene groups. This caused the C-10 and C-12 methylene signals to separate just enough to distinguish two coupling patterns in the ^1H NMR. When the TBS ether derivative (**105**) was characterized using an H,H-COSY experiment, each of the protons were positively assigned. The 2,6-*cis* stereochemistry was then verified using a 2D NOESY experiment. The NOESY spectrum revealed a strong cross peak between the C-11 and C-15 methine protons (Figure 80).

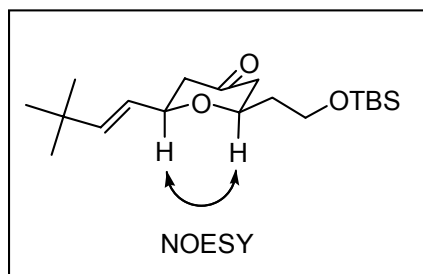


Figure 80 NOESY for tetrahydropyranone (**105**)

This indicates a syn-relationship at the C-11 and C-15 methine positions.

In order to complete the B ring of bryostatin 1, the C-13 ketone in the tetrahydropyranone substrate (**105**) needs to be selectively converted to the (*Z*)- α,β -unsaturated methyl ester (**106**). When the phosphonate derived from trimethylphosphonoacetate and NaHMDS was added to this ketone (**105**), an inseparable 1:1 mixture of *E* and *Z* isomers was obtained. Interestingly, the ^1H NMR resembled a single product, but examination of the ^{13}C NMR spectrum clearly confirmed the presence of two isomers. Separation difficulties with similar tetrahydropyran ring systems have also been encountered in previous bryostatin syntheses.^{85, 121-122} The best solution to this problem would be to use a chiral phosphonate to improve selectivity. Evans has demonstrated that the asymmetric Horner-Emmons method developed by Fuji and coworkers¹²³⁻¹²⁴ will give the desired selectivity in a related system (Figure 81).⁸⁵ Fuji's method utilizes a chiral binol-derived phosphonate to control the stereochemical outcome of the Horner-Emmons reaction. Future work should evaluate if this reagent will give the desired result for this ketone (**105**).

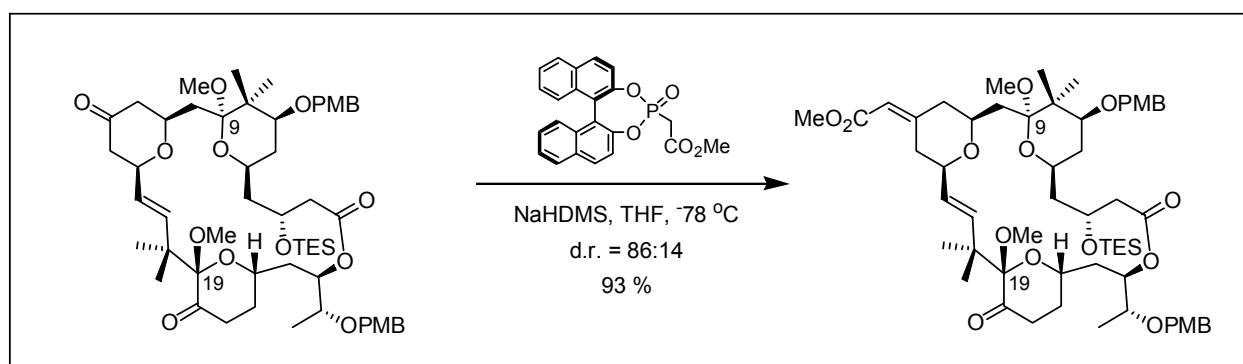


Figure 81 Evans' application of Fuji's binol phosphonate reagent

4.6. Summary

We have demonstrated that an intramolecular Mukaiyama aldol reaction can be used to selectively synthesize chiral 2,6-*cis*-tetrahydropyranones (Figure 82). The substrates for this reaction can be readily prepared, in a convergent manner, from achiral aldehydes and chiral diols.

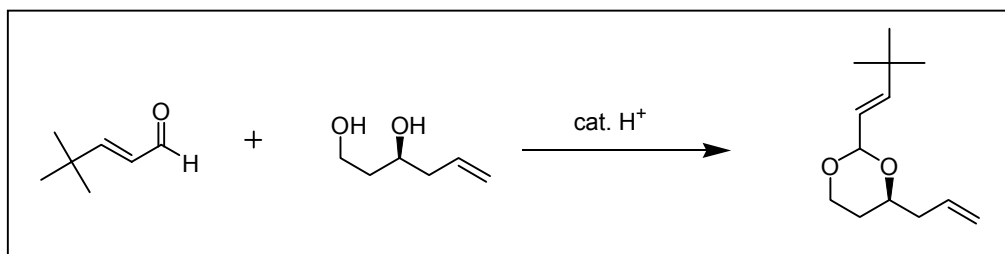


Figure 82 A convergent preparation of Mukaiyama aldol precursors

The major advantage of our new method is the especially mild conditions used to generate oxocarbenium ions from acetals. These conditions utilize $\text{Ce}(\text{NO}_3)_3$, a commercially available, inexpensive, and non-toxic Lewis acid. Additionally, this method is attractive given that cyclic acetals are utilized as oxocarbenium ion precursors. This is a particularly important feature for complex molecule syntheses, since acetals can be made using very mild procedures.¹²⁵

To demonstrate the utility of this method, the C-9 to C-19 fragment, or B ring, of bryostatin 1 was synthesized. The 2,6-*cis*-tetrahydropyranone ring (**104**) was synthesized in four steps (Figure 83), from a known diol (**98**),¹²⁶ in an overall yield of 42%. Initial experiments

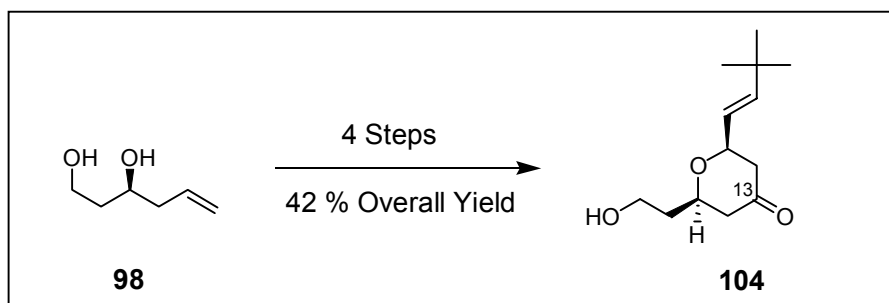


Figure 83 A brief route to the C-9 to C-19 fragment of bryostatin 1

demonstrated that the C-13 ketone could be converted to the required α,β -unsaturated methyl ester in high yield, but as an inseparable mixture of diastereomers. The stereoselective introduction of this exocyclic ester has previously been addressed by the Evans^{85, 121} and the Hoffmann¹²² groups, therefore we did not pursue this transformation further.

One improvement to be addressed in the future is how to increase the enantiomeric excess of the 1,3-diol starting materials. For our purpose, a 78% ee was acceptable, but in a total synthesis this would not be ideal. Additional boron allylation procedures should be evaluated to see if the enantiomeric purity of the starting materials could be improved.

The Wacker oxidation¹¹⁷ is a superb method for generating methyl ketones from terminal olefins. In our case, difficulties were encountered when the pH became too acidic due to the presence of the acid labile acetal group. Attempting to buffer the Wacker oxidation with Li_2CO_3 causes precipitation of palladium metal, which effectively removes the catalyst from the reaction. An interesting experiment would be to replace PdCl_2 and CuCl_2 with $\text{Pd}(\text{OAc})_2$ and $\text{Cu}(\text{OAc})_2$, since the use of the acetate salts would generate acetic acid in the catalytic cycle instead of HCl. Acetic acid ($\text{pK}_a = 4.8$) is a substantially weaker acid compared to HCl ($\text{pK}_a = -8.0$) and may prevent acetal hydrolysis. The amount of palladium needed to achieve good conversions would also be reduced if no buffer were added, since this would prevent palladium metal precipitation.

Furthermore, the application of this method for constructing other tetrahydropyran rings, with complex substitution patterns, needs to be investigated. We expect that this approach can be easily adapted to synthesize similar natural products, such as (+) phorboxazole A or (+) dactylolide. The macrolide (+) phorboxazole A¹²⁷ (Figure 84) contains a persubstituted THP ring that can be constructed from a silyl enol ether (**107**), making it a suitable candidate for this Mukaiyama aldol method.

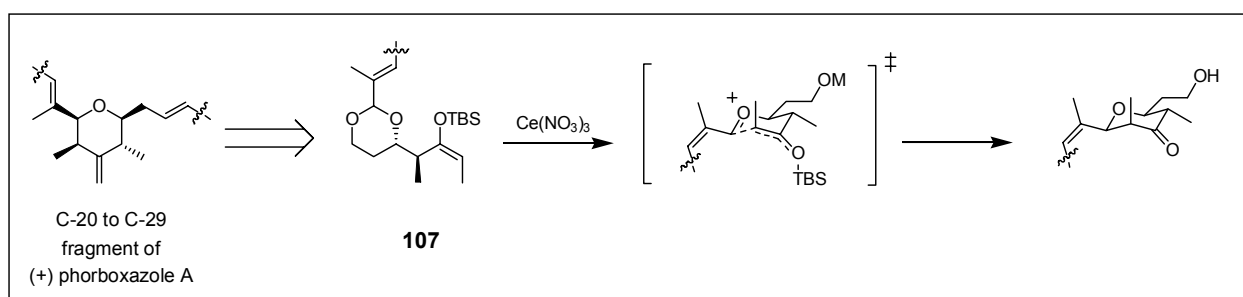
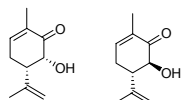


Figure 84 C-20 to C-29 fragment of (+) phorboxazole A

The required silyl enol ether (**107**) can be synthesized in high enantiomeric purity by a number of asymmetric aldol methods. For example, a chiral oxazolidinone¹²⁸ and Paterson's boron enolate method¹²⁹ can be used to create the 1,2-*anti*-stereochemical relationship. This strategy would produce the (+) phorboxazole A fragment in an exceptionally short sequence.

Experimental Procedures

General Procedures. THF and Et₂O were dried by distillation over Na/benzophenone ketyl under N₂. Alternatively, anhydrous, non-stabilized, THF and Et₂O were purchased from Aldrich in sure-pack™ drums. Using this method, solvents were dried by passing through a cylinder of activated Al₂O₃ immediately before use. Benzene and CH₂Cl₂ were dried by distillation over CaH₂. All reagents were used as received unless otherwise noted. Ce(NO₃)₃ heptahydrate was dried under high vacuum at 80 °C for 24 hours, then pulverized using a mortar and pestle. This fine white powder was dried for another 12 hours at 80 °C under high vacuum. Column/Flash Chromatography was performed using ICN Silitech 32-63 D (60 Å) grade silica gel. Thin layer chromatography was performed using plates from EM Science (silica gel 60 F₂₅₄ / 250 μm thickness). NMR experiments were performed using Bruker 300 and 500 MHz instruments. IR spectra were recorded on a Matheson FT-IR. Mass Spectra were obtained using a VG high resolution MS. Chemical shifts (δ) are reported in ppm relative to TMS. All reactions were carried out under a nitrogen atmosphere using thoroughly dried glassware unless otherwise noted.



Rubottom oxidation of (*R*)-(-)-Carvone:

6-Hydroxy-5-isopropenyl-2-methyl-cyclohex-2-enones (31a and 31b)

TMSCl was purified by distillation over Na₂CO₃ under a nitrogen atmosphere. *m*-CPBA was purified by dissolving 77% commercially available *m*-CPBA in CH₂Cl₂, then washing the organic layer three times with a dibasic sodium phosphate solution adjusted to pH 7.4. The organic layer was then dried over MgSO₄, filtered, and solvents removed in vacuo. The slightly

yellow crystals were then recrystallized from hexanes and stored in a plastic bottle in a $-20\text{ }^{\circ}\text{C}$ freezer until use. TLC plates were deactivated prior to use by dipping into a solution 3% Et_3N in hexanes, then drying.

To a flask equipped with a Claisen adapter, rubber septum, and N_2 adapter was added dry (*i*-Pr) $_2$ NH (12.35 g, 121.7 mmol) and THF (60 mL). The vessel was cooled to $-40\text{ }^{\circ}\text{C}$ and *n*-BuLi (1.6M hexanes, 76.1 mL, 121.7 mmol) was added. The reaction was warmed to $0\text{ }^{\circ}\text{C}$ for 30 minutes, then cooled to $-78\text{ }^{\circ}\text{C}$ and diluted with THF (100 mL). A solution of (*R*)-(-)-carvone (15.0 g, 98.5 mmol) in THF (85 mL) was prepared added by cannula to the LDA solution at $-78\text{ }^{\circ}\text{C}$. This was stirred at $-78\text{ }^{\circ}\text{C}$ for 60 minutes, and then quenched at $-78\text{ }^{\circ}\text{C}$ by adding TMSCl (21.4 g, 197.1 mmol). The reaction was allowed to warm to ambient temperature and stirred there for an additional 60 minutes. TLC analysis (deactivated with Et_3N , 15:85 EtOAc:Hexanes) showed the silyl enol-ether at $R_f = 0.82$. The reaction mixture was then concentrated by rotovap. Some celite was added and the slurry was taken up in pentanes and filtered through a pad of celite. Pentanes were then used to rinse the solids and the solvents were removed by rotovap to give the crude TMS enol ether (**29**) as a viscous yellow oil. The crude silyl enol-ether was placed in a dry flask equipped with a claisen adapter, rubber septum, and an addition funnel. CH_2Cl_2 (450 mL) and solid NaHCO_3 were added and the vessel was cooled to $0\text{ }^{\circ}\text{C}$. A solution of *m*-CPBA (21.0 g, 121.7 mmol) in CH_2Cl_2 (200 mL) was added drop wise via addition funnel, and when complete, the reaction was warmed to ambient temperature and stirred there for 45 minutes. Then the reaction mixture was filtered through a pad of celite to remove the solids and the filtrate was concentrated in vacuo. The resulting green slurry was taken up in pentanes and again filtered through celite to remove more solids. Removal of solvents this time afforded a yellow oil free of solids. Both diastereomers of the hydroxy ketone (**31a**) and (**31b**) as well as

both diastereomers of the desired silyl ether (**30a**) and (**30b**) were detected by GC analysis. The crude silyl ethers were directly converted to the hydroxy ketone by treatment with HF/MeOH.

6-Hydroxy-5-isopropenyl-2-methyl-cyclohex-2-enones (31a) and (31b)

To a stirred solution of (**30**) and (**31**) (8.01 g, 33.4 mmol) in MeOH (75 mL) at 25 °C was added 48% aq. HF (2.17 mL, 62.7 mmol). The reaction was monitored by GC and/or TLC. After 40 minutes the reaction was complete. The reaction was carefully neutralized by adding solid NaHCO₃, and then H₂O followed by EtOAc (60 mL). The layers were separated and the aqueous layer extracted with EtOAc (5x50 mL). The organic layer was dried over MgSO₄, filtered, and solvents removed in vacuo. This gives a yellow/green oil as the crude products which were purified by column chromatography (20:80 EtOAc:Hexanes) to give a 2:1 ratio of anti(**31b**):syn(**31a**) diastereomers (1.48 g, 27%) and (3.27 g, 59%). Overall yield from (*R*)-carvone is 63%.

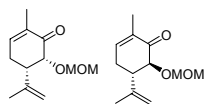
6(*R*)-Hydroxy-5(*S*)-isopropenyl-2-methyl-cyclohex-2-enone (31a)

¹H NMR (300 MHz, CDCl₃) δ 6.65 (t, *J* = 0.8 Hz, 1H), 4.82 (s, 1H), 4.68 (s, 1H), 4.39 (d, *J* = 5.8 Hz, 1H), 3.63 (s, 1H), 3.15 (s, 1H), 2.74-2.47 (m, 3H), 1.80 (s, 3H), 1.66 (s, 3H); ¹³C NMR (75 MHz, CDCl₃) δ 199.8, 144.2, 143.1, 133.8, 113.8, 74.7, 46.9, 29.7, 23.1, 15.3; IR (neat) 3483, 3055, 2976, 2924, 1674, 1670, 1450, 1360, 1265, 1189, 1134, 1030, 900, 738 cm⁻¹; HRMS (EI) *m/z* calc for C₁₀H₁₄O₂ (M)⁺ 166.0993, found 166.0996; [α]_D²³ -30.5 ° (MeOH, c 1.0).

6(*S*)-Hydroxy-5(*S*)-isopropenyl-2-methyl-cyclohex-2-enone (31b)

¹H NMR (300 MHz, CDCl₃) δ 6.77 (t, *J* = 1.7 Hz, 1H), 4.95-4.96 (m, 2H), 4.17 (d, *J* = 12.7 Hz, 1H), 3.80 (s, 1H), 2.74-2.2.67 (m, 1H), 2.49-2.42 (m, 2H), 1.86 (s, 6H); ¹³C NMR (75 MHz, CDCl₃) δ 200.7, 145.7, 144.3, 133.2, 113.7, 74.5, 51.2, 30.8, 18.9, 15.4; IR (thin film) 3483,

3056, 2976, 2925, 1674, 1647, 1437, 1373, 1266, 1138, 1045, 898, 734 cm^{-1} ; HRMS (EI) m/z calc for $\text{C}_{10}\text{H}_{14}\text{O}_2$ (M)⁺ 166.0993, found 166.0990; $[\alpha]_{\text{D}}^{23}$ -10.5° (MeOH, c 1.0).



5(S)-Isopropenyl-6(R)-methoxymethoxy-2-methyl-cyclohex-2-enone (32a)
and 5(S)-Isopropenyl-6(S)-methoxymethoxy-2-methyl-cyclohex-2-enone and (32b)

To a flask equipped with a reflux condenser and N_2 adapter were added a mixture of diastereomers of (**31**) (4.75 g, 28.58 mmol), diisopropylethylamine (25 mL), DMAP (100 mg), and chloromethyl methylether (5.76 g, 71.44 mmol). The reaction was heated to 40°C and after 15 hours was complete. The reaction was cooled to ambient temperature and then quenched with $\text{NH}_4\text{Cl}_{(\text{aq. sat.})}$ (10 mL). The mixture was transferred to a separatory funnel using EtOAc (50 mL) and an additional amount of aq. sat. NH_4Cl (60 mL) was added. The layers were then separated and the aqueous layer extracted with EtOAc (5x40 mL). The combined organic layers were the washed with dilute $\text{HCl}_{(\text{aq.})}$ (25 mL), then with brine (2x50 mL), dried over MgSO_4 , filtered, and solvents removed in vacuo. This gave a yellow oil as the crude products which were then purified by column chromatography (15:85 EtOAc: Hexanes, $R_f = 0.31$ anti (**32b**), $R_f = 0.38$ syn (**32a**)) to give the desired compounds (5.05g, 84%) anti (**32b**) and (901 mg, 15%) syn (**32a**) as slightly yellow oils.

5(S)-Isopropenyl-6(R)-methoxymethoxy-2-methyl-cyclohex-2-enone (32a)

^1H NMR (300MHz, CDCl_3) δ 6.69 (t, $J = 2.3$ Hz, 1H), 4.89 (s, 1H), 4.80 (s, 1H), 4.67 (d, $J = 6.7$ Hz, 1H), 4.65 (d, $J = 6.7$ Hz, 1H), 4.09 (d, $J = 2.2$ Hz, 1H), 3.24 (s, 3H), 2.66-2.63 (m, 2H), 2.33-2.26 (m, 1H), 1.75 (s, 3H), 1.74 (s, 3H); ^{13}C NMR (75 MHz, CDCl_3) δ 197.3, 144.8, 143.7, 133.4, 112.9, 95.5, 76.9, 55.8, 46.6, 27.2, 22.2, 15.8; IR (thin film) 3087, 2925, 2847, 1674,

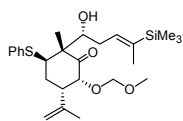
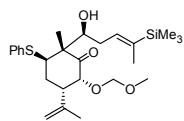
1641, 1451, 1373, 1152, 1125, 1029, 922, 898, 842 cm^{-1} ; LRMS (CI / CH_4) m/z calc for $\text{C}_{12}\text{H}_{18}\text{O}_3$ ($\text{M}+\text{H}$)⁺ 211, found 211; $[\alpha]_{\text{D}}^{23} +55.3$ ° (MeOH, c 1.0).

5(S)-Isopropenyl-6(S)-methoxymethoxy-2-methyl-cyclohex-2-enone (32b)

^1H NMR (300 MHz, CDCl_3) δ 6.69-6.67 (m, 1H), 4.91 (s, 2H), 4.93 (d, $J = 7.1$ Hz, 2H), 4.74 (d, $J = 7.1$ Hz, 1H), 4.18 (d, $J = 12.1$ Hz, 1H), 3.39 (s, 3H), 2.89-2.83 (m, 1H), 2.53-2.35 (m, 2H), 1.83 (s, 3H), 1.81 (d, $J = 0.9$ Hz, 3H); ^{13}C NMR (75 MHz, CDCl_3) δ 198.9, 144.2, 143.6, 134.6, 113.7, 97.0, 78.8, 56.0, 49.5, 30.7, 19.2, 15.6; IR (thin film) 3024, 2955, 2897, 1683, 1647, 1440, 1381, 1267, 1151, 1076, 1032, 918, 899, 738 cm^{-1} ; HRMS (EI) m/z calc for $\text{C}_{11}\text{H}_{15}\text{O}_2$ ($\text{M}-\text{CH}_3\text{O}$)⁺ 179.1072, found 179.1070; $[\alpha]_{\text{D}}^{23} -110.0$ ° (MeOH, c 1.0).

5(S)-Isopropenyl-6(R)-methoxymethoxy-2-methyl-cyclohex-2-enone (32a)

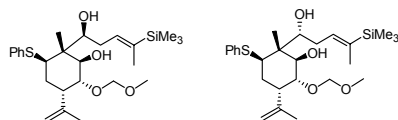
To a flask containing diisopropylamine (1.11 g, 11.0 mmol) and THF (10 mL) was added *n*-BuLi (6.88 mL, 11.0 mmol) at -50 °C. The reaction was warmed to 0 °C and stirred for 30 min under N_2 . Then the LDA solution was cooled to -78 °C and a solution of (**32b**) (2.1 g, 10.0 mmol) in THF (40 mL) was added. The reaction was stirred at -78 °C for 30 minutes and then quenched at -78 °C with glacial acetic acid (1.80 g, 30.0 mmol), then warmed to ambient temperature. The reaction mixture was poured into a separatory funnel and washed with NaHCO_3 (aq. sat.) (2x15 mL), and then with brine (2x15 mL). The organic layers were dried over MgSO_4 , filtered, and solvents removed in vacuo. This gave the crude products as yellowish oil. The syn and anti diastereomers were then separated by column chromatography (15:85 EtOAc:Hexanes, $R_f = 0.38$ syn (**32a**), $R_f = 0.31$ anti (**32b**)) to give the desired product (**32a**) (1.45 g, 69%) and recovered starting material (**32b**) (484 mg, 23%).



2(R)-(1(R,S)-Hydroxy-4-trimethylsilyl-pent-3-enyl)-5(S)-isopropenyl-6(R)-methoxymethoxy-2(R)-methyl-3(R)-phenylsulfanyl-cyclohexanone (35 and 36)

To a flask cooled to 0 °C was added thiophenol (53.7 mg, 0.48 mmol), CH₂Cl₂ (1.0 mL), and then AlMe₃ (2M hexanes, 0.48 mL, 0.96 mmol). This solution was then stirred at 0 °C for 35 minutes then cooled to -50 °C and a solution of (**32a**) (100 mg, 0.48 mmol) in CH₂Cl₂ (1.0 mL) was added. Stirring was continued for 5 hours at -50 °C. TLC (15:85 EtOAc:Hexanes) can be used to monitor the 1,4 addition. After stirring for 5 hours, the reaction was diluted with THF (1.0 mL) and a solution of 4-trimethylsilyl-pent-3-enal (**34**) (170 mg, 0.96 mmol) in THF (1.0 mL) was added. After stirring for another 5 hours at -50 °C the reaction was diluted with EtOAc (5 mL) and quenched with aq. sat. NaK tartrate (3 mL). The mixture was allowed to warm to 25 °C and stirred until two layers separated from the aluminum emulsion. The aqueous layer extracted with EtOAc (3x10 mL). The combined organic layers were then washed with aq. sat. NaHCO₃ and brine, dried over Na₂SO₄, filtered, and solvents removed in vacuo. The two diastereomers of the product were then purified by column chromatography (15:85 EtOAc:Hexanes) to give a 2:1 mixture of diastereomers (58.1 mg, 25%). The enone starting material (**32a**) was also recovered (74.2 mg, 74.2%). Major diastereomer (**35**): ¹H NMR (300 MHz, CDCl₃) δ 7.40-7.26 (m, 5H), 5.75-5.78 (m, 1H), 5.01 (s, 1H), 4.81 (s, 1H), 4.66 (s, 2H), 4.46 (d, *J*=5.5 Hz, 1H), 4.01-4.04 (m, 1H), 3.58 (dd, *J*= 4.0, 11.2 Hz, 1H), 3.35 (s, 3H), 2.99 (d, *J*= 4.6 Hz, 1H), 2.39-2.18 (m, 5H), 1.62 (s, 3H), 1.57 (s, 3H), 1.48 (s, 3H), 0.05 (s, 9H); ¹³C NMR (75 MHz, CDCl₃) δ 213.0, 141.4, 138.4, 136.0, 134.7, 132.6, 132.4, 129.4, 127.7, 114.9, 95.8, 78.0, 75.6, 56.8, 56.1, 49.6, 45.9, 31.4, 30.7, 22.6, 18.7, 14.9, -1.9; IR (thin film) 3437, 3004, 2954, 1706, 1648, 1618, 1584, 1439, 1247, 1154, 1018, 837, 746, 691 cm⁻¹; HRMS (EI) *m/z* calc for C₂₆H₄₀O₄SiS (M)⁺ 476.2416, found 476.2406. Minor diastereomer (**36**): ¹H NMR (300 MHz, CDCl₃) δ 7.51-7.42 (m, 5H), 5.89 (t, *J*= 1.7 Hz, 1H), 4.96 (s, 1H), 4.80 (s, 1H), 4.74-4.66 (dd, *J*= 6.9, 19.6 Hz, 2H), 4.48 (d, *J*= 5.5 Hz, 1H), 4.29-4.26 (m, 1H), 3.87 (dd, *J*= 4.0, 10.4 Hz, 1H), 3.36 (s, 3H), 3.01 (d, *J*= 5.2 Hz, 1H), 2.63-2.50 (m, 1H), 2.41-2.27 (m, 3H), 2.22-2.17 (m, 1H), 1.71 (s, 3H), 1.56-1.54 (m, 3H), 1.34 (s, 3H), 0.07 (s, 9H); ¹³C NMR (75 MHz, CDCl₃) δ 210.1, 141.6, 138.7, 136.1, 134.4, 132.3, 129.4, 129.2, 127.7, 114.7, 96.2, 79.0, 74.4, 57.2, 56.1, 50.0, 45.8, 32.2, 30.2, 29.9, 22.7, 17.5, 15.0, -1.9; IR (thin film) 3477, 3002, 2953,

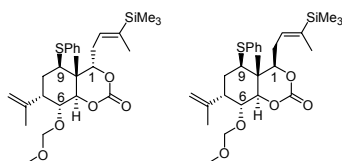
1714, 1439, 1152, 1023, 837, 739 cm^{-1} ; HRMS (EI) m/z calc for $\text{C}_{26}\text{H}_{40}\text{O}_4\text{SiS}$ (M)⁺ 476.2416, found 476.2426.



General procedure for $\text{NaBH}(\text{OAc})_3$ directed reduction:

Syntheses of 2(*R*)-(1(*S*)-Hydroxy-4-trimethylsilyl-pent-3-enyl)-5(*S*)-isopropenyl-6(*R*)-methoxymethoxy-2(*R*)-methyl-3(*R*)-phenylsulfanyl-1(*R*)-cyclohexanol (37**) and 2(*R*)-(1(*R*)-Hydroxy-4-trimethylsilyl-pent-3-enyl)-5(*S*)-isopropenyl-6(*R*)-methoxymethoxy-2(*R*)-methyl-3(*R*)-phenylsulfanyl-1(*R*)-cyclohexanol (**39**).**

To a flask containing NaBH_4 (129 mg, 3.4 mmol) was added glacial acetic acid (4.0 mL) at 0 °C. The mixture stirred until bubbling subsided. A solution of (**35** or **36**) (160 mg, 0.34 mmol) in CH_2Cl_2 (1.0 mL) was then added and the reaction warmed to 25 °C. After 2.5 hours the reaction was quenched using aq. sat. NaHCO_3 . The reaction was then extracted with Et_2O (4x10 mL), and then washed with aq. sat. NaHCO_3 and brine. The ether layer was then dried over Na_2SO_4 , filtered, and solvents removed in vacuo. The product was then purified by column chromatography (20:80 EtOAc:Hexanes) to give the desired product as a colorless oil. Diol adduct (**37**) from the major aldol diastereomer: (49.7%) ^1H NMR (300 MHz, CDCl_3) δ 7.37-7.22 (m, 5H), 5.82 (t, $J = 1.3$ Hz, 1H), 5.02 (d, $J = 17.0$ Hz, 2H), 4.72 (s, 2H), 4.39 (d, $J = 9.9$ Hz, 1H), 4.06 (dd, $J = 3.0, 9.6$ Hz, 1H), 3.80 (dd, $J = 5.9, 9.9$ Hz, 1H), 3.39 (s, 3H), 3.20-3.24 (m, 2H), 2.78-2.80 (m, 1H), 2.40-2.45 (m, 2H), 2.00-2.03 (m, 3H), 1.68 (s, 3H), 1.58 (s, 3H), 1.30 (s, 3H), 0.05 (s, 9H); ^{13}C NMR (75 MHz, CDCl_3) δ 142.9, 140.1, 135.4, 131.8, 129.3, 127.2, 114.7, 96.8, 79.9, 78.1, 71.5, 56.1, 48.0, 46.4, 43.7, 31.6, 30.3, 29.9, 24.4, 15.0, 12.6, -1.9; IR (thin film) 3448, 3054, 2986, 1422, 1265, 1100, 839, 738, 705 cm^{-1} . Diol adduct (**39**) from the minor aldol diastereomer: (94.2%) ^1H NMR (300 MHz, CDCl_3) δ 7.43-7.21 (m, 5H), 5.81-5.83 (m, 1H), 5.02 (s, 1H), 4.98 (s, 1H), 4.69 (s, 2H), 4.33 (d, $J = 9.2$ Hz, 1H), 4.11 (d, $J = 10.4$ Hz, 1H), 3.77 (dd, $J = 5.6, 8.7$ Hz, 1H), 3.65 (dd, $J = 3.5, 11.2$ Hz, 1H), 3.39 (s, 3H), 2.73-2.75 (m, 3H), 2.37-2.41 (m, 1H), 2.07-2.11 (m, 1H), 1.95-1.99 (m, 2H), 1.72 (s, 3H), 1.58 (s, 3H), 1.12 (s, 3H), 0.06 (s, 9H); ^{13}C NMR (75 MHz, CDCl_3) δ 139.7, 136.9, 135.0, 131.3, 129.0, 126.8, 114.2, 96.7, 81.2, 76.7, 74.8, 69.2, 56.0, 48.0, 47.6, 46.8, 32.0, 30.8, 23.8, 14.9, 11.7, -2.0; IR (thin film) 3465, 3053, 2955, 1645, 1583, 1481, 1439, 1265, 1214, 1151, 1035, 965, 896, 838, 738, 704 cm^{-1} .

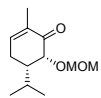


General procedure for cyclic carbonate formation:

Syntheses of 7(*S*)-Isopropenyl-8(*R*)-methoxymethoxy-4(*R*)-methyl-5(*R*)-phenyl sulfanyl-4(*S*)-(3-trimethylsilyl-but-2-enyl)-hexahydro-8(*R*)benzo[1,3]dioxin-2-one (38**) and 7(*S*)-Isopropenyl-8(*R*)-methoxymethoxy-4(*R*)-methyl-5(*R*)-phenylsulfanyl-4(*R*)-(3-trimethylsilyl-but-2-enyl)-hexahydro-8(*R*)benzo[1,3]dioxin-2-one (**40**).**

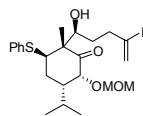
To a dry flask was added (**37** or **39**) (28.1 mg, 59.1 μmol), pyridine (58.7 mg, 0.71 mmol), and CH_2Cl_2 (1.5 mL). The flask was then cooled to $-78\text{ }^\circ\text{C}$ and a solution of triphosgene (26.3 mg, 89.2 μmol) in CH_2Cl_2 (1.0 mL) was added. The reaction was then warmed to ambient temperature. After 3.5 hours the reaction was quenched by adding aq. sat. NH_4Cl (1.5 mL). The aqueous layer was separated and extracted with EtOAc. The combined organic layers were then washed with 1M HCl (aq), then with aq. sat. NaHCO_3 , then with brine. Then dried over Na_2SO_4 , filtered, and solvents removed in vacuo. The products were then purified by column chromatography (60:30:10 Et_2O :Hexanes: CH_2Cl_2) to give oils which solidified upon storing at $0\text{ }^\circ\text{C}$. Carbonate adduct (**38**) from the major aldol diastereomer: (96.6%) ^1H NMR (500 MHz, CDCl_3) δ 7.38-2.27 (m, 5H), 5.89-5.88 (m, 1H), 5.06 (d, $J = 21.0$ Hz, 2H), 4.87 (d, $J = 10.5$ Hz, 1H), 4.73 (dd, $J = 7.0, 23.9$ Hz, 2H), 4.48 (dd, $J = 2.5, 10.5$ Hz, 1H), 4.01 (q, $J = 6.2$, 1H), 3.39 (s, 3H), 3.17 (dd, $J = 4.5, 11.7$ Hz, 1H), 2.86 (s, 1H), 2.75 (m, 1H), 2.40-2.51 (m, 1H), 2.09-2.02 (m, 2H), 1.65 (s, 3H), 1.59 (s, 3H), 1.32 (s, 3H), 0.06 (s, 9H); ^{13}C NMR (75 MHz, CDCl_3) δ 187.9, 148.5, 142.2, 141.1, 133.4, 131.9, 131.4, 129.6, 128.1, 115.4, 96.7, 88.0, 76.3, 74.4, 56.0, 46.0, 44.1, 40.5, 31.3, 28.9, 24.4, 15.0, 14.3, 14.0, -2.0; IR (thin film) 3054, 2986, 1750, 1422, 1265, 1120, 896, 737, 704 cm^{-1} ; HRMS (EI) m/z calc for $\text{C}_{27}\text{H}_{40}\text{O}_5\text{SiS}$ (M) $^+$ 504.2365, found 504.2383. Carbonate adduct (**40**) from the minor aldol diastereomer: (58.0%) ^1H NMR (500 MHz, CDCl_3) δ 7.40-7.29 (m, 5H), 5.88 (t, $J = 5.3$ Hz, 1H), 5.05-4.99 (d, $J = 28.9$ Hz, 2H), 4.71 (dd, $J = 26.4, 7.0$ Hz, 2H), 4.58 (d, $J = 10.7$ Hz, 1H), 4.43 (d, $J = 10.4$ Hz, 1H), 4.04 (q, $J = 6.2$ Hz, 1H), 3.48 (dd, $J = 15.6, 6.9$ Hz, 1H), 3.39 (s, 3H), 3.10 (dd, $J = 12.1, 3.4$ Hz, 1H), 2.81 (s, 1H), 2.39-2.32 (m, 1H), 2.11-2.00 (m, 2H), 1.72 (s, 3H), 1.54 (s, 3H), 1.19 (s, 3H), 0.07 (s, 9H); ^{13}C NMR (75 MHz, CDCl_3) δ 232.9, 149.0, 141.7, 139.7, 133.6, 132.4, 129.4, 128.0, 115.2, 96.6, 91.8, 80.2, 79.4, 73.4, 55.8, 48.8, 43.4, 41.5, 32.3, 32.0, 29.7, 24.0, 15.1, 8.0, -2.1; IR (thin film)

3054, 2986, 1753, 1470, 1265, 1248, 1215, 1120, 1097, 738, 704 cm^{-1} ; HRMS (EI) m/z calc for $\text{C}_{27}\text{H}_{40}\text{O}_5\text{SiS}$ (M)⁺ 504.2365, found 504.2381.



5(S)-Isopropyl-6(R)-methoxymethoxy-2-methyl-cyclohex-2-enone (52)

To a Morton style flask equipped with a three way adapter was added freshly prepared Wilkinson's catalyst ($(\text{PPh}_3)_3\text{RhCl}$, 317 mg, 0.34 mmol), dry benzene (40 mL), and trifluoroethanol (3 mL). This solution was pump/purged using a H_2 filled balloon and a water aspirator five times. The catalyst was then stirred under H_2 for 20 min, then a solution of (**32a**) (2.82 g, 13.41 mmol) in dry benzene (15 mL) and trifluoroethanol (3 mL) was added to the reaction vessel. The Morton flask was pump/purged with H_2 several more times and the reaction left stirring under 1 atm of H_2 at ambient temperature overnight. The reaction mixture was then filtered through a pad of SiO_2 and the SiO_2 washed with EtOAc. Solvents were then removed in vacuo and the residue purified by column chromatography (5:30:65 EtOAc: CH_2Cl_2 : Hexanes) to give the desired product (2.47 g, 87%) and recovered starting material (286 mg, 10%). The product was a slightly yellow oil. ^1H NMR (300 MHz, CDCl_3) δ 6.71 (t, $J = 1.6$ Hz, 1H), 4.71 (d, $J = 6.7$ Hz, 1H), 4.57 (d, $J = 6.7$ Hz, 1H), 4.04 (d, $J = 2.3$ Hz, 1H), 3.31 (s, 3H), 2.37-2.32 (m, 2H), 1.91-1.85 (m, 1H), 1.79 (t, $J = 1.6$ Hz, 3H), 1.66-1.62 (m, 1H), 0.99-0.93 (dd, $J = 6.6, 13.4$ Hz, 6H); ^{13}C NMR (75 MHz, CDCl_3) δ 198.3, 145.3, 132.9, 95.4, 77.2, 55.9, 46.8, 28.1, 27.2, 20.4(6), 20.4(3), 15.7; IR (thin film) 3031, 2985, 1734, 1374, 1266, 1246, 1047, 739, 704 cm^{-1} ; HRMS (EI) m/z calc for $\text{C}_{11}\text{H}_{17}\text{O}_2$ (M- CH_3O)⁺ 181.1228, found 181.1226; $[\alpha]_{\text{D}}^{23} +13.1^\circ$ (MeOH, c 1.0).

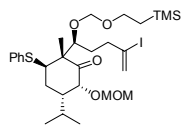


2(S)-(1(S)-Hydroxy-4-iodo-pent-4-enyl)-5(S)-isopropyl-6(R)-methoxymethoxy-

2(S)-methyl-3(R)-phenylsulfanyl-cyclohexanone (**53** and **54**)

Note: The following procedure was carried out in the absence of light. To a dry flask was added CH₂Cl₂ (3.5 mL) and thiophenol (258 mg, 2.36 mmol). The flask was then cooled to 0 °C and AlMe₂Cl (1.0M in hexanes, 4.71 mL, 4.71 mmol) added. The mixture was stirred at 0 °C for 60 minutes, then cooled to -50 °C and a solution of (**52**) (500 mg, 2.36 mmol) in CH₂Cl₂ (3.0 mL) was added. The progress of the 1,4 addition was monitored by TLC (15:85 EtOAc:Hexanes). After stirring for 5 hours at -50 °C, a solution of 4-iodo-pent-4-enal (**51**) (876 mg, 4.21 mmol) in THF (1.5 mL) was added to the reaction flask. After stirring for 2.5 hours at -50 °C, the reaction was diluted with EtOAc (15 mL) and slowly quenched using NaK tartrate (aq. sat.) (8 mL). The reaction was warmed to ambient temperature and vigorously stirred until the aluminum emulsion separated, then diluted with brine (20 mL) and extracted with EtOAc (3x20 mL). The combined organic layers were then washed with NaHCO₃ (aq. sat.) and brine, then dried over MgSO₄, filtered, and solvents removed in vacuo. Purification by column chromatography (10:10:80 EtOAc:Hexanes:CH₂Cl₂) to separate the enone, aldehyde, and aldol diastereomers, and then (60:30:10 Et₂O:Hexanes:CH₂Cl₂) to separate the two aldol diastereomers in a 6:1 ratio, (major diastereomer (**53**), R_f = 0.64 / minor diastereomer (**54**) R_f = 0.56). The major diastereomer was the desired product and isolated as an oil (303 mg, 25%). ¹H NMR (300 MHz, CDCl₃) δ 7.50-7.48 (m, 2H), 7.33-7.27 (m, 3H), 6.01 (d, *J* = 1.3 Hz, 1H), 5.67 (d, *J* = 1.3 Hz, 1H), 4.62-4.60 (m, 2H), 4.27 (d, *J* = 4.0 Hz, 1H), 4.02 (t, *J* = 9.7 Hz, 1H), 3.88 (dd, *J* = 9.5, 5.3 Hz, 1H), 3.39 (s, 3H), 2.62-2.68 (m, 1H), 2.24-2.16 (m, 3H), 2.08-1.99 (m, 1H), 1.85-1.82 (m, 1H), 1.71-1.41 (m, 3H), 1.40 (s, 3H), 0.97 (d, *J* = 6.4 Hz, 3H), 0.77 (d, *J* = 6.4 Hz, 3H); ¹³C NMR (75 MHz, CDCl₃) δ 212.5, 134.6, 132.8, 129.2, 127.6, 125.8, 111.7, 95.3, 79.3, 74.1, 56.1, 50.1, 43.8, 42.7, 31.5, 29.8, 27.9, 22.6, 21.3, 20.7, 17.6; IR (thin film) 3457, 3010, 2970, 2871, 1699, 1612, 1584, 1473,

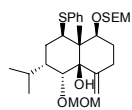
1438, 1374, 1149, 1116, 1085, 1002, 915 cm^{-1} ; HRMS (EI) m/z calc for $\text{C}_{23}\text{H}_{33}\text{O}_4\text{SI}$ (M)⁺ 532.1144, found 532.1124; $[\alpha]_{\text{D}}^{23} +5.3^\circ$ (MeOH, c 1.0).



2(S)-[4-Iodo-1(S)-(2-trimethylsilyl-ethoxymethoxy)-pent-4-enyl]-5(S)-isopropyl-6(R)-methoxymethoxy-2(S)-methyl-3(R)-phenylsulfanyl-cyclohexanone (55)

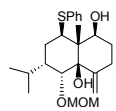
Note: The following procedure was carried out in the absence of light. To a flask was added dimethylaminopyridine (20 mg, cat.), diisopropylethylamine (1.0 mL), and a solution of (**53**) (100.1 mg, 0.188 mmol) in CH_2Cl_2 (1.0 mL). A reflux condenser was attached and 2-chloromethoxyethyltrimethylsilane (62.2 mg, 0.413 mmol) was added. The reaction was then heated to 40 $^\circ\text{C}$ and after 4 hours quenched with NH_4Cl (aq. sat.) (6 mL). The reaction mixture was then extracted with EtOAc (5x10 mL) and the organic layer washed with dilute HCl (2x5 mL), then with brine. The mixture was then dried over MgSO_4 , filtered, and solvents removed in vacuo. The product was then purified by column chromatography (10:90 EtOAc:Hexanes) to give the product as a colorless oil (99.8 mg, 80.1%) ^1H NMR (300 MHz, CDCl_3) δ 7.43-7.22 (m, 5H), 6.00 (s, 1H), 5.68 (s, 1H), 4.80 (dd, $J = 11.0, 7.1$ Hz, 2H), 4.64 (d, $J = 6.6$ Hz, 1H), 4.50 (d, $J = 6.5$ Hz, 1H) 4.41-4.38 (d, $J = 9.1$ Hz, 1H), 4.12-4.11 (m, 2H), 3.73-3.58 (m, 2H), 3.39 (s, 3H), 2.68 (t, $J = 11.2$ Hz, 1H), 2.49 (s, 1H), 2.33 (t, $J = 10.6$ Hz, 1H), 2.15-2.09 (m, 1H), 2.04-2.00 (m, 1H), 1.85-1.68 (m, 3H), 1.26 (s, 3H), 1.02-0.91 (m, 5H), 0.76-0.74 (d, $J = 6.7$ Hz, 3H), 0.05 (s, 9H); ^{13}C NMR (75 MHz, CDCl_3) δ 208.5, 135.2, 132.4, 129.1, 127.3, 125.4, 110.9, 97.4, 95.8, 80.7, 80.5, 66.3, 58.6, 56.6, 53.2, 43.9, 43.2, 33.1, 27.3, 25.4, 20.7, 20.5, 18.2, 15.2, -1.3; IR (thin film) 3054, 2949, 2894, 2069, 2003, 1939, 1741, 1698, 1605, 1580, 1485, 1432, 1380,

1247, 1207, 1089, 1000, 894, 854, 833, 755, 691 cm^{-1} ; HRMS (EI) m/z calc for $\text{C}_{29}\text{H}_{47}\text{O}_5\text{SiSI}$ (M^+) 662.1958, found 662.1968; $[\alpha]_{\text{D}}^{23} +31.1^\circ$ (MeOH, c 1.0).



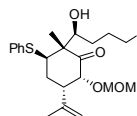
3(S)-Isopropyl-4(R)-methoxymethoxy-8a(S)-methyl-5-methylene-1(R)-phenylsulfanyl-8(S)-(2-trimethylsilyl-ethoxymethoxy)-octahydro-naphthalen-4a(S)-ol (56)

Note: The following procedure was carried out in the absence of light. To a flask was added (**55**) (50 mg, 75 μmol) and THF (3.0 mL). The reaction was cooled to -78°C and *sec*-butyl lithium (1.07 M in hexanes, 77 μL , 83 μmol) was added. The reaction was stirred at -78°C and after 100 minutes quenched at -78°C with NH_4Cl (aq. sat.) (1.5 mL). The reaction was warmed to ambient temperature, neutralized with NaHCO_3 (aq. sat.) (2.0 mL) and then extracted with EtOAc (3x10 mL). The combined organic layers were dried over MgSO_4 , filtered, and concentrated in vacuo. The crude product was purified by column chromatography (5:20:75 THF: CH_2Cl_2 :Hexanes, $R_f=0.41$) to give a clear oil (29 mg, 72.5%) ^1H NMR (300 MHz, CDCl_3) δ 7.44-7.19 (m, 5H), 5.26 (s, 1H), 4.98 (s, 1H), 4.79 (d, $J=7.1$ Hz, 1H), 4.65 (d, $J=7.1$ Hz, 1H), 4.59 (s, 2H), 4.48-4.39 (dd, $J=14.4, 2.1$ Hz, 1H), 4.03 (d, $J=3.0$ Hz, 1H), 3.62-3.54 (m, 3H), 3.38 (s, 3H), 2.37-2.46 (m, 2H), 2.06-1.97 (m, 2H), 1.77-1.59 (m, 3H), 1.16 (s, 3H), 1.00 (d, $J=6.5$ Hz, 3H), 0.94-0.88 (td, $J=9.3, 3.4$ Hz, 4H), 0.85-0.83 (d, $J=6.5$ Hz, 3H), -0.02 (s, 9H); ^{13}C NMR (75 MHz, CDCl_3) δ 150.9, 138.0, 131.2, 128.9, 126.4, 111.3, 98.7, 93.6, 86.0, 80.2, 74.3, 69.7, 65.6, 56.7, 51.9, 47.0, 39.5, 30.6, 26.9, 25.0, 21.3, 20.8, 18.2, 13.4, -1.5; IR (thin film) 3484, 3070, 2946, 2922, 2084, 2019, 1942, 1630, 1580, 1481, 1435, 1383, 1244, 1151, 1098, 1049, 1024, 938, 857, 830 cm^{-1} ; HRMS (EI) m/z calc for $\text{C}_{29}\text{H}_{48}\text{O}_5\text{SiS}$ (M^+) 536.2991, found 536.2999; $[\alpha]_{\text{D}}^{23} -56.2^\circ$ (MeOH, c 1.0).



6(S)-Isopropyl-5-methoxymethoxy-8a-methyl-4-methylene-8-phenylsulfanyl-octahydro-naphthalene-1,4a-diol (57)

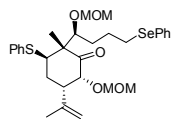
To a flask containing (**56**) (30 mg, 56 μ mol) was added a solution of (1.0 M) potassium aminopropyl amide in 1,3-diaminopropane (KAPA) (1.0 mL, 1.0 mmol) at 0 °C under N₂. After 90 min, the reaction was quenched with brine (2 mL) and dilute HCl_(aq) (3 mL). This mixture was extracted with EtOAc and the organic layer washed with 1 M HCl_(aq), then with brine. The organic layer was dried over MgSO₄, filtered, and concentrated and purified by column chromatography (25:75 / EtOAc:Hexane, R_f = 0.25). This gave the diol (**57**) as a clear oil (17 mg, 75% yield). ¹H NMR (300 MHz, CDCl₃) δ 7.41-7.44 (m, 2H), 7.18-7.29 (m, 3H), 5.26 (t, 1H, *J* = 1.8 Hz), 4.97 (s, 1H), 4.58 (d, 2H, *J* = 1.4 Hz), 4.48-4.53 (m, 1H), 4.07 (d, 1H, *J* = 3.1 Hz), 3.51 (s, 1H), 3.36 (s, 3H), 2.55-2.65 (m, 1H), 2.44-2.40 (m, 2H), 2.04-2.00 (m, 2H), 1.86-1.83 (m, 1H), 1.77-1.75 (m, 1H), 1.68-1.64 (m, 3H), 1.09 (s, 3H), 0.98 (d, 3H, *J* = 6.5 Hz), 0.82 (d, 3H, *J* = 6.5 Hz); ¹³C NMR (75 MHz, CDCl₃) δ 150.9, 137.9, 131.6, 129.2, 126.8, 111.8, 99.1, 86.3, 78.6, 68.7, 57.0, 52.0, 47.8, 39.8, 31.0, 27.2, 25.1, 21.7, 21.0, 13.7; IR (thin film) 3478, 3048, 2822, 1584, 1262, 1142, 1095, 1021, 743, 702 cm⁻¹; HRMS (EI) *m/z* calc for C₂₃H₃₄O₄S (M)⁺ 406.2178, found 406.2191; [α]_D²³ -5.3 ° (MeOH, c 1.0).



2(S)-(1(S)-Hydroxy-4-phenylselanyl-butyl)-5(S)-isopropenyl-6(R)-methoxymethoxy-2(S)-methyl-3(R)-phenylsulfanyl-cyclohexanone (60 and 61)

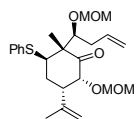
To a flask was added CH₂Cl₂ (3.0 mL) and thiophenol (182 mg, 1.62 mmol). The flask was then cooled to 0 °C and AlMe₂Cl (1.0M in hexanes, 3.25 mL, 3.25 mmol) was added and the mixture stirred at 0 °C for 45 minutes. Then the reaction flask was cooled to -45 °C and a solution of

(**32a**) (341 mg, 1.62 mmol) in CH₂Cl₂ (2.5 mL) was added. The progress of the 1,4 addition was monitored by TLC (15:85 EtOAc:Hexanes). After stirring for 4 hours at -50 °C, a solution of 4-phenylselenobutanal (**59**) (516 mg, 2.27 mmol) in THF (2.0 mL) was added to the reaction flask. After stirring for 2 hours at -45 °C, the reaction was diluted with EtOAc (7 mL) and slowly quenched using NaK tartrate (aq. sat) (2 mL). The reaction was warmed to ambient temperature and vigorously stirred until the aluminum emulsion separated, then diluted with brine (10 mL) and extracted with EtOAc (4x15 mL). The combined organic layers were then washed with NaHCO₃ (aq. sat.) and brine, then dried over Na₂SO₄, filtered, and solvents removed in vacuo. Purification by column chromatography (gradient: 5:30:65 EtOAc: CH₂Cl₂: Hexanes to separate the enone and aldehyde, then 50:50 EtOAc:Hexanes to elute aldol adducts) to give recovered enone (195 mg, 57%) and aldehyde (424 mg, 82%). The aldol adducts were then separated by another column (20:30:50 EtOAc: CH₂Cl₂: Hexanes) to give the desired product as two diastereomers in a 6:1 ratio. Major Diastereomer (**60**) (R_f= 0.47, 164 mg, 19%) ¹H NMR (300 MHz, CDCl₃) δ 7.47-7.38 (m, 4H), 7.33-7.20 (m, 6H), 4.98 (s, 1H), 4.75 (s, 1H), 4.66 (d, *J* = 0.7 Hz, 2H), 4.45 (d, *J* = 5.7 Hz, 1H), 3.89 (t, *J* = 10.1 Hz, 1H), 3.50 (dd, *J* = 11.4, 4.4 Hz, 1H), 3.36 (s, 3H), 2.98-2.86 (m, 1H), 2.87 (t, *J* = 6.6 Hz, 2H), 2.18-2.28 (m, 2H), 2.01-2.05 (m, 1H), 1.75-1.57 (m, 4H), 1.52 (s, 3H), 1.48 (s, 3H); ¹³C NMR (75 MHz, CDCl₃) δ 213.3, 141.4, 134.8, 133.0, 132.9, 132.8, 132.7, 132.6, 130.9, 129.5, 129.3, 127.9, 126.9, 115.2, 96.1, 78.2, 75.9, 56.9, 56.2, 49.6, 46.2, 32.2, 31.0, 28.2, 27.6, 22.7, 18.9 ppm; IR (thin film) 3506, 3073, 3054, 2943, 1735, 1704, 1648, 1571, 1438, 1374, 1240, 1027, 922 cm⁻¹; HRMS (EI) *m/z* calc for C₂₈H₃₆O₄SSe (M)⁺ 548.1499, found 548.1498; [α]_D²³ +4.4 ° (MeOH, c 1.0).



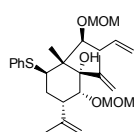
5(S)-Isopropenyl-6(R)-methoxymethoxy-2(S)-(1(S)-methoxymethoxy-4-phenylselanyl-butyl)-2-methyl-3(R)-phenylsulfanyl-cyclohexanone (62)

To a flask equipped with a reflux condenser was added (**60**) (160 mg, 0.29 mmol), CH₂Cl₂ (2.0 mL), diisopropylethylamine (1.5 mL), and dimethylaminopyridine (50 mg). Chloromethyl methyl ether (74.2 mg, 0.88 mmol) was added and the reaction heated to 40 °C. After stirring for 20 hours the reaction was quenched by adding NH₄Cl (aq. sat.) (4 mL). The mixture was then extracted with EtOAc (4x10 mL) and the organic layers were washed with a 50:50 solution of brine: 1M HCl_(aq) (2x5 mL). The organic layers were then dried over Na₂SO₄, filtered, and solvents removed in vacuo. The resulting yellow residue was purified by column chromatography (10:30:60 EtOAc:CH₂Cl₂:Hexanes) to give the desired product as a slightly yellow oil (170 mg, 99%) ¹H NMR (300 MHz, CDCl₃) δ 7.67-7.48 (m, 2H), 7.49-7.38 (m, 2H), 7.29-7.25 (m, 6H), 4.94 (d, *J* = 1.1 Hz, 1H), 4.81 (s, 1H), 4.71 (s, 2H), 4.55 (d, *J* = 6.8 Hz, 1H), 4.32 (d, *J* = 7.2 Hz, 2H), 4.23 (d, *J* = 3.6 Hz, 1H), 4.08 (t, *J* = 4.2 Hz, 1H), 3.36 (s, 3H), 3.27 (s, 3H), 3.00-3.04 (m, 1H), 2.94-2.84 (m, 2H), 2.55-2.58 (m, 1H), 1.99-1.98 (m, 1H), 1.90 (t, *J* = 4.2 Hz, 1H), 1.89-1.85 (m, 1H), 1.78 (s, 3H), 1.68-1.61 (m, 2H), 1.29 (s, 3H); ¹³C NMR (75 MHz, CDCl₃) δ 207.6, 142.8, 135.4, 132.2, 131.7, 130.2, 128.9, 126.9, 126.6, 112.8, 99.0, 95.1, 81.4, 79.1, 58.6, 56.0, 52.6, 43.9, 33.2, 27.9, 27.5, 26.3, 21.9, 15.5 ppm ; IR (thin film) 3057, 2946, 1710, 1475, 1148, 1089, 1024, 922, 737 cm⁻¹; HRMS (EI) *m/z* calc for C₃₀H₄₀O₅SSe (M)⁺ 592.1584 , found 592.1598; [α]_D²³ +6.7 ° (MeOH, c 1.0).



5(S)-Isopropenyl-6(R)-methoxymethoxy-2(R)-(1(S)-methoxymethoxy-but-3-enyl)-2-methyl-3(R)-phenylsulfanyl-cyclohexanone (63)

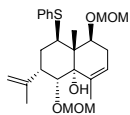
To a flask was added (**62**) (145 mg, 0.245 mmol) and dry CH₂Cl₂ (3 mL). This solution was then cooled to -78 °C and a solution of purified *m*-CPBA (42.3 mg, 0.245 mmol) in CH₂Cl₂ (2.0 mL) was added slowly. When the addition was complete, the reaction was allowed to slowly warm to ambient temperature. After 90 minutes a reflux condenser was attached. Then pyridine (78.2 mg, 0.98 mmol) and 3,4-dihydro-2H-pyran (618 mg, 7.35 mmol) were added and the reaction heated to reflux (oil bath temp 75 °C). After 3 hours, the reaction was cooled to ambient temperature and the volatile compounds removed by rotovap. The residue was taken up in EtOAc (20 mL) and washed with brine, 10% HCl (aq), and NaHCO₃ (aq. sat.). The organic layer was then dried over Na₂SO₄, filtered, and solvents removed in vacuo. The residue was then purified by column chromatography (15:85 EtOAc:Hexanes) to give the desired product as a white waxy solid (103 mg, 97%). ¹H NMR (300 MHz, CDCl₃) δ 7.39-7.21 (m, 5H), 5.82-5.87 (m, 1H), 5.06 (d, *J* = 15.2 Hz, 1H), 5.03 (d, *J* = 8.2 Hz, 1H), 4.91 (s, 1H), 4.80 (s, 1H), 4.76 (d, *J* = 7.0 Hz, 1H), 4.65 (d, *J* = 7.1 Hz, 1H), 4.57 (d, *J* = 6.7 Hz, 1H), 4.50-4.51 (m, 1H), 4.47 (d, *J* = 6.6 Hz, 1H), 4.23 (d, *J* = 3.4 Hz, 1H), 4.08 (t, *J* = 3.6 Hz, 1H), 3.39 (s, 3H), 3.31 (s, 3H), 3.02 (d, *J* = 11.1 Hz, 1H), 2.61 (t, *J* = 11.4 Hz, 1H), 2.32 (quint, *J* = 7.8 Hz, 1H), 1.76-1.87 (m, 2H), 1.77 (s, 3H), 1.29 (s, 3H); ¹³C NMR (75 MHz, CDCl₃) δ 207.9, 143.3, 136.2, 135.9, 132.2, 129.3, 127.4, 117.3, 113.2, 98.8, 95.7, 80.0, 79.6, 58.8, 56.5, 56.4, 53.2, 44.3, 37.7, 26.6, 22.3, 15.8 ppm; IR (thin film) 3076, 2946, 1704, 1438, 1157, 1018, 909, 733 cm⁻¹; HRMS (EI) *m/z* calc for C₂₄H₃₄O₅S (M)⁺ 434.2126, found 434.2146; [α]_D²³ +2.7 ° (MeOH, c 1.0).



1(R),5(S)-Diisopropenyl-6(R)-methoxymethoxy-2(R)-(1(S)-methoxymethoxy-but-3-enyl)-2-methyl-3(R)-phenylsulfanyl-cyclohexanol (64)

Preparation of 2-propenylmagnesium bromide: To a flask equipped with a reflux condenser was added oven dried magnesium turnings (241 mg, 10.0 mmol), iodine (20 mg), and THF (10 mL). Then 2-bromopropene (1.20 g, 10.0 mmol) was added drop-wise to the flask. After all of the metal had dissolved, the Grignard was stirred for an additional 10 minutes prior to use.

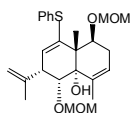
To a flask was added (**63**) (60 mg, 0.14 mmol) and THF (2.5 mL). The reaction vessel was cooled to $-78\text{ }^{\circ}\text{C}$ and 2-propenyl magnesium bromide (1.0M THF, 0.70 mL, 0.70 mmol) was added. The reaction was warmed to ambient temperature and after 3 hours quenched by adding NaHCO_3 (aq. sat.) (1.0 mL). The mixture was then extracted with EtOAc (3x10 mL) and the organic layer washed with brine (5 mL). The organic layer was dried over Na_2SO_4 , filtered, and solvents removed in vacuo. The product was separated from the starting material by column chromatography (5:30:65 EtOAc: CH_2Cl_2 :Hexanes) to give the starting material (**63**) (45 mg, 75%) as a waxy solid and the product (**64**) as a slightly yellow oil (13.2 mg, 20%). ^1H NMR (300 MHz, CDCl_3) δ 7.51 (d, $J = 7.1$ Hz, 2H), 7.25-7.29 (m, 3H), 5.82-5.89 (m, 1H), 5.11 (s, 2H), 5.09 (s, 1H), 5.02 (s, 2H), 4.94 (s, 1H), 4.77 (d, $J = 7.9$ Hz, 2H), 4.71 (d, $J = 6.9$ Hz, 1H), 4.54 (d, $J = 7.0$ Hz, 1H), 4.67 (d, $J = 0.9$ Hz, 2H), 4.18 (d, $J = 7.1$ Hz, 1H), 4.10 (dd, $J = 11.9, 4.2$ Hz, 1H), 4.00 (dd, $J = 7.0, 4.3$ Hz, 1H), 3.37 (s, 3H), 3.33 (s, 3H), 2.89-2.92 (m, 1H), 2.78-2.81 (m, 2H), 2.21 (dt, $J = 14.6, 3.6$ Hz, 1H), 2.01-2.04 (m, 2H), 1.94 (s, 3H), 1.76 (s, 3H), 1.23 (s, 3H); ^{13}C NMR (75 MHz, CDCl_3) δ 148.6, 146.3, 138.6, 135.8, 132.7, 129.6, 127.2, 116.0, 113.9, 98.5, 96.2, 85.4, 83.7, 78.7, 56.8, 56.5, 50.0, 48.7, 42.2, 38.3, 32.6, 24.3, 23.3, 17.5 ppm; IR (thin film) 3556, 3069, 2923, 1636, 1442, 1153, 1093, 1034, 911, 745, 689 cm^{-1} ; HRMS (EI) m/z calc for $\text{C}_{27}\text{H}_{40}\text{O}_5\text{S}$ (M) $^+$ 476.2596, found 476.2613; $[\alpha]_{\text{D}}^{23} -3.3^{\circ}$ (MeOH, c 1.0).



3(S)-Isopropenyl-4(R),8(S)-bis-methoxymethoxy-5,8a(S)-dimethyl-1(R)-phenylsulfanyl-1,3,4,7,8,8a-hexahydro-2H-naphthalen-4a(S)-ol (65)

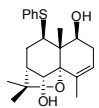
Note: Grubbs 2nd generation catalyst was prepared according to the literature procedure starting from bis(tricyclohexylphosphine)methylidene ruthenium dichloride and 1,3-dimesityl-4,5-dihydroimidazolium chloride.

To a flask equipped with a greased reflux condenser was added (**64**) (12.0 mg, 25 μ mol) and CH_2Cl_2 (0.63 mL). Then Grubbs 2nd generation catalyst (0.6 mg, 2.5 mole%) was added and the reaction heated to reflux. After stirring for 15 minutes at reflux the reaction was cooled to ambient temperature and filtered through a plug of silica gel to remove most of the catalyst. The plug was washed with 50:50 EtOAc:Hexanes to elute product. Solvents were then removed in vacuo to give a brown oily residue (10.9mg, 94% yield). ^1H NMR (300 MHz, CDCl_3) δ 7.25-7.38 (m, 4H), 7.15-7.17 (m, 1H), 5.42 (t, $J = 1.5$ Hz, 1H), 4.90 (s, 1H), 4.87 (s, 1H), 4.83 (d, $J = 5.0$ Hz, 1H), 4.76 (d, $J = 3.7$ Hz, 2H), 4.70 (d, $J = 5.0$ Hz, 1H), 4.34 (dd, $J = 9.3, 6.7$ Hz, 1H), 3.87 (d, $J = 5.7$ Hz, 1H), 3.78 (s, 1H), 3.77 (d, $J = 4.8$ Hz, 1H), 3.42 (s, 3H), 3.34 (s, 3H), 3.05 (ddd, $J = 10.3, 5.5, 2.64$ Hz, 1H), 2.78 (td, $J = 13.5, 6.5$ Hz, 1H), 2.49-2.54 (m, 1H), 2.02-2.13 (m, 1H), 1.62-1.66 (m, 1H), 1.84 (s, 3H), 1.80 (s, 3H), 1.29 (s, 3H); ^{13}C NMR (75 MHz, CDCl_3) δ 145.9, 137.6, 137.5, 129.4, 128.9, 125.4, 124.4, 116.1, 114.1, 111.3, 98.1, 97.2, 79.7, 78.6, 76.9, 57.3, 55.8, 48.6, 43.8, 41.5, 31.6, 31.4, 22.7, 20.0, 14.3 ppm; IR (thin film) 3521, 3061, 2919, 1640, 1584, 1434, 1141, 1101, 1038, 911, 737 cm^{-1} ; HRMS (EI) m/z calc for $\text{C}_{25}\text{H}_{36}\text{O}_5\text{S}$ (M)⁺ 448.2283, found 448.2267; $[\alpha]_D^{23} -6.3^\circ$ (MeOH, c 1.0). H,H-COSY and 1D NOE are consistent with proposed structure.



6(S)-Isopropenyl-1(S),5(R)-bis-methoxymethyl-4,8a(S)-dimethyl-8-phenylsulfanyl-1,5,6,8a-tetrahydro-2H-naphthalen-4a(S)-ol (66)-(67)

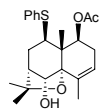
A solution of (**65**) (50 mg, 0.11 mol) in CH₂Cl₂ (5 mL) was cooled to -78 °C under N₂. A solution on purified *m*-CPBA (20 mg, 0.12 mmol) in CH₂Cl₂ (1.0 mL) was added dropwise and the reaction stirred for 40 min before warming to 25 °C for 30 min. Pyridine (87mg, 1.10 mmol) was added followed by TFAA (116 mg, 0.55 mmol) to the crude sulfoxide (**66**) and the mixture stirred for 5 hrs. The reaction was quenched with NaHCO₃ (aq. sat.) (2 mL) and then diluted with EtOAc. The organic layer was separated and washed with 1 M HCl (aq.), dried over Na₂SO₄, concentrated, and purified by prep. TLC (15:85 / EtOAc:Hexane, R_f= 0.25). This gave the vinyl sulfide (**67**) as a clear oil. (43 mg, 87% yield) ¹H NMR (300 MHz, CDCl₃) δ 7.53-7.56 (m, 2H), 7.26-7.33 (m, 3H), 5.46-5.47 (m, 1H), 4.98 (d, *J* = 2.7 Hz, 1H), 4.90 (d, *J* = 6.9 Hz, 1H), 4.76 (d, *J* = 6.9 Hz, 1H), 4.73 (d, *J* = 5.0 Hz, 1H), 4.71 (s, 2H), 4.66 (d, *J* = 5.0 Hz, 1H), 4.36 (dd, *J* = 14.6, 7.6 Hz, 1H), 4.03 (d, *J* = 8.8 Hz, 1H), 3.41 (dd, *J* = 8.8, 2.7 Hz, 1H), 3.38 (s, 3H), 3.36 (s, 3H), 2.78-2.84 (m, 1H), 2.16-2.25 (m, 1H), 1.87 (s, 3H), 1.58 (s, 3H), 1.17 (s, 3H); ¹³C NMR (75 MHz, CDCl₃) δ 146.8, 143.3, 136.3, 135.8, 134.6, 129.1, 127.8, 127.4, 124.9, 115.2, 98.5, 98.2, 77.3, 76.8, 57.5, 56.2, 49.2, 48.6, 31.9, 21.6, 21.4, 15.7 ppm; IR (thin film) 3514, 3063, 2935, 1634, 1440, 1373, 1152, 1096, 1030, 902, 737, 646 cm⁻¹; HRMS (EI) *m/z* calc for C₂₅H₃₄O₅S (M)⁺ 446.2126, found 446.2143; [α]_D²³ -2.7 ° (MeOH, c 1.0).



2,6(R),10,10-Tetramethyl-7(R)-phenylsulfanyl-11(S)-oxa-9(R)-tricyclo[7.2.1.0^{1,6}]dodec-2-ene-5(S),12(R)-diol (68)

To a solution of (**65**) (10.0 mg, 22 μmol) in THF (0.5 mL) at 25 °C was added a solution of trifluoromethanesulfonic acid (4.35 mg, 29 μmol) in THF (1.0 mL). The reaction was stirred for

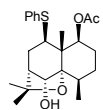
25 minutes and then quenched by adding solid NaHCO₃ (20 mg). The reaction was concentrated to half volume then purified by preparatory TLC (20:30:50 / EtOAc:CH₂Cl₂:Hexanes, R_f = 0.29) This gave the desired product as a white residue (2.5 mg, 30% yield). ¹H NMR (300 MHz, CDCl₃) δ 7.51-7.54 (m, 2H), 7.27-7.36 (m, 3H), 5.64 (d, *J* = 5.6 Hz, 1H), 4.63 (s, 1H), 4.28 (dd, *J* = 9.6, 5.9 Hz, 1H), 4.14 (s, 1H), 3.67 (dd, *J* = 11.7, 6.8 Hz, 1H), 2.31-2.35 (m, 1H), 2.14-2.17 (m, 1H), 2.06-2.07 (m, 2H), 2.05 (s, 3H), 1.99-2.03 (m, 1H), 1.97-1.98 (m, 1H), 1.51 (s, 3H), 1.17 (s, 3H), 1.15 (s, 3H); ¹³C NMR (75 MHz, CDCl₃) δ 133.2, 132.7, 132.1, 129.3, 128.1, 127.9, 91.5, 82.3, 80.7, 73.5, 52.6, 51.0, 47.9, 35.9, 31.1, 29.4, 24.1, 22.8, 12.3; IR (thin film) 3534, 3053, 1617, 1421, 1106, 908, 733 cm⁻¹; HRMS (EI) *m/z* calc for C₂₁H₂₈O₃S (M)⁺ 360.1759, found 360.1753; [α]_D²³ -8.5° (MeOH, c 1.0); H,H-COSY and 1D NOE experiments are consistent with proposed structure.



Acetic acid 12(R)-hydroxy-2(R),6(S),10,10-tetramethyl-7(R)-phenylsufanyl-11(S)-oxa-tricyclo [7.2.1.01,6]dodec-2-en-5(S)-yl ester (69)

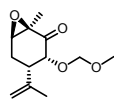
To a solution of (**68**) (12.0 mg, 32 μmol) in CH₂Cl₂ (1.0 mL) was added triethylamine (6.5 mg, 64 μmol), DMAP (1mg), and finally Ac₂O (3.3 mg, 32 μmol) in CH₂Cl₂ (0.15 mL) at 25 °C under N₂. After 2.5 hrs the reaction was concentrated and purified by prep. TLC. (15:30:55 / EtOAc:CH₂Cl₂:Hexane, R_f = 0.31). This gave the desired product (7.2 mg, 56 % yield). ¹H NMR (300 MHz, CD₂Cl₂) δ 7.41-7.44 (m, 2H), 7.22-7.30 (m, 2H), 5.62-5.67 (m, 2H), 4.58 (s, 1H), 3.77 (dd, *J* = 11.3, 6.3 Hz, 1H), 2.14-2.18 (m, 2H), 2.04 (s, 3H), 2.02 (dd, *J* = 5.2, 3.4 Hz, 3H), 1.90-1.92 (m, 2H), 1.81-1.84 (m, 1H), 1.62 (s, 1H), 1.51 (s, 3H), 1.24 (s, 3H), 1.19 (s, 3H); ¹³C NMR (75 MHz, CDCl₃) δ 171.6, 134.6, 133.2, 132.3, 128.9, 127.0, 92.3, 91.3, 82.4, 80.7, 73.2, 51.1, 48.8, 48.1, 36.0, 29.5, 29.0, 24.3, 22.7, 22.2, 13.7; IR (thin film) 3435, 3053, 1722, 1265,

733 cm^{-1} ; HRMS (EI) m/z calc for $\text{C}_{23}\text{H}_{30}\text{O}_4\text{S}$ (M^+) 402.1864, found 402.1868; $[\alpha]_{\text{D}}^{23}$ -4.3° (MeOH, c 1.0).



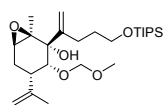
Acetic acid 5(S)-12(R)-hydroxy-2(R),6(S),10,10-tetramethyl-7(R)-phenylsulfanyl-11(S)-oxa-tricyclo[7.2.1.01,6]dodec-5(S)-yl ester (70)

A solution of (**69**) (16.8 mg, 42 μmol) was dissolved in CH_2Cl_2 (2.0 mL). The mixture was flushed with H_2 and $[\text{Ir}(\text{cod})\text{py}(\text{PCy}_3)]\text{PF}_6$ (3.4 mg, 4.2 μmol) was added by dissolving in CH_2Cl_2 (0.4 mL) and adding by syringe pump over a 45 min period. This addition was made once more to total 20 mol% catalyst. After a total of 3 hrs, the reaction was concentrated and purified by prep. TLC (25:75 / EtOAc:Hexane, $R_f = 0.35$) to give recovered starting material (**69**) (7.6 mg, 45% recovery) and desired product (**70**) (5.5 mg, 33% yield), both waxy solids. ^1H NMR (300 MHz, CDCl_3) δ 7.44-7.45 (m, 2H), 7.20-7.27 (m, 3H), 5.49 (dd, $J = 12.0, 3.6$ Hz, 1H), 4.37 (s, 1H), 3.60-3.63 (m, 1H), 2.18-2.21 (m, 2H), 2.03-2.07 (m, 1H), 2.03 (s, 3H), 1.86-1.89 (m, 2H), 1.69-1.74 (m, 3H), 1.53-1.57 (m, 4H), 1.26 (s, 3H), 1.18 (d, $J = 7.5$ Hz, 3H), 1.11 (s, 3H); ^{13}C NMR (75 MHz, CDCl_3) δ 171.5, 134.8, 133.1, 128.9, 127.3, 116.5, 95.9, 93.4, 78.1, 78.0, 71.2, 50.6, 35.5, 34.1, 30.7, 29.8, 26.8, 24.3, 23.9, 22.3, 17.9, 13.3 ppm; IR (thin film) 3498, 3057, 1731, 1260, 1028 cm^{-1} ; HRMS (EI) m/z calc for $\text{C}_{23}\text{H}_{32}\text{O}_4\text{S}$ (M^+) 404.2021, found 404.2027; $[\alpha]_{\text{D}}^{23}$ -3.6° (MeOH, c 1.0); H,H-COSY and 1D NOE experiments are consistent with proposed structure.



4(S)-Isopropenyl-3(R)-methoxymethoxy-1(R)-methyl-7-oxa-bicyclo[4.1.0]heptan-2-one (71)

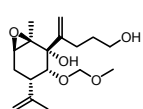
A solution of (**32a**) (1.58 g, 7.52 mmol) and K₂CO₃ (2.08 g, 15.04 mmol) in THF (22.5 mL) and H₂O (7.5 mL) was cooled to 0 °C. H₂O₂ (30% aq.) (4.26 mL, 37.60 mmol) was added slowly by syringe. After stirring for 2 hrs another addition of H₂O₂ (30% aq.) (4.26 mL, 37.60 mmol) was made and the reaction allowed to warm to 25 °C. After 17 hrs, the reaction was cooled back to 0 °C and a final addition of H₂O₂ (30% aq.) (4.26 mL, 37.60 mmol) was made. The reaction was allowed to warm to 25 °C and after a total reaction time of 37 hrs poured into brine (60 mL) and extracted with EtOAc. The combined organic layers were washed with Na₂S₂O₃ (aq.sat.) and then with brine. The organic layer was dried over MgSO₄, filtered, concentrated, and purified by column chromatography (50:50 / Ether:Hexane, R_f = 0.50). This gave the desired compound as a clear oil (1.31 g, 77% yield). ¹H NMR (300 MHz, CDCl₃) δ 4.93 (s, 1H), 4.77 (s, 1H), 4.65 (d, *J* = 6.7 Hz, 1H), 4.61 (d, *J* = 6.7 Hz, 1H), 4.40 (d, *J* = 3.8 Hz, 1H), 3.48 (t, *J* = 2.3 Hz, 1H), 3.35 (s, 3H), 2.76-2.78 (m, 1H), 2.29-2.34 (m, 2H), 1.78 (s, 3H), 1.45 (s, 3H); ¹³C NMR (75 MHz, CDCl₃) δ 202.3, 143.9, 112.7, 95.3, 75.7, 62.8, 59.3, 55.8, 43.3, 25.9, 22.5, 15.1; IR (thin film) 1721, 1148, 922 cm⁻¹; HRMS (EI): *m/z* calc for C₁₁H₁₅O₄ (M-CH₃)⁺ 211.0970, found 211.0968; [α]_D²³ +2.7 ° (MeOH, c 1.0).



4(S)-Isopropenyl-3(R)-methoxymethoxy-1(S)-methyl-2(R)-(1-methylene-4-triisopropylsilyloxy-butyl)-7-oxa-bicyclo[4.1.0]heptan-2(R)-ol (73)

A solution of (**71**) (1.03 g, 4.55 mmol) in THF (14 mL) was cooled to -78 °C under N₂. In a separate flask, (4-Bromopent-4-enyloxy)-triisopropylsilane (**72**) (2.08 g, 6.47 mmol) was dissolved in THF (16 mL) and cooled to -78 °C under N₂. Then *t*-butyl lithium (7.61 mL, 12.94 mmol) was added to the solution of (**72**) and the resulting yellow solution stirred for 10 min. The vinyl lithium reagent was then added by syringe to the epoxy ketone (**71**) solution at -78 °C.

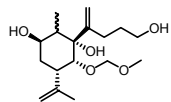
After 45 min, the reaction was quenched by pouring into a solution of brine (25 mL) and 1 M HCl (aq) (20 mL). This mixture was extracted with EtOAc and the organic layers dried over MgSO₄, filtered, concentrated, and purified by column chromatography (10:90 / EtOAc:Hexane, R_f= 0.30). This gave separable diastereomers as a 12:1 (β:α) ratio in favor of the desired diastereomer (1.23 g, 58% yield). ¹H NMR (300 MHz, CDCl₃) δ 5.42 (s, 1H), 5.08 (s, 1H), 4.88 (d, *J* = 0.8 Hz, 1H), 4.78 (s, 1H), 4.64 (d, *J* = 6.4 Hz, 1H), 4.56 (d, *J* = 6.4 Hz, 1H), 3.83 (d, *J* = 1.7 Hz, 1H), 3.75 (t, *J* = 6.4 Hz, 2H), 3.59 (s, 1H), 3.38 (s, 3H), 3.05 (t, *J* = 2.1 Hz, 1H), 2.40 (dd, *J* = 10.7, 6.4 Hz, 1H), 2.34 (t, *J* = 20.4 Hz, 2H), 2.20 (td, *J* = 14.4, 2.2 Hz, 1H), 1.92 (ddd, *J* = 14.4, 4.5, 1.9 Hz, 1H), 1.80 (s, 3H), 1.78-1.83 (m, 2H), 1.39 (s, 3H), 0.96-1.10 (m, 21H); ¹³C NMR (75 MHz, CDCl₃) δ 149.4, 145.5, 111.9, 111.8, 98.3, 78.8, 74.5, 63.3, 61.2, 59.3, 56.3, 37.9, 31.9, 28.2, 24.9, 22.8, 20.3, 18.0, 11.9; IR (thin film) 3508, 1639, 1465, 1378, 1152, 1107, 912, 887, 784, 733 cm⁻¹; HRMS (EI): *m/z* calc for C₂₃H₄₁SiO₅ (M-C₃H₇)⁺ 425.2723, found 425.2724; [α]_D²³ -26.2 ° (MeOH, c 1.0).



2(R)-(4-Hydroxy-1-methylene-butyl)-4(S)-isopropenyl-3(R)-methoxymethoxy-1(S)-methyl-7-oxa-bicyclo[4.1.0]heptan-2-ol (75)

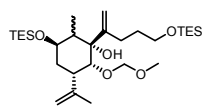
To a solution of (73) (705 mg, 1.50 mmol) in THF (20 mL) was added TBAF hydrate (511 mg, 1.96 mmol) at 25 °C. After 2.5 hrs, the reaction was concentrated and purified by column chromatography (75:25 / EtOAc:Hexane, R_f= 0.50). This gave the desired diol as a clear oil (437 mg, 93% yield). ¹H NMR (300 MHz, CDCl₃) δ 5.43 (s, 1H), 5.03 (s, 1H), 4.83 (s, 1H), 4.72 (s, 1H), 4.59 (d, *J* = 6.4 Hz, 1H), 4.50 (d, *J* = 6.4 Hz, 1H), 3.75 (d, *J* = 1.4 Hz, 1H), 3.58-3.63 (m, 2H), 3.32 (s, 3H), 3.00 (t, *J* = 1.9 Hz, 1H), 2.35 (dd, *J* = 6.5, 4.1 Hz, 1H), 2.24 (t, *J* = 7.4 Hz, 2H), 2.15 (td, *J* = 10.8, 2.2 Hz, 1H), 1.84 (ddd, *J* = 14.4, 1.9, 1.8 Hz, 1H), 1.75 (s, 3H), 1.72-1.74

(m, 1H), 1.34 (s, 3H), 1.18-1.22 (m, 1H); ^{13}C NMR (75 MHz, CDCl_3) δ 148.4, 145.2, 112.7, 111.8, 98.2, 78.5, 74.5, 61.6, 60.2, 59.1, 56.8, 37.6, 31.5, 27.2, 24.6, 22.6, 20.8; IR (thin film) 3452, 1147, 917 cm^{-1} ; HRMS (EI): m/z calc for $\text{C}_{16}\text{H}_{24}\text{O}_4$ ($\text{M}-\text{CH}_4\text{O}$) $^+$ 280.1674, found 280.1677; $[\alpha]_{\text{D}}^{23}$ -57.8° (MeOH, c 1.0).



1(R)-(4-Hydroxy-1-methylene-butyl)-5(S)-isopropenyl-6(R)-methoxymethoxy-2(R,S)-methyl-cyclohexane-1(R),3(R)-diol (76)

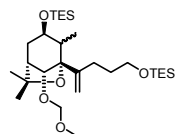
To a solution of (**75**) (437 mg, 1.40 mmol) in THF (17 mL) was added 1,4-cyclohexadiene (1.12 g, 14.0 mmol), collidine hydrochloride (883 mg, 5.60 mmol), Mn powder (246 mg, 4.48 mmol) and titanocene dichloride (70 mg, 0.28 mmol) at 25 $^\circ\text{C}$ under N_2 . After stirring for 23 hrs, the reaction was poured into a flask containing 1 M $\text{HCl}_{(\text{aq})}$. The mixture was extracted with EtOAc and the organic layer washed with 1 M $\text{HCl}_{(\text{aq})}$ then dried over MgSO_4 , filtered, concentrated, and purified by column chromatography (85:15 / EtOAc:Hexane, note: the starting material (**75**) and product (**76**) have exactly the same $R_f = 0.50$). This gave the desired product as a clear oil (352 mg, 80% yield). ^1H NMR (300 MHz, CDCl_3) δ 5.99 (s, 1H), 5.28 (s, 1H), 5.18 (s, 1H), 4.83 (s, 1H), 4.71 (s, 1H), 4.66 (d, $J = 6.3$ Hz, 1H), 4.50 (d, $J = 6.3$ Hz, 1H), 3.97 (dd, $J = 3.6$ Hz, 1H), 3.67 (s, 1H), 3.56-3.68 (m, 3H), 3.38 (s, 3H), 2.57 (d, $J = 1.2$ Hz, 1H), 2.09-2.27 (m, 2H), 2.07 (td, $J = 13.4, 3.7$ Hz, 1H), 1.95 (q, $J = 3.4$ Hz, 1H), 1.77-1.81 (m, 2H), 1.73 (s, 3H), 1.51-1.54 (m, 1H), 1.10 (d, $J = 7.4$ Hz, 3H); ^{13}C NMR (75 MHz, CDCl_3) δ 147.1, 145.6, 116.9, 111.4, 98.9, 81.5, 79.5, 69.9, 60.9, 56.4, 42.7, 38.6, 32.9, 31.6, 27.5, 22.3, 11.7; IR (thin film) 3421, 1434 cm^{-1} ; HRMS (EI): m/z calc for $\text{C}_{17}\text{H}_{30}\text{O}_5$ (M) $^+$ 314.2093, found 314.2092; $[\alpha]_{\text{D}}^{23}$ -42.1° (MeOH, c 1.0).



3(S)-Isopropenyl-2(R)-methoxymethoxy-6(R,S)-methyl-1(R)-(1-methylene-4-triethylsilyly-butyl)-5(R)-triethylsilyl-cyclohexanol (77)

To a solution of (76) (342 mg, 1.09 mmol) in CH₂Cl₂ (10 mL) was added pyridine (342 mg, 4.35 mmol), DMAP (13 mg, 0.11 mmol), and then TESCl (341 mg, 2.29 mmol) at 25 °C under N₂.

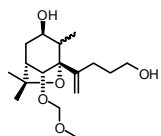
After 20 hrs, the reaction was quenched by adding brine (10 mL) and 1 M HCl (aq). This mixture was extracted with CH₂Cl₂ and the organic layer dried over MgSO₄, filtered, concentrated, and purified by column chromatography (15:85 / Ether:Hexane, R_f = 0.33). This gave the desired product as a clear oil (326 mg, 55% yield). ¹H NMR (300 MHz, CDCl₃) δ 6.01 (s, 1H), 5.11 (s, 1H), 4.83 (s, 1H), 4.69 (s, 1H), 4.67 (d, *J* = 6.4 Hz, 1H), 4.53 (d, *J* = 6.4 Hz, 1H), 3.98 (dd, *J* = 6.6, 3.3 Hz, 1H), 3.65 (t, *J* = 6.7 Hz, 3H), 3.39 (s, 3H), 3.02 (s, 1H), 2.61 (d, *J* = 12.4 Hz, 1H), 1.99-2.21 (m, 3H), 1.77-1.84 (m, 3H), 1.75 (s, 3H), 1.45 (d, *J* = 14.3 Hz, 1H), 1.03 (d, *J* = 7.3 Hz, 3H), 0.96 (t, *J* = 6.5 Hz, 9H), 0.94 (t, *J* = 7.7 Hz, 9H), 0.61 (q, *J* = 7.9 Hz, 6H), 0.59 (q, *J* = 6.7 Hz, 6H); ¹³C NMR (75 MHz, CDCl₃) δ 147.1, 146.4, 115.8, 111.0, 98.9, 81.4, 79.6, 70.7, 62.9, 56.4, 43.8, 38.5, 32.7, 32.2, 28.9, 22.4, 12.2, 6.8, 6.7, 4.9, 4.4; IR (thin film) 3544, 1644, 1096 cm⁻¹; HRMS (EI): *m/z* calc for C₁₇H₂₈O₃ (M)⁺ 542.3822, found 542.3821; [α]_D²³ -25.4 ° (MeOH, c 1.0).



8(R)-Methoxymethoxy-4(R,S),7,7-trimethyl-5(R)-(1-methylene-4-triethylsilyly-butyl)-3(R)-triethylsilyly-6(R)-oxa-bicyclo[3.2.1]octane (78)

To a solution of (77) (256 mg, 0.47 mmol) in CH₂Cl₂ (7 mL) was added pyridine (150 mg, 1.90 mmol) and added I₂ (240 mg, 0.94 mmol) at 25 °C, in the dark, under N₂. After stirring for 22 hrs the reaction was quenched with sodium bisulfite (aq.sat.) and extracted with CH₂Cl₂. The organic layers were washed with 1 M HCl (aq), dried over MgSO₄, filtered, and concentrated. The crude

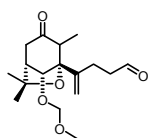
diastereomeric alkyl iodides were dissolved in toluene (3 mL) and AIBN (10 mg, 0.06 mmol) was added followed by Bu₃SnH (112 mg, 0.39 mmol). The mixture was immersed into a preheated oil bath (120 °C) and refluxed for 40 min. The mixture was cooled to 25 °C and ether, saturated with H₂O, (4 mL) was added followed by DBU (61 mg, 0.40 mmol). Bu₃SnOH was precipitated by stirring for 10 min. This slurry was filtered through a plug of cotton, sand, and MgSO₄. The plug was washed with ether and the combined organic layers concentrated and purified by column chromatography (9:91 / EtOAc:Hexane, R_f = 0.40). This gave the desired product as a clear oil (141 mg, 55% yield, 2 steps). ¹H NMR (300 MHz, CDCl₃) δ 5.05 (s, 1H), 4.84 (s, 1H), 4.77 (d, *J* = 7.1 Hz, 1H), 4.62 (d, *J* = 7.1 Hz, 1H), 4.43 (dt, *J* = 13.7, 6.9 Hz, 1H), 4.14 (s, 1H), 3.64 (t, *J* = 6.7 Hz, 2H), 3.41 (s, 1H), 3.38 (s, 3H), 2.10-2.21 (m, 3H), 1.90-1.94 (m, 1H), 1.67-1.72 (m, 2H), 1.47 (s, 3H), 1.37 (s, 3H), 1.19-1.30 (m, 1H), 0.96 (t, *J* = 6.6 Hz, 9H), 0.95 (t, *J* = 6.6 Hz, 9H), 0.90 (d, *J* = 7.2 Hz, 3H), 0.61 (q, *J* = 6.6 Hz, 6H), 0.56 (q, *J* = 6.6 Hz, 6H); ¹³C NMR (75 MHz, CDCl₃) δ 147.1, 111.5, 96.6, 92.8, 83.1, 81.8, 67.4, 63.0, 56.2, 46.9, 45.6, 34.6, 31.9, 30.6, 28.9, 28.7, 24.5, 24.0, 19.1, 16.6, 15.1, 13.5, 11.6, 10.6, 9.6, 6.4, 5.3, 5.0, 4.8; IR (thin film) 1685, 1091, cm⁻¹; HRMS (EI): *m/z* calc for C₁₇H₂₈O₃ (M)⁺ 542.3822, found 542.3826; [α]_D²³ -18.4° (MeOH, c 1.0).



5(R)-(4-Hydroxy-1-methylene-butyl)-8(R)-methoxymethoxy-4(R,S),7,7-trimethyl-6(R)-oxa-bicyclo[3.2.1]octan-3(R)-ol (79)

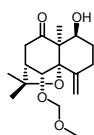
To a solution of (78) (137 mg, 0.25 mmol) in THF (4 mL) was added TBAF hydrate (165 mg, 0.63 mmol). After 1 hr, the reaction was concentrated and purified by column chromatography (5:20:75 / MeOH:CH₂Cl₂:EtOAc, R_f = 0.5). This gave the desired products as a clear oil (72.9 mg, 92% yield). ¹H NMR (300 MHz, CDCl₃) δ major diastereomer: 5.15 (s, 1H), 4.83 (s, 1H),

4.74 (d, $J = 6.9$ Hz, 1H), 4.64 (d, $J = 6.9$ Hz, 1H), 4.51 (dt, $J = 11.4, 6.9$ Hz, 1H), 4.15 (s, 1H), 3.61-3.65 (m, 3H), 3.41 (s, 3H), 2.10-2.27 (m, 3H), 1.62-1.76 (m, 4H), 1.49 (s, 3H), 1.41 (s, 3H), 0.94 (d, $J = 7.3$ Hz, 3H); ^{13}C NMR (75 MHz, CDCl_3) δ major diastereomer: 145.7, 113.4, 96.4, 93.2, 82.6, 71.2, 66.9, 61.6, 56.4, 46.8, 43.9, 32.3, 29.9, 27.9, 24.5, 17.5, 11.2; IR (thin film) 3396, 1629 cm^{-1} ; HRMS (EI): m/z calc for $\text{C}_{17}\text{H}_{30}\text{O}_5$ (M) $^+$ 314.2093, found 314.2079; $[\alpha]_{\text{D}}^{23} -7.1$ (MeOH, c 1.0).



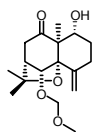
4-(8(R)-Methoxymethoxy-4(S),7,7-trimethyl-3-oxo-6(R)-oxa-bicyclo[3.2.1]oct-5(R)-yl)-pent-4-enal (80)

To a solution of (**79**) (49 mg, 0.16 mmol) in CH_2Cl_2 (5.5 mL) was added NaHCO_3 (50 mg) and then DMPI (159 mg, 0.38 mmol). After 2 hrs, the reaction was quenched by adding $\text{Na}_2\text{S}_2\text{O}_3$ (aq.sat) and NaHCO_3 (aq.sat). The mixture was stirred for 15 min, then extracted with CH_2Cl_2 , dried over MgSO_4 , filtered, concentrated, and purified by column chromatography (50:50 / EtOAc:Hexane, $R_f = 0.35$). This gave the desired product as a clear oil (38.4 mg, 80% yield). ^1H NMR (300 MHz, CD_2Cl_2) δ 9.74 (t, $J = 1.6$ Hz, 1H), 5.06 (s, 1H), 4.79 (s, 1H), 4.76 (d, $J = 6.9$ Hz, 1H), 4.69 (d, $J = 6.9$ Hz, 1H), 4.43 (s, 1H), 3.40 (s, 3H), 2.61-2.65 (m, 4H), 2.50-2.58 (m, 2H), 2.36-2.47 (m, 2H), 1.41 (s, 3H), 1.19 (s, 3H), 1.02 (d, $J = 7.8$ Hz, 3H); ^{13}C NMR (75 MHz, CD_2Cl_2) δ 212.7, 202.4, 144.1, 113.5, 96.9, 91.3, 82.9, 82.8, 56.9, 56.7, 46.8, 43.2, 43.1, 29.6, 26.9, 25.6, 16.3; IR (thin film) 1721, 1644, 1460 cm^{-1} ; HRMS (EI): m/z calc for $\text{C}_{17}\text{H}_{26}\text{O}_5$ (M) $^+$ 310.1780, found 310.1794; $[\alpha]_{\text{D}}^{23} -11.4$ (MeOH, c 1.0).



5(S)-Hydroxy-12(R)-methoxymethoxy-6(S),10,10-trimethyl-2-methylene-11(S)-oxatricyclo[7.2.1.01,6]dodecan-7-one (81)

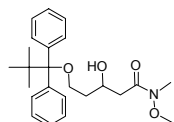
To a solution of (**80**) (4.4 mg, 14 μ mol) in CH_2Cl_2 (0.5 mL) was added DBU (3 mg, 18 μ mol) and the reaction stirred for 5 hrs at 25 $^\circ\text{C}$ under N_2 . The reaction was then concentrated to \sim 0.1 mL and purified by column chromatography (50:50 / EtOAc:Hexane, R_f = 0.52). This gave the desired product as a waxy solid (3.1 mg, 71% yield). ^1H NMR (300 MHz, CD_2Cl_2) δ 5.24 (s, 1H), 5.09 (dd, J = 2.8, 1.1 Hz, 1H), 4.95 (unresolved dd, J = 1.9 Hz, 1H), 4.73 (d, J = 6.9 Hz, 1H), 4.63 (d, J = 6.9 Hz, 1H), 3.99 (d, J = 2.9 Hz, 1H), 3.36 (s, 3H), 2.68 (dd, J = 18.5, 3.0 Hz, 1H), 2.50 (dd, J = 18.5, 3.9 Hz, 1H), 2.39 (t, J = 3.2 Hz, 2H), 2.17-2.21 (m, 1H), 1.91 (d, J = 3.9 Hz, 1H), 1.82 (tdd, J = 14.1, 4.6, 1.6 Hz, 1H), 1.65 (dq, J = 14.1, 2.5 Hz, 1H), 1.43 (s, 3H), 1.15 (s, 3H), 0.98 (s, 3H); ^{13}C NMR (75 MHz, CD_2Cl_2) δ 215.7, 144.6, 110.6, 96.3, 89.7, 83.7, 82.4, 76.4, 60.9, 56.2, 46.5, 46.1, 31.4, 29.9, 28.9, 26.9, 18.6; IR (thin film) 3421, 1701, 1649 cm^{-1} ; HRMS (EI): m/z calc for $\text{C}_{17}\text{H}_{26}\text{O}_5$ (M) $^+$ 310.1780, found 310.1769; $[\alpha]_{\text{D}}^{23} +42.2^\circ$ (MeOH, c 1.0).



5(R)-Hydroxy-12(R)-methoxymethoxy-6(S),10,10-trimethyl-2-methylene-11(S)-oxatricyclo[7.2.1.01,6]dodecan-7-one (82**)**

To a solution of (**80**) (38.4 mg, 0.12 mmol) in CH_2Cl_2 (3.5 mL) was added DBU (24.5 mg, 0.16 mmol) and the reaction stirred for 6 hrs. Then an additional amount of DBU (24.5 mg, 0.16 mmol) was added and the reaction stirred for a total of 24 hrs at 25 $^\circ\text{C}$ under N_2 . The reaction was then concentrated to \sim 0.2 mL and purified by column chromatography (50:50 / EtOAc:Hexane, R_f = 0.5 and 0.25) This gave (**82**) as a waxy solid (25.8 mg, 67% yield) and (**81**) as a minor product (8.8 mg, 23% yield). ^1H NMR (300 MHz, CD_2Cl_2) δ 5.15 (dd, J = 2.6, 1.3 Hz, 1H), 4.96 (t, J = 2.1 Hz, 1H), 4.75 (d, J = 7.0 Hz, 1H), 4.61 (d, J = 7.0 Hz, 1H), 4.42 (s, 1H), 3.85 (ddd, J = 12.4, 4.9, 1.1 Hz, 1H), 3.36 (s, 3H), 2.67 (td, J = 19.2, 2.9 Hz, 2H), 2.62 (dd, J =

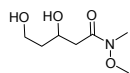
19.0, 3.9 Hz, 1H), 2.46 (t, $J = 3.2$ Hz, 1H), 2.32 (ddd, $J = 13.9, 4.7$ Hz, 1H), 1.99-2.05 (m, 1H), 1.83-1.85 (m, 1H), 1.43-1.45 (m, 1H), 1.44 (s, 3H), 1.19 (s, 3H), 1.00 (s, 3H); ^{13}C NMR (75 MHz, CD_2Cl_2) δ 216.9, 142.9, 111.6, 96.2, 89.6, 83.4, 82.7, 71.1, 61.8, 56.5, 46.2, 44.1, 29.8, 29.4, 29.2, 26.8, 11.4; IR (thin film) 3457, 1696, 1649 cm^{-1} ; HRMS (EI): m/z calc for $\text{C}_{17}\text{H}_{26}\text{O}_5$ (M) $^+$ 310.1780, found 310.1780; $[\alpha]_{\text{D}}^{23} +8.6^\circ$ (MeOH, c 1.0).



5-(2,2-Dimethyl-1,1-diphenyl-propoxy)-3-hydroxypentanoic acid

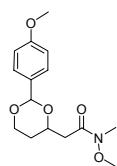
methoxymethylamide (84)

To a stirring solution of N-Methoxy-N-methyl-acetamide (**83**) (5.18 g, 50.24 mmol) in THF (50 mL) at -78°C , under N_2 , was added LDA (1.0 M THF, 50.24 mL, 50.24 mmol). After stirring for 100 min., 3-(*tert*-butyldiphenylsilyl)-hydroxy propionaldehyde (7.89 g, 41.87 mmol) in THF (15 mL) was added at -78°C to the orange enolate solution. After stirring for 2.5 hrs. at -78°C , the reaction was warmed to 30°C for 30 min., then quenched by adding 1% HCl (aq.) (55 mL). The organic layer was separated and the aqueous layer extracted with ethyl acetate (5x60 mL). The combined organic layers were washed with brine, dried over MgSO_4 , filtered, and concentrated by rotovapor to give clear oil. The product was purified by passing through a plug of silica gel using EtOAc to elute (17.13 g, 41.22 mmole, 98 % yield). ^1H NMR (300 MHz, CDCl_3) δ 7.67-7.70 (m, 4H), 7.39-7.42 (m, 6H), 4.33-4.35 (m, 1H), 3.87-3.91 (m, 1H), 3.88 (dd, $J = 9.1, 15.4$ Hz, 2H), 3.68 (s, 3H), 3.21 (s, 3H), 2.61-2.67 (m, 2H), 1.79-1.84 (m, 2H), 1.07 (s, 9H); ^{13}C NMR (75 MHz, CDCl_3) δ 173.5, 135.5, 133.5, 133.4, 129.6, 127.7, 66.4, 61.5, 61.2, 38.7, 31.9, 26.8, 19.1; IR (thin film) 3467, 3062, 3042, 1639, 1107 cm^{-1} ; HRMS (EI): m/z calc for $\text{C}_{19}\text{H}_{24}\text{SiNO}_4$ ($\text{M}-\text{C}_4\text{H}_9$) $^+$ 358.1474, found 358.1465.



2-(2-Hex-1-en-[1,3]dioxan-4)-N-methoxy-N-methylacetamide (**85**)

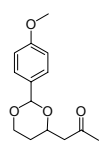
The TBDPS ether (**84**) (17.13g, 41.22 mmol) was dissolved in THF (70 mL) and TBAF hydrate (11.52 g, 41.22 mmol) was added. The mixture was stirred at 25 °C for 60 min., then concentrated by rotovapor to a volume ~15 mL. The crude brown oil was loaded onto a plug of silica gel and washed with 10% ethyl acetate in hexane, then eluted with 15% methanol in ethyl acetate. This gave the semi-purified diol as clear oil with trace solids (5.59g, 31.54 mmol, 77%). ¹H NMR (300 MHz, CDCl₃) δ 4.32 (ddt, *J* = 8.9, 3.6 Hz, 1H), 3.87 (t, *J* = 5.8 Hz, 2H), 3.71 (s, 3H), 3.21 (s, 3H), 2.51-2.71 (m, 2H), 1.68-1.82 (m, 2H); ¹³C NMR (75 MHz, CDCl₃) δ 172.9, 66.5, 60.9, 59.7, 38.3, 38.0, 31.4; IR (thin film) 3411, 1644 cm⁻¹; Could not obtain a satisfactory HRMS on this diol. Both EI and CI (CH₄) were experiments tried.



N-Methoxy-2-[2-(4-methoxyphenyl)-[1,3]dioxan-4-yl]-N-methylacetamide (**86**)

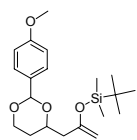
To a solution of (**85**) (1.0 g, 5.64 mmol) in benzene (54 mL) was added 4-anisaldehyde diethylacetal (1.16 g, 5.50 mmol) and PPTS (100 mg, cat. H⁺). A short path distillation head was attached and the mixture heated to 110 °C for 70 min to remove ethanol. After cooling to 25 °C, the brown residue was purified by flash column chromatography (70% ethyl acetate: hexane) to give the product as a pale yellow oil (1.15 g, 3.91 mmol, 71%). ¹H NMR (300 MHz, CD₂Cl₂) δ 7.38 (d, *J* = 8.9 Hz, 2H), 6.87 (d, *J* = 8.8 Hz, 2H), 5.49 (s, 1H), 4.34-4.37 (m, 1H), 4.20 (dd, *J* = 11.4, 4.9 Hz, 1H), 3.96 (td, *J* = 11.9, 2.8 Hz, 1H), 3.77 (s, 3H), 3.67 (s, 3H), 3.15 (s, 3H), 2.90 (dd, *J* = 15.7, 6.9 Hz, 1H), 2.52 (dd, *J* = 15.8, 5.8 Hz, 1H), 1.80 (ddd, *J* = 25.0, 12.9, 5.0 Hz, 1H), 1.63-1.68 (m, 1H); ¹³C NMR (75 MHz, CD₂Cl₂) δ 171.4, 160.2, 131.8, 127.7, 113.7, 101.4, 74.1, 67.1, 61.6, 55.5, 38.6, 32.1, 31.6; IR (thin film) 3052,

1726, 1654, 1245, 1102 cm^{-1} ; HRMS (EI): m/z calc for $\text{C}_{15}\text{H}_{21}\text{NO}_5$ (M)⁺ 295.1419, found 295.1415.



1-[2-(4-Methoxyphenyl)-[1,3]dioxan-4-yl]-propan-2-one (88)

To a solution of (**86**) (1.00 g, 3.39 mmol) in THF (60 mL) at -78 °C under N_2 was added MeLi (1.4M Ether, 6.10 mL, 8.48 mmol). After stirring for 1 hr. aqueous saturated NH_4Cl (20 mL) was added followed by hexane (24 mL) and CH_2Cl_2 (12 mL) and the reaction was warmed to 25 °C. The organic layer was separated and the aqueous layer extracted with methylene chloride (3x10 mL). The combined organic layers were washed with brine, dried over MgSO_4 , filtered, and concentrated by rotovapor. The crude yellow oil was then purified by flash column chromatography (70% diethyl ether: pentane) to give the desired product as colorless oil (823 mg, 97%). ^1H NMR (300 MHz, CD_2Cl_2) δ 7.36 (d, $J = 8.5$ Hz, 2H), 6.88 (d, $J = 8.5$ Hz, 2H), 5.47 (s, 1H), 4.28-4.31 (m, 1H), 4.20 (ddd, $J = 11.5, 4.9, 1.3$ Hz, 1H), 3.95 (td, $J = 12.0, 2.7$ Hz, 1H), 3.78 (s, 3H), 2.80 (dd, $J = 16.3, 7.4$ Hz, 1H), 2.55 (dd, $J = 16.3, 5.2$ Hz, 1H), 2.16 (s, 3H), 1.45 (ddd, $J = 23.5, 12.2, 5.0$ Hz, 1H), 1.54-1.59 (m, 1H); ^{13}C NMR (75 MHz, CD_2Cl_2) δ 206.3, 160.4, 131.9, 127.8, 113.9, 101.5, 73.7, 67.2, 55.7, 50.0, 31.6, 31.1; IR (thin film) 3062, 1706, 1614, 1522, 1096 cm^{-1} ; HRMS (EI): m/z calc for $\text{C}_{14}\text{H}_{18}\text{O}_4$ ($\text{M}-\text{H}$)⁺ 249.1127, found 249.1138.

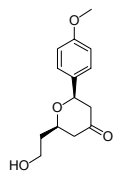


***tert*-Butyl-{1-[2-(4-methoxyphenyl)-[1,3]dioxan-4-ylmethyl]-vinyl}oxy-**

dimethylsilane (90)

The ketone (**88**) (500 mg, 1.99 mmol) and Et_3N (2.01 g, 19.90 mmol) were dissolved in CH_2Cl_2 (15 mL), then cooled to -78 °C under N_2 . TBSOTf (528 mg, 2.00 mmol) was added and after 10 min the reaction was slowly warmed to 25 °C. After 2.5 hrs, the mixture was poured into

NaHCO₃ (aq. sat.) (10 mL). The organic layer was separated and the aqueous layer extracted with CH₂Cl₂. The combined organic layers were dried over MgSO₄, filtered, concentrated, and purified by column chromatography (4:94:2 / Ether:Hexane:Et₃N, Rf=0.33) This gave the desired kinetic silyl enoether (**90**) as a pale yellow oil (406 mg, 56% yield) The thermodynamic enol ether (**90b**) was isolated in 19% yield. ¹H NMR (300 MHz, CD₂Cl₂) δ 7.36 (d, *J* = 6.9 Hz, 2H), 6.86 (d, *J* = 6.7 Hz, 2H), 5.43 (s, 1H), 4.19 (ddd, *J* = 11.4, 4.9, 1.2 Hz, 1H), 4.14 (s, 1H), 4.12 (d, *J* = 0.6 Hz, 1H), 4.05-4.09 (m, 1H), 3.90 (td, *J* = 11.9, 2.7 Hz, 1H), 3.78 (s, 3H), 2.46 (dd, *J* = 13.9, 6.8 Hz, 1H), 2.19 (dd, *J* = 13.9, 6.8 Hz, 1H), 1.68-1.74 (m, 1H), 1.55-1.60 (m, 1H), 0.95 (s, 9H), 0.18 (s, 6H); ¹³C NMR (75 MHz, CD₂Cl₂) δ 160.3, 155.9, 132.1, 127.8, 113.7, 101.5, 92.3, 75.0, 67.4, 55.6, 43.9, 31.5, 25.9, 18.4, -4.5, -4.6; IR (thin film) 1618, 1516, 1250, 1107, 1020 cm⁻¹; HRMS (ED): *m/z* calc for C₂₀H₃₂SiO₄ (M)⁺ 364.2070, found 364.2077.

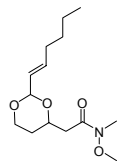


2-(2-Hydroxyethyl)-6-(4-methoxyphenyl)-tetrahydropyran-4-one (92)

To a flask containing dry Ce(NO₃)₃ (1.07 g, 3.29 mmol) was added CH₃CN (8 mL).

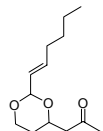
This slurry was stirred at 25 °C under N₂ for 10 min, then a solution of (**90**) (300 mg, 0.82 mmol) in CH₃CN (4 mL) was added and the solids slowly began to dissolve. After 80 min, TBAF hydrate (230 mg, 0.82 mmol) was added and the mixture stirred for 60 min. The mixture was then poured into NaHCO₃ (aq. sat.) (20 mL) and slowly neutralized by adding 1 M HCl. The biphasic mixture was concentrated by rotovapor to remove most of the CH₃CN and the remaining solution was extracted with EtOAc. The organic layers were dried over MgSO₄, filtered, concentrated, and purified by column chromatography (100 % Ether). This gave the desired product as a clear oil (166 mg, 81%). ¹H NMR (300 MHz, CD₂Cl₂) δ 7.28 (d, *J* = 8.8 Hz, 2H), 6.89 (d, *J* = 8.8 Hz, 2H), 4.61 (dd, *J* = 9.9, 4.5 Hz, 1H), 3.93-3.99 (m, 1H), 3.78 (s, 3H),

3.75-3.76 (m, 2H), 2.56 (d, $J = 7.2$ Hz, 1H), 2.54 (s, 1H), 2.43 (d, $J = 5.0$ Hz, 1H), 2.41 (s, 1H), 2.20 (t, $J = 4.9$ Hz, 1H), 1.67-1.94 (m, 2H); ^{13}C NMR (75 MHz, CD_2Cl_2) δ 206.4, 159.9, 133.4, 127.5, 114.3, 79.0, 76.7, 60.4, 55.7, 49.7, 47.9, 39.1; IR (thin film) 3442, 1716, 1511, 1250 cm^{-1} ; HRMS (EI): m/z calc for $\text{C}_{20}\text{H}_{32}\text{SiO}_4$ (M) $^+$ 250.1205, found 250.1216.



2-(2-Hex-1-en-[1,3]dioxan-4)-N-methoxy-N-methyl-acetamide (87)

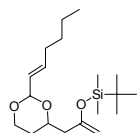
To a solution of (**85**) (3.0 g, 17.23 mmol) in benzene (160 mL) was added (*E*)-2-heptenal diethylacetal (3.06 g, 16.71 mmol) and PPTS (300 mg, cat. H^+). A short path distillation head was attached and the mixture heated to 110 $^\circ\text{C}$ for 70 min to remove ethanol. After cooling to 25 $^\circ\text{C}$, the brown residue was purified by flash column chromatography (75% ethyl acetate: hexane) to give the product as a pale yellow oil (3.46 g, 12.75 mmol, 74%). ^1H NMR (300 MHz, CDCl_3) δ 5.83 (dt, $J = 15.6, 6.7$ Hz, 1H), 5.40 (dd, $J = 15.6, 5.1$ Hz, 1H), 4.92 (d, $J = 3.4$ Hz, 1H), 4.09-4.19 (m, 1H), 4.07 (dd, $J = 11.3, 4.7$ Hz, 1H), 3.79 (td, $J = 11.3, 3.0$ Hz, 1H), 3.61 (s, 3H), 3.12 (s, 3H), 2.84 (dd, $J = 15.7, 6.2$ Hz, 1H), 2.45 (dd, $J = 15.7, 6.3$ Hz, 1H), 1.98 (dd, $J = 13.2, 7.6$ Hz, 2H), 1.58-1.65 (m, 2H), 1.21-1.32 (m, 4H), 0.82 (t, $J = 6.8$ Hz, 3H); ^{13}C NMR (75 MHz, CDCl_3) δ 171.0, 135.6, 126.6, 100.7, 73.1, 66.2, 61.1, 38.0, 31.7, 31.5, 31.0, 30.5, 21.9, 13.7; IR (thin film) 1665, 1475, 1419, 1383, 1116 cm^{-1} ; HRMS (EI): m/z calc for $\text{C}_{14}\text{H}_{25}\text{NO}_4$ (M) $^+$ 271.1783, found 271.1773.



1-(2-Hex-1-en-[1,3]dioxan-4)-propan-2-one (89)

To a solution of (**87**) (1.05 g, 3.87 mmol) in THF (60 mL) at -78 $^\circ\text{C}$ under N_2 was added MeLi (1.4M Ether, 6.91 mL, 9.68 mmol). After stirring for 1 hr. aqueous saturated NH_4Cl (20 mL) was added followed by hexane (24 mL) and CH_2Cl_2 (12 mL) and the reaction was warmed

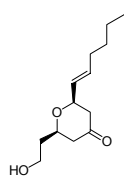
to 25 °C. The organic layer was separated and the aqueous layer extracted with methylene chloride (3x10 mL). The combined organic layers were washed with brine, dried over MgSO₄, filtered, and concentrated by rotovapor. The crude yellow oil was then purified by flash column chromatography (70% diethyl ether: pentane) to give the desired product as colorless oil (697 mg, 89%). ¹H NMR (300 MHz, CDCl₃) δ 5.38 (dt, *J* = 14.3, 6.7 Hz, 1H), 5.41 (dd, *J* = 15.7, 3.5 Hz, 1H), 4.90 (d, *J* = 4.9 Hz, 1H), 4.04-4.12 (m, 2H), 3.78 (t, *J* = 11.9 Hz, 1H), 2.76 (d, *J* = 16.4, 6.8 Hz, 1H), 2.46 (dd, *J* = 16.4, 5.6 Hz, 1H), 2.13 (s, 3H), 2.00 (dd, *J* = 13.4, 6.5 Hz, 2H), 1.61 (qd, *J* = 12.2, 4.9 Hz, 2H), 1.48 (d, *J* = 13.1 Hz, 1H), 1.22-1.34 (m, 4H), 0.82 (t, *J* = 6.6 Hz, 3H); ¹³C NMR (75 MHz, CDCl₃) δ 205.9, 135.6, 126.7, 100.7, 72.6, 66.2, 49.4, 31.5, 31.0, 30.8, 30.6, 22.0, 13.6; IR (thin film) 1716, 1419, 1363, 1132 cm⁻¹; HRMS (EI): *m/z* calc for C₁₃H₂₂O₃ (M)⁺ 225.1490, found 225.1493.



***tert*-Butyl-[1-(2-hex-1-en-[1,3]dioxan-4-methyl)-vinyloxy]-dimethylsilane (**91**)**

To a solution of (**89**) (300 mg, 1.33 mmol) in CH₂Cl₂ (10 mL) was added Et₃N (1.34 g, 13.26 mmol) under N₂. The reaction flask was cooled to -78 °C and *tert*-butyldimethylsilyl triflate (357 mg, 1.35 mmol) was added. The reaction was stirred for 10 min. at -78 °C, then warmed to 25 °C and stirred for 1 hour, monitoring by TLC. The reaction was quenched by adding aqueous saturated sodium bicarbonate (8 mL) and the CH₂Cl₂ layer was separated. The aqueous layer was extracted with ethyl acetate (3x15 mL). The combined organic layers were washed with brine, dried over MgSO₄, filtered, and concentrated by rotovapor. The crude brown oil was purified by column flash chromatography (5:93:2 diethyl ether: hexane: triethylamine) to give the desired product (**91**) as colorless oil (227 mg, 50%). The undesired thermodynamic enol (**91b**) ether was the major byproduct (20%). ¹H NMR (300 MHz, CD₂Cl₂) δ 5.85 (dt, *J* = 15.6,

6.8 Hz, 1H), 5.45 (ddt, $J = 15.6, 5.1, 1.5$ Hz, 1H), 4.88 (d, $J = 5.1$ Hz, 1H), 4.09 (d, $J = 2.4$ Hz, 2H), 4.06 (dd, $J = 5.0, 1.4$ Hz, 2H), 3.83-3.88 (m, 1H), 3.74 (td, $J = 11.7, 2.9$ Hz, 1H), 2.36 (dd, $J = 13.9, 6.7$ Hz, 1H), 2.12 (dd, $J = 13.9, 6.7$ Hz, 1H), 2.04 (dd, $J = 13.1, 6.7$ Hz, 2H), 1.55-1.56 (m, 1H), 1.50 (qd, $J = 11.8, 1.5$ Hz, 2H), 1.32-1.36 (m, 4H), 0.94 (s, 9H), 0.87-0.91 (m, 3H), 0.17 (s, 6H); ^{13}C NMR (75 MHz, CD_2Cl_2) δ 156.1, 135.5, 128.0, 101.5, 92.3, 74.8, 67.0, 44.0, 32.2, 31.7, 31.5, 26.1, 22.8, 18.5, 14.1, -4.4, -4.5; IR (thin film) 1654, 1634, 1132, 1009, 963 cm^{-1} ; HRMS (EI): m/z calc for $\text{C}_{19}\text{H}_{36}\text{SiO}_3$ (M) $^+$ 339.2355, found 339.2359.



2-Hex-1-en-6-(2-hydroxy-ethyl)-tetrahydro-pyran-4-one (93)

To a flask containing dry $\text{Ce}(\text{NO}_3)_3$ (1.73g, 5.30 mmol) was added CH_3CN (8 mL).

This slurry was stirred at 25 $^\circ\text{C}$ under N_2 for 10 min, then a solution of (**91**) (300 mg, 1.33 mmol) in CH_3CN (4 mL) was added and the solids slowly began to dissolve. After 80 min, TBAF hydrate (307 mg, 1.18 mmol) was added and the mixture stirred for 60 min. The mixture was then poured into NaHCO_3 (aq. sat.) (20 mL) and slowly neutralized by adding 1 M HCl. The biphasic mixture was concentrated by rotovapor to remove most of the CH_3CN and the remaining solution was extracted with EtOAc. The organic layers were dried over MgSO_4 , filtered, concentrated, and purified by column chromatography (100 % Ether). This gave the desired product as a clear oil (248 mg, 93%). ^1H NMR (300 MHz, CD_2Cl_2) δ 5.71 (dtd, $J = 15.4, 6.7, 0.9$ Hz, 1H), 5.49 (ddt, $J = 14.1, 6.2, 1.3$ Hz, 1H), 4.07 (dd, $J = 13.8, 6.7$ Hz, 1H), 3.82-3.86 (m, 2H), 3.72-3.76 (m, 1H), 2.32 (t, $J = 7.3$ Hz, 5H), 2.03 (dd, $J = 13.2, 6.5$ Hz, 2H), 1.76-1.87 (m, 2H), 1.30-1.39 (m, 4H), 0.89 (t, $J = 7.0$ Hz, 3H); ^{13}C NMR (75 MHz, CD_2Cl_2) δ 206.4, 133.9, 129.5, 78.1, 76.6, 60.6, 48.2, 48.0, 38.9, 32.3, 31.5, 22.6, 14.1; IR (thin film) 3437, 1721, 1065 cm^{-1} ; HRMS (EI): m/z calc for $\text{C}_{13}\text{H}_{22}\text{O}_3$ (M) $^+$ 226.1568, found 226.1565.

 **(S)-1-Triisopropylsilyloxyhex-5-en-3-ol (95)**

(-)-Ipc₂B-allyl was prepared according to the procedure of Brown, H.C. *JACS* **1983**, 105, 2092. A flask containing the (-)-Ipc₂B-allyl reagent (9.79g, 30.0 mmol) in ether (75 mL) was cooled to -78 °C under N₂. Then a solution of 3-(triisopropylsilyl)-hydroxy propanal (**94**) (6.21g, 26.9 mmol) in ether (20 mL) was added dropwise and stirred for 1 hr. The mixture was then warmed to 25 °C over 1 hr, and stirred for 95 min before carefully quenching with 3 N NaOH (22 mL). Then H₂O₂ (30% aq, 10.2 mL, 90 mmol) was slowly added. After bubbling subsided the reaction refluxed for 45 min, then cooled to 25 °C and diluted with H₂O (50 mL). The mixture was extracted with EtOAc, the organic layer washed with H₂O, then with brine. The organic layer was dried over MgSO₄, filtered, concentrated, and product purified by column chromatography (15:85 / EtOAc:Hexane, R_f= 0.40). This gave the desired product (**95**) as a clear oil (6.59 g, 90% yield). ¹H NMR (300 MHz, CDCl₃) δ 5.87 (ddt, *J* = 10.0, 9.9, 2.9 Hz, 1H), 5.10 (d, *J* = 10.8 Hz, 1H), 5.04 (d, *J* = 1.6 Hz, 1H), 3.95 (qt, *J* = 10.0, 5.3 Hz, 2H), 3.89 (t, *J* = 6.3 Hz, 1H), 3.50 (br s, 1H), 2.24 (dt, *J* = 14.1, 7.9 Hz, 2H), 1.68 (dd, *J* = 5.6, 5.0 Hz, 2H), 1.05 (d, *J* = 4.7 Hz, 21H); ¹³C NMR (75 MHz, CDCl₃) δ 135, 117, 71, 63, 42, 38, 18, 12; IR (thin film) 3457, 1101, 1000 cm⁻¹; HRMS (EI): *m/z* calc for C₁₂H₂₈SiO₂ (M-C₃H₄)⁺ 231.1780, found 231.1784; [α]_D²³ +7.7° (CHCl₃, c 1.0).

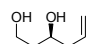
 **(S)-Benzoic acid 1-(2-triisopropylsilyloxy-ethyl)-but-3-enyl ester (96)**

The secondary alcohol (**95**) (500 mg, 1.83 mmol) was dissolved in CH₂Cl₂ (15 mL) at 25 °C under N₂. Next Et₃N (371 mg, 3.67 mmol) was added followed by DMAP (10 mg) and BzCl (245 mg, 1.74 mmol). The mixture was heated to reflux and after stirring for 24 hrs cooled to 25

°C. The mixture was poured into NaHCO₃ (aq. sat.) (20 mL) and extracted with CH₂Cl₂. The combined organic layers were dried over MgSO₄, filtered, concentrated, and purified by column chromatography (10:90 Ether:Hexane, R_f = 0.25). This gave the desired product (**96**) as a clear oil (644 mg, 98% yield). ¹H NMR (300 MHz, CDCl₃) δ 8.05 (dd, *J* = 5.0 Hz, 2H), 7.53-7.58 (m, 1H), 7.41-7.46 (m, 1H), 5.82-5.87 (m, 1H), 5.34 (dt, *J* = 12.7, 6.0 Hz, 1H), 5.13 (d, *J* = 15.4 Hz, 1H), 5.07 (d, *J* = 0.9 Hz, 1H), 3.82 (t, *J* = 6.7 Hz, 2H), 2.50-2.56 (m, 2H), 2.00 (ddd, *J* = 7.6, 5.7, 2.3 Hz, 2H), 1.05 (s, 21H); ¹³C NMR (75 MHz, CDCl₃) δ 166, 134, 133, 131, 130.7, 129.5, 128, 118, 72, 60, 39, 37, 10, 12; IR (thin film) 3078, 3032, 1721, 1270, 1107 cm⁻¹; HRMS (EI): *m/z* calc for C₁₉H₂₉SiO₃ (M-C₃H₇)⁺ 333.1885, found 333.1891; [α]_D²³ +19.1° (CHCl₃, c 1.0).

 (**S**)-Benzoic acid 1-(2-hydroxyethyl)-but-3-enyl ester (**97**)

The TIPS ether (**96**) (177 mg, 0.47 mmol) was dissolved in CH₂Cl₂ (3 mL). Then TBAF hydrate (160 mg, 0.61 mmol) was added and after stirring at 25 °C for 10 hrs the mixture was concentrated. The resulting oil was purified by column chromatography (25:75 / EtOAc:Hexane, R_f = 0.30). This gave the desired product (**97**) as a clear oil (72 mg, 70% yield). Chiral HPLC (Chiracel ODH, flow rate 0.4 mL/min, 10:90 iPrOH:Hexane) shows (**97**) to have an % ee of 78%. This is consistent with Browns' results using the (Ipc)₂B-allyl reagent with sterically undemanding aldehydes. ¹H NMR (300 MHz, CDCl₃) δ 8.02-8.05 (m, 2H), 7.53-7.55 (m, 1H), 7.41-7.46 (m, 2H), 5.79-5.86 (m, 1H), 5.16 (ddd, *J* = 14.2, 2.15, 1.02 Hz, 1H), 5.12 (t, *J* = 1.0 Hz, 1H), 4.53-4.58 (m, 1H), 4.43-4.43 (m, 1H), 3.85 (ddt, *J* = 7.4, 3.7, 2.6 Hz, 1H), 2.36 (s, 1H), 2.31-2.13 (m, 2H), 2.00-2.04 (m, 1H), 1.88-1.92 (m, 1H); ¹³C NMR (75 MHz, CDCl₃) δ 167, 134, 133, 130.1, 129.5, 128, 118, 68, 62, 42, 36; IR (thin film) 3452, 1721, 1271 cm⁻¹; HRMS (EI): *m/z* calc for C₁₃H₁₇O₃ (M+H)⁺ 221.1177, found 221.1184; [α]_D²³ +15.9° (CHCl₃, c 1.0).

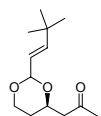
 **(S)-Hex-5-ene-1,3-diol (98)**

The TIPS ether (**95**) (3.0 g, 11.01 mmol) was dissolved in THF (100 mL) and TBAF hydrate (3.17 g, 12.11 mmol) was added in one portion at 25 °C. After 90 min, the mixture was concentrated and purified by column chromatography (100 % EtOAc, $R_f = 0.33$) This gave the known diol (**98**) (Hosokawa, T. *Chem. Lett.* **1989**, 2001) as a clear oil (1.18 g, 92% yield) ^1H NMR (300 MHz, CDCl_3) δ 5.81 (qt, $J = 10.0, 7.6, 6.7$ Hz, 1H), 5.18 (d, $J = 2.0$ Hz, 1H), 5.15 (d, $J = 14.0$ Hz, 1H), 3.84-3.93 (m, 3H), 2.25-2.32 (m, 4H), 1.72 (dt, $J = 4.8, 2.6$ Hz, 2H); ^{13}C NMR (75 MHz, CDCl_3) δ 134, 118, 70, 61, 42, 38; IR (thin film) 3365, 1055 cm^{-1} ; $[\alpha]_{\text{D}}^{23} +11.6^\circ$ (CHCl_3 , c 1.0).

 **(S)-4-Allyl-2-(3,3-dimethylbut-1-enyl)-[1,3]dioxane (101)**

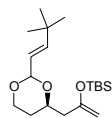
The diol (**98**) (1.08 g, 9.32 mmol) was dissolved in benzene (55 mL) and 4,4-Dimethylpent-2-enal (**100**) (983 mg, 8.76 mmol) was added followed by PPTS (128 mg). A reflux condenser and dean stark trap filled with molecular sieves was attached and the reaction heated to 110 °C under N_2 for 2.5 hrs. The reaction was then cooled to 25 °C and Et_3N (0.2 mL) was added. The reaction was concentrated and purified by column chromatography (5:30:65 / EtOAc: CH_2Cl_2 :Hexane, $R_f = 0.40$). This gave the desired product (**101**) as a clear oil (1.38 g, 91% yield). ^1H NMR (300 MHz, CDCl_3) δ 5.86 (dd, $J = 16.0, 0.8$ Hz, 1H), 5.80 (qt, $J = 13.0, 7.3, 2.8$ Hz, 1H), 5.40 (dd, $J = 16.0, 5.1$ Hz, 1H), 5.10 (d, $J = 13.5$ Hz, 1H), 5.05 (d, $J = 5.0$ Hz, 1H), 4.91 (d, $J = 5.1$ Hz, 1H), 4.12 (dd, $J = 11.4, 4.9$ Hz, 1H), 3.80 (dd, $J = 12.2, 2.6$ Hz, 1H), 3.62-3.68 (m, 1H), 2.30 (dq, $J = 17.8, 11.3$ Hz, 2H), 1.66 (qd, $J = 12.8, 7.8$ Hz, 1H), 1.43 (d, $J = 13.3$ Hz, 1H), 0.99 (s, 9H); ^{13}C NMR (75 MHz, CDCl_3) δ 146, 134, 122, 117, 101, 75, 66,

40, 33, 31, 29; IR (thin film) 1111, 1101, 1000 cm^{-1} ; HRMS (EI): m/z calc for $\text{C}_{13}\text{H}_{22}\text{O}_2$ (M)⁺ 209.1541, found 209.1547; $[\alpha]_{\text{D}}^{23} +3.9^\circ$ (CHCl_3 , c 1.0).



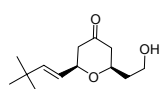
(S)-1-[2-(3,3-Dimethylbut-1-enyl)-[1,3]dioxan-4-yl]-propan-2-one (102)

The terminal olefin (**101**) (1.0 g, 4.80 mmol) was dissolved in THF (25 mL), and H_2O (4 mL). Li_2CO_3 (3.55 g, 48.0 mmol) was added followed by CuCl_2 (320 mg, 2.40 mmol) and PdCl_2 (143mg, 0.80 mmol). The reaction mixture was stirred vigorously under 1 atm of O_2 for 1 hour, then another addition of PdCl_2 (143 mg, 0.80 mmol) was made. After stirring for another 1 hour under O_2 , a third and final addition of PdCl_2 (143 mg, 0.80 mmol) was made. After 3 hrs total, the mixture was diluted with ether and filtered through a plug of celite. Additional ether was added and the mixture washed with brine, dried over MgSO_4 , filtered, concentrated, and purified by column chromatography (20:80 / EtOAc:Hexane, $R_f = 0.25$). This gave the desired product (**102**) as a clear oil (685 mg, 84% yield). ^1H NMR (300 MHz, CDCl_3) δ 5.90 (dd, $J = 16.0, 0.8$ Hz, 1H), 5.39 (dd, $J = 16.0, 5.0$ Hz, 1H), 4.95 (d, $J = 5.0$ Hz, 1H), 4.13-4.17 (m, 1H), 3.84 (td, $J = 11.2, 2.7$ Hz, 1H), 2.84 (q, $J = 6.7$ Hz, 1H), 2.57 (q, $J = 6.7$ Hz, 1H), 2.20 (s, 3H), 1.70 (qd, $J = 11.4, 4.2$ Hz, 1H), 1.54 (dq, $J = 13.2, 1.5$ Hz, 1H), 1.02 (s, 3H); ^{13}C NMR (75 MHz, CDCl_3) δ 206, 146, 122, 101, 72, 66, 60, 49, 30, 29, 28; IR (thin film) 1716, 1142, 1081 cm^{-1} ; HRMS (EI): m/z calc for $\text{C}_{13}\text{H}_{22}\text{O}_3$ (M-H)⁺ 225.1490, found 225.1493; $[\alpha]_{\text{D}}^{23} +4.1^\circ$ (CHCl_3 , c 1.0).



(S)-tert-Butyl-{1-[2-(3,3-dimethylbut-1-enyl)-[1,3]dioxan-4-ylmethyl]-vinyl}oxydimethylsilane (103)

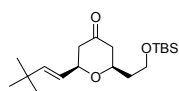
The methyl ketone (**102**) (575 mg, 2.54 mmol) and Et₃N (2.57 g, 25.40 mmol) were dissolved in CH₂Cl₂ (18 mL), then cooled to -78 °C under N₂. TBSOTf (698 mg, 2.64 mmol) was added and after 10 min the reaction was slowly warmed to 25 °C. After 2.5 hrs, the mixture was poured into NaHCO₃ (aq. sat.) (10 mL). The organic layer was separated and the aqueous layer extracted with CH₂Cl₂. The combined organic layers were dried over MgSO₄, filtered, concentrated, and purified by column chromatography (4:94:2 / Ether:Hexane:Et₃N, R_f = 0.33) This gave the desired kinetic silyl enol ether (**103**) as a pale yellow oil (542 mg, 63% yield). ¹H NMR (300 MHz, CD₂Cl₂) δ 5.85 (dd, *J* = 16.0, 0.9 Hz, 1H), 5.35 (d, *J* = 5.1 Hz, 1H), 4.88 (dd, *J* = 5.1, 0.8 Hz, 1H), 4.10 (s, 1H), 4.08 (d, *J* = 0.8 Hz, 1H), 4.06 (dd, *J* = 5.0, 1.4 Hz, 1H), 3.88-3.92 (m, 1H), 3.74 (td, *J* = 11.8, 2.9 Hz, 1H), 2.38 (q, *J* = 6.7 Hz, 1H), 2.15 (q, *J* = 6.7 Hz, 1H), 1.60 (qd, *J* = 13.3, 5.0 Hz, 1H), 1.49 (dq, *J* = 13.3, 2.7 Hz, 1H), 1.00 (s, 9H), 0.93 (s, 9H), 0.17 (s, 6H); ¹³C NMR (75 MHz, CD₂Cl₂) δ 156, 146, 123, 102, 92, 75, 67, 44, 33, 32, 30, 26, 18, -4.4, -4.6; IR (thin film) 1148, 1019 cm⁻¹; HRMS (EI): *m/z* calc for C₁₉H₃₆SiO₃ (M)⁺ 340.2433, found 340.2431; [α]_D²³ +2.0° (CHCl₃, c 1.0).



2-(3,3-Dimethylbut-1-enyl)- 6(S)-(2(R)-hydroxyethyl)-tetrahydropyran-4-one
(104)

To a flask containing dry Ce(NO₃)₃ (1.50 g, 4.72 mmol) was added CH₃CN (8 mL). This slurry was stirred at 25 °C under N₂ for 10 min, then a solution of (**103**) (400 mg, 1.18 mmol) in CH₃CN (4 mL) was added and the solids slowly began to dissolve. After 80 min, TBAF hydrate (307 mg, 1.18 mmol) was added and the mixture stirred for 60 min. The mixture was then poured into NaHCO₃ (aq. sat.) (20 mL) and slowly neutralized by adding 1 M HCl. The biphasic mixture was concentrated by rotovapor to remove most of the CH₃CN and the remaining solution was

extracted with EtOAc. The organic layers were dried over MgSO₄, filtered, concentrated, and purified by column chromatography (100 % Ether, R_f= 0.45). This gave the desired product (**104**) as a clear oil (182 mg, 69% yield). ¹H NMR (300 MHz, CD₂Cl₂) δ 5.71 (dd, *J* = 15.8, 1.0 Hz, 1H), 5.40 (dd, *J* = 15.8, 6.2 Hz, 1H), 4.08 (q, *J* = 6.8 Hz, 1H), 3.83-3.86 (m, 1H), 3.75 (t, *J* = 5.4 Hz, 2H), 2.32 (t, *J* = 6.8 Hz, 4H), 1.73-1.87 (m, 3H), 1.00 (s, 9H); ¹³C NMR (75 MHz, CD₂Cl₂) δ 206, 144, 125, 78, 77, 61, 48.3, 48.0, 39, 33, 29; IR (thin film) 3432, 1726 cm⁻¹; HRMS (EI): *m/z* calc for C₁₃H₂₂O₃ (M)⁺ 226.1568, found 226.1573; [α]_D²³ +24.7° (CHCl₃, c 1.0).



2-(R)-[2-(*tert*-butyldimethylsilyl)-ethyl]-6-(S)-(3,3-dimethyl-but-1-enyl)-tetrahydropyran-4-one (105)

The primary alcohol (**104**) (50.0 mg, 0.22 mmol) was dissolved in CH₂Cl₂ (1 ml) at 25 °C under N₂. Imidazole (30 mg, 0.44 mmol) was added followed by TBSCl (35 mg, 0.44 mmol). The reaction was stirred for 2 hrs, then quenched by adding H₂O (1 mL). The organic layer was separated and the aqueous layer extracted with CH₂Cl₂. The combined organic layers were dried over MgSO₄, filtered, concentrated, and purified by column chromatography (25:75 / Ether:Hexane, R_f= 0.45). This gave the desired product (**105**) as a clear oil (69mg, 92% yield). ¹H NMR (300 MHz, CD₂Cl₂) δ 5.74 (dd, *J* = 15.7 0.4 Hz, 1H), 5.40 (dd, *J* = 15.7, 6.2 Hz, 1H), 4.02 (qd, *J* = 6.2, 1.0 Hz, 1H), 3.75-3.81 (m, 1H), 3.71 (ddt, *J* = 18.1, 5.0 Hz, 2H), 2.25-2.32 (m, 4H), 1.69-1.79 (m, 2H), 1.00 (s, 9H), 0.88 (s, 9H), 0.03 (s, 6H); ¹³C NMR (75 MHz, CD₂Cl₂) δ 207, 144, 125, 78, 74, 59, 49, 48, 40, 33, 30, 26, 19, -5.2, -5.3; IR (thin film) 1716, 1260, 1086 cm⁻¹; HRMS (EI): *m/z* calc for C₁₈H₃₃SiO₃ (M-CH₃)⁺ 325.2198, found 325.2203; [α]_D²³ +29.0° (CHCl₃, c 1.0).

BIBLIOGRAPHY

1. Gottesman, M. M.; Pastan, I.; Ambudkar, S. *Curr. Opin. Genet. Dev.* **1996**, *6*, 610.
2. Gottesman, M. M. and Pastan, I. *Annu. Rev. Biochem.* **1993**, *62*, 385.
3. Brennan, R. G. *Semin. Cell Dev. Biol.* **2001**, *12*, 201.
4. Ambudkar, S.; Dey, S.; Hrycyna, C.; Ramachandra, M.; Pastan, I.; Gottesman, M. M. *Annu. Rev. Pharmacol. Toxicol.* **1999**, *39*, 361.
5. Sharom, F. J. *J. Membr. Biol.* **1997**, *160*, 161.
6. Thiebaut, F.; Tsuruo, T.; Hamada, H.; Gottesman, M. M.; Pastan, I.; Willingham, M. C. *Proc. Natl. Acad. Sci. USA* **1987**, *84*, 7735.
7. Cordon-Cardo, C.; O'Brien, J. P.; Casals, D.; Rittman-Grauer, L.; Biedler, J. L.; Melamed, M. R.; Bertino, J. R. *Proc. Natl. Acad. Sci. USA* **1989**, *86*, 695.
8. Synold, T. W.; Dussault, I.; Forman, B. M. *Nature Med.* **2001**, *7*, 584.
9. Schuetz, E. and Strom, S. *Nature Med.* **2001**, *7*, 536.
10. van Veen, H. W. *Semin. Cell Dev. Biol.* **2001**, *12*, 239.
11. Saier, M. H.; Paulsen, I. T. *Semin. Cell Dev. Biol.* **2001**, *12*, 205.
12. Ueda, K.; Cardarelli, C.; Gottesman, M. M.; Pastan, I. *Proc. Natl. Acad. Sci. USA* **1987**, *84*, 3004.
13. Seelig, A. *Eur. J. Biochem.* **1998**, *251*, 252.
14. Chin, K. V.; Pastan, I.; Gottesman, M. M. *Adv. Cancer Res.* **1993**, *60*, 157.
15. Gupta, S.; Gollapudi, S. *J. Clin. Immunol.* **1993**, *13*, 289.
16. Liu, R.; Sharom, F. J. *Biochemistry* **1996**, *35*, 11865.
17. Sharom, F. J.; Liu, R.; Qu, Q.; Romsicki, Y. *Semin. Cell Dev. Biol.* **2001**, *12*, 257.
18. Senior, A. E. *Acta. Physiol. Scand.* **1998**, *163*, Suppl. 213.
19. Seelig, A.; Blatter, X. L.; Wohnsland, F. *Int. J. Clin. Pharm. Ther.* **2000**, *38*, 111.
20. Chang, G.; Roth, C. B. *Science* **2001**, *293*, 1793.

21. Zamora, J. M.; Pearce, H. L.; Beck, W. T. *Mol. Pharmacol.* **1988**, *33*, 454.
22. Schinkel, A. H.; Wagenaar, E.; Mol, C. A. A. M.; van Deemter, L. *J. Clin. Invest.* **1996**, *97*, 2517.
23. Ueda, K.; Okamura, N.; Hirai, M.; Tanigawara, Y.; Saeki, T.; Kioka, N.; Komano, T.; Hori, K. *J. Biol. Chem.* **1992**, *267*, 24248.
24. Higgins, C. F. *Ann. Rev. Cell Biol.* **1992**, *8*, 67.
25. Rosenberg, M. F.; Callaghan, R.; Ford, R. C.; Higgins, C. F. *J. Biol. Chem.* **1997**, *272*, 10685.
26. Kajiji, S.; Dreslin, J. A.; Grizzuti, K.; Gros, P. *Biochemistry* **1994**, *33*, 5041.
27. Zhang, X.; Collins, K. I.; Greenberger, L. M. *J. Biol. Chem.* **1995**, *270*, 5441.
28. Hrycyna, C. A. *Semin. Cell Dev. Biol.* **2001**, *12*, 247.
29. Tsuruo, T.; Tomida, A. *Anti-Cancer Drugs* **1995**, *6*, 213.
30. Kim, S. E.; Kim, Y. H.; Kim, Y. C.; Lee, J. J. *J. Nat. Prod.* **1998**, *61*, 108.
31. Kim, S. E.; Kim, H. S.; Hong, Y. S.; Kim, Y. C.; Lee, J. J. *J. Nat. Prod.* **1999**, *62*, 697.
32. Sadis, S.; Hightower, L. E. *Biochemistry* **1992**, *31*, 9406.
33. Wandel, C.; Kim, R. B.; Kajiji, S.; Guengerich, P. F.; Wilkinson, G. R.; Wood, A. J. J. *Cancer Res.* **1999**, *59*, 3944.
34. Schinkel, A. H.; Mol, C. A. A. M.; Wagenaar, E.; van Deemter, L.; Smit, J. J. M.; Borst, P. *Eur. J. Cancer* **1995**, *31A*, 1295.
35. Spivey, A. C.; Weston, M.; Woodhead, S. *Chem. Soc. Rev.* **2002**, *31*, 43.
36. Huffmann, J. W.; Raveendranath, P. C. *J. Org. Chem.* **1986**, *51*, 2148
37. Li, W. Z.; Zhou, G.; Gao, X.; Li, Y. *Tetrahedron. Lett.* **2001**, *42*, 4649.
38. Cortes-Selva, F.; Campillo, M.; Reyes, C. P.; Jimenez, I. A.; Castanys, S.; Bazzocchi, I., L.; Pardo, L.; Gamarro, F.; Ravelo, A. G. *J. Med. Chem.* **2004**, *47*, 576.
39. Tsuruo, T.; Iida, H.; Tsukagoshi, S. *Cancer Res.* **1981**, *41*, 1967.
40. Andrus, M. B.; Turner, T. M.; Updegraff, E. P.; Sauna, Z. E.; Ambudkar, S. V. *Tetrahedron Lett.* **2001**, *42*, 3819.
41. Barrett, H. C.; Büchi, G. *J. Am. Chem. Soc.* **1967**, *89*, 5665.

42. Marshall, J. A.; Pike, M. T. *J. Org. Chem.* **1968**, *33*, 435.
43. Asselin, A.; Mongrain, M.; Deslongchamps, P. *Can. J. Chem.* **1968**, *46*, 2817.
44. Büchi, G.; Wüest, H. *J. Org. Chem.* **1979**, *44*, 546.
45. White, J. D.; Shin, H.; Kim, T.; Cutshall, N. S. *J. Am. Chem. Soc.* **1997**, *119*, 2404.
46. Rubottom, G. M.; Gruber, J. M. *J. Org. Chem.* **1978**, *43*, 1599.
47. Dess, D. B.; Martin, J. C.; *J. Org. Chem.* **1983**, *48*, 4155.
48. Itoh, A.; Ozawa, S.; Oshima, K.; Nozaki, H. *Tetrahedron Lett.* **1980**, *21*, 361.
49. Saksena, A. K.; Mangiaracina, P. *Tetrahedron Lett.* **1983**, *24*, 273.
50. Evans, D. A.; Allison, B. D.; Yang, M. G.; Masse, C. E. *J. Am. Chem. Soc.* **2001**, *123*, 10840.
51. Ireland, R. E.; Bey, P. *Org. Synth.* **1973**, *43*, 1599.
52. Gras, J. L.; Kong Win Chang, Y. Y.; Bertrand, M. *Tetrahedron Lett.* **1982**, *23*, 3571.
53. Brown, C. A.; Jadhav, P. K. *Org. Synth.* **1987**, *65*, 224.
54. Corey, E. J.; Suggs, J. W. *J. Org. Chem.* **1973**, *38*, 3224.
55. Crimmins, M. T.; Kirincich, S. J.; Wells, A. J.; Choy, A. L. *Synth. Commun.* **1998**, *28*, 3675.
56. Scholl, M.; Ding, S.; Lee, C. W.; Grubbs, R. H. *Org. Lett.* **1999**, *1*, 953.
57. Scarborough, R. M., Jr.; Smith, A. B. *Tetrahedron Lett.* **1977**, *50*, 4361.
58. Dowd, P.; Kennedy, P. *Synth. Commun.* **1981**, *11*, 935.
59. Jones, D. N.; Mundy, D.; Whitehouse, R. D. *J. Chem. Soc. Chem. Commun.* **1970**, *2*, 86.
60. For an example, see: Mastalerz, H.; Menard, M.; Vinet, V.; Desiderio, J.; Functomc, J.; Kessler, R.; Tsai, Y. *J. Med. Chem.* **1988**, *31*, 1190.
61. Grubbs, R. H. *Acc. Chem. Res.* **2001**, *34*, 18.
62. Garbaccio, R. M.; Danishefsky, S. J. *Org. Lett.* **2000**, *2*, 3127.
63. For a review, see: DeLuchi, O.; Miotti, U.; Modena, G. *Org. React.* **1991**, *40*, 157.
64. Crabtree, R. H.; Davis, M. W. *J. Org. Chem.* **1986**, *51*, 2655.

65. Brown, L.; Koreeda, M. *J. Org. Chem.* **1984**, *49*, 3875.
66. Payne, G. B.; Williams, P. H. *J. Org. Chem.* **1961**, *26*, 651.
67. Wipf, P. W.; Jung, J. K. *J. Org. Chem.* **2000**, *65*, 6319.
68. Gansauer, A.; Bluhm, H.; Pierobon, M. *J. Am. Chem. Soc.* **1998**, *120*, 12849.
69. Lee, C. A.; Floreancig, P. E. *Tetrahedron Lett.* **2004**, *45*, 7193.
70. Still, W. C. *J. Comp. Chem.* **1990**, *11*, 440.
71. Petasis, N. A.; Lu, S. P. *Tetrahedron Lett.* **1996**, *37*, 141.
72. Spitaler, M.; Utz, I.; Hilbe, W.; Hofmann, J.; Grunicke, H. H. *Biochem. Pharmacol.* **1998**, *56*, 861.
73. Searle, P. A.; Molinski, T. F. *J. Am. Chem. Soc.* **1995**, *117*, 8126.
74. For a recent example, see: Paterson, I.; Tudge, M. *Tetrahedron* **2003**, *59*, 6833.
75. For a recent example, see: Mandai, T.; Ueda, M.; Kashiwagi, K.; Kawada, M.; Tsuji, J. *Tetrahedron Lett.* **1993**, *34*, 111.
76. Burke, S. D.; Armistead, D. M.; Schoenen, F. J. *Tetrahedron* **1986**, *42*, 2787.
77. Mulzer, J.; Hanbauer, M. *Tetrahedron Lett.* **2000**, *41*, 33 and references therein
78. For a recent example, see: Overman, L. E.; Pennington, L. D. *J. Org. Chem.* **2003**, *68*, 7143 and references therein.
79. Aubele, D. A.; Lee, C. A.; Floreancig, P. E. *Org. Lett.* **2003**, *23*, 4521.
80. Keck, G. E.; Covell, J. A.; Schiff, T.; Yu, T. *Org. Lett.* **2002**, *4*, 1189.
81. Huang, H.; Panek, J. S. *J. Am. Chem. Soc.* **2000**, *122*, 9836.
82. Rychnovsky, S. D.; Marumoto, S.; Jaber, J. J. *Org. Lett.* **2001**, *3*, 3815.
83. Rychnovsky, S. D.; Thomas, C. R. *Org. Lett.* **2000**, *2*, 1217.
84. Kopecky, D. J.; Rychnovsky, S. D. *J. Am. Chem. Soc.* **2001**, *123*, 8420.
85. Evans, D. A.; Carter, P. H.; Carreira, E. M.; Prunet, J. A.; Charette, A. B.; Lautens, M. *Angew. Chem. Int. Ed.* **1998**, *37*, 2354.
86. Smith, A. B.; Verhoest, P. R.; Minbiole, K. P.; Lim, J. J. *Org. Lett.* **1999**, *1*, 909.
87. Petasis, N. A.; Lu, S. P. *Tetrahedron Lett.* **1996**, *36*, 141.

88. Jaber, J. J.; Mitsui, K.; Rychnovsky, S. D. *J. Org. Chem.* **2001**, *66*, 4679.
89. For a discussion, see: Aubele, Danielle A., Ph.D. Thesis, University of Pittsburgh August 2004.
90. Mohr, P. *Tetrahedron Lett.* **1993**, *34*, 6251.
91. Paquette, L. A.; Tae, J. *J. Org. Chem.* **1996**, *61*, 7860.
92. Sano, T.; Oriyama, T. *Synlett* **1997**, 716.
93. Suginome, M.; Iwanami, T.; Ito, Y. *J. Org. Chem.* **1998**, *63*, 6096.
94. Chen, C.; Mariano, P. S. *J. Org. Chem.* **2000**, *65*, 3252.
95. Manabe, K.; Mori, Y.; Wakabayashi, T.; Nagayama, T.; Kobayashi, S. *J. Am. Chem. Soc.* **2000**, *122*, 7202.
96. Mukaiyama, T.; Narasaka, K.; Banno, K. *Chem. Lett.* **1973**, *9*, 1011.
97. For a recent review, see: Mikami, K.; Terada, M.; Matsuzawa, H. *Angew. Chem. Int. Ed.* **2002**, *41*, 3554.
98. Crosby, S. R.; Harding, J. R.; King, C. D.; Parker, G. D.; Willis, C. D. *Org. Lett.* **2002**, *4*, 577.
99. Pettit, G. R.; Day, J. F.; Hartwell, J. L.; Wood, H. B.; *Nature* **1970**, *227*, 962.
100. Pettit, G. R.; Herald, C. L.; Doubek, D. L.; Herald, D. L.; Arnold, E.; Clardy, J. *J. Am. Chem. Soc.* **1982**, *104*, 6846.
101. Pettit, G. R. *J. Nat. Prod.* **1996**, *59*, 812.
102. For a review, see: Pettit, G. R. The Bryostatins. In *Progress in the Chemistry of Organic Natural Products*; Herz, W., Ed.; Springer-Verlag: New York, 1991; No. 57, pp 153-195.
103. Schuchter, L. M.; Esa, A. H.; May, W.; Laulis, M. K.; Pettit, G. R.; Hess, A. D. *Cancer Res.* **1991**, *51*, 682.
104. Drexler, H. G.; Cignac, S. M.; Pettit, G. R.; Hoffbrand, A. V. *Eur. J. Immunol.* **1990**, *20*, 119 and references therein.
105. DeVries, D. J.; Herald, C. L.; Pettit, G. R.; Blumberg, P. M.; *Biochem. Pharm.* **1988**, *37*, 4069 and references therein.
106. Scala, S.; Dickstein, B.; Regis, J.; Szallasi, Z.; Blumberg, P. M.; Bates, S. E. *Clinical Cancer Res.* **1995**, *1*, 15851.

107. Kageyama, M.; Tamura, T.; Nantz, M. H.; Roberts, J. C.; Somfai, P.; Whritenour, D. C.; Masamune, S. *J. Am. Chem. Soc.* **1990**, *112*, 7407
108. Ohmori, K.; Ogawa, Y.; Obitsu, T.; Ishikawa, Y.; Nishiyama, S.; Yamamura, S. *Angew. Chem. Int. Ed.* **2000**, *39*, 2290.
109. Wender, P. A.; De Brabander, J.; Harran, P. G.; Jimenez, J. M.; Koehler, M. F. T.; Lippa, B.; Park, C. M.; Shiozaki, M. *J. Am. Chem. Soc.* **1998**, *120*, 4534.
110. Wender, P. A.; De Brabander, J.; Harran, P. G.; Hinkle, K. W.; Lippa, B.; Pettit, G. R. *Tetrahedron Lett.* **1998**, *39*, 8625.
111. Wender, P. A.; Hinkle, K. W. *Tetrahedron Lett.* **2000**, *41*, 6725.
112. Wender, P. A.; Lippa, B. *Tetrahedron Lett.* **2000**, *41*, 1007.
113. Wender, P. A.; Baryza, J. L.; Bennett, C. E.; Bi, F. C.; Brenner, S. E.; Clarke, M. O.; Horan, J. C.; Kan, C.; Lacote, E.; Lippa, B.; Nell, P. G.; Turner, T. M. *J. Am. Chem. Soc.* **2002**, *124*, 13648.
114. Wender, P. A.; Koehler, M. F. T.; Sendzik, M. *Org. Lett.* **2003**, *5*, 4549.
115. Wender, P. A.; Matweg, A. V. W.; VanDeusen, C. L. *Org. Lett.* **2003**, *5*, 277.
116. Nahm, S.; Weinreb, S. M. *Tetrahedron Lett.* **1981**, *22*, 3815.
117. For a review, see: Tsuji, J. *Synthesis* **1984**, *5*, 369.
118. Brown, H. C.; Jadhav, P. K. *J. Am. Chem. Soc.* **1983**, *105*, 2092.
119. Brown, H. C.; Desai, M. C.; Jadhav, P. K. *J. Org. Chem.* **1982**, *47*, 5065.
120. Chini, M.; Crotti, P.; Flippin, L. A.; Gardelli, C.; Giovani, E.; Macchia, F.; Pineschi, M. *J. Org. Chem.* **1993**, *58*, 1221.
121. Evans, D. A.; Carter, P. H.; Carreira, E. M.; Charette, A. B.; Prunet, J. A.; Lautens, M. *J. Am. Chem. Soc.* **1999**, *121*, 7540.
122. Lampe, T. F. J.; Hoffmann, H. M. R. *Tetrahedron Lett.* **1996**, *37*, 7695.
123. Tanaka, K.; Ohta, Y.; Fuji, K. *Tetrahedron Lett.* **1993**, *34*, 4071.
124. Tanaka, K.; Otsubo, K.; Fuji, K. *Tetrahedron Lett.* **1996**, *37*, 3735.
125. Tsunoda, T.; Suzuki, M.; Noyori, R. *Tetrahedron Lett.* **1980**, *21*, 1357.
126. Hosokawa, T. *Chem. Lett.* **1989**, 2001.

127. For a recent synthesis, see: Smith, A. B.; Minbirole, K. P.; Verhoest, P. R.; Schelhass, M. *J. Am. Chem. Soc.* **2001**, *123*, 10942.
128. Evans, D. A.; Ennis, M. D.; Mathre, D. J. *J. Am. Chem. Soc.* **1982**, *104*, 1737.
129. Goodman, J. M.; Paterson, I. *Tetrahedron Lett.* **1992**, *33*, 7223.